REMOVAL OF SULPHATES FROM ACID MINE DRAINAGE USING BARIUM AND ORGANICALLY MODIFIED CLAY

by

MABATHO MOREROA

Student Number: 201002676

Dissertation in fulfilment of the requirement for the degree

MAGISTER TECHNOLOGIAE

in

CHEMICAL ENGINEERING

in the

FACULTY OF ENGINEERING AND THE BUILT ENVIRONMENT

of the

UNIVERSITY OF JOHANNESBURG

Supervisor : PROF. F. NTULI

2015

DECLARATION

I hereby declare that this dissertation, which I herewith submit for the research qualification

MAGISTER TECHNOLOGIAE IN CHEMICAL ENGINEERING

to the University of Johannesburg, Department of Chemical Engineering, is, apart from the recognised assistance of my supervisors, my own work and has not previously been submitted by me to another institution to obtain a research diploma or degree.

_____ on this ____ day of _____

(Candidate)

_____ on this ____ day of _____

(Supervisor)

DEDICATIONS

I would like to dedicate this work to my family: Mother (Tryphosa), Phetogo, Jack, Ishmael and Harry Moreroa for the great support they've given me during the completion of this degree. It wouldn't have been possible without family.

ACKNOLEDGEMENTS

I would like to extend my profound gratitude to:

- Prof. F. Ntuli for the excellent supervision and financial support he granted me.
- Mr Thabo Falayi for playing the role of a co-supervisor by assisting in experimental work and availing himself throughout my master's degree.
- Dr. Thabo Nkambule for proof reading my dissertation.
- The Metallurgy department for availing analytical equipment in the department and assisting during the operation of the equipment.
- The Chemistry department for availing and training of analytical equipment.
- The department of Chemical Engineering and the University of Johannesburg for granting me the opportunity to complete my master's degree.
- My mother Miss TM Moreroa, son Phetogo, brothers Jack, Ishmael and Harry for the support and understanding my absence during my academic career.
- My colleagues and dearest friend Abigail Ramohlale for the support they've given me throughout.
- Lastly I'd like to thank God, almighty for giving me the knowledge and wisdom to complete this dissertation.

ABSTRACT

Attapulgite and Mozambican bentonite (MB) were modified by using barium chloride and ammonium cations such as hexadecyltrimethylammonium bromide (HDTMA) and trimethyldecylammonium bromide (TDTMA) to enhance the removal capacity of sulphates from acid mine drainage (AMD). Through the modification process the surface properties of the clays was rendered organophilic. Batch adsorption experiments of the modified clays were done in a thermostatic shaker at different temperatures, mass loading of adsorbent, and cation exchange capacity (CEC) percentages to investigate the sorption behaviour of sulphates from AMD. Characterization of the modified clay that gave the highest removal of sulphates was done using XRF, XRD, FTIR and SEM to investigate the chemical composition of the clay, removal mechanism and structural change of the clay as a result of sorption of sulphates.

Attapulgite showed higher removal of sulphates (70.8%) when modified with $BaCl_2$ than the other two surfactants. This maximum removal was achieved at 25^{o}C and 10% w/v clay to AMD. The reaction fitted the Temkin adsorption isotherm and the second order kinetic model. Adsorption of sulphates on attapulgite was not dependent on temperature as the difference in recovery was not statistically significant when temperature was varied. The value of activation energy (23.7kJ/mol) showed that chemisorption was the dominant mechanism of sulphate removal.

MB showed higher removal of sulphates (74.0%) when modified with TDTMA. The reaction was endothermic and fitted the Temkin isotherm model and the second order kinetic model. More sulphates were adsorbed at higher temperatures, suggesting that this was an endothermic reaction, which was supported by the positive value of enthalpy. The activation energy for this reaction (-124.8 kJ/mol) showed that physisorption was the dominant mechanism of sulphate removal.

Characterization of both clays showed that the sulphates were removed by adsorption and that the modifiers were only adsorbed on the surface of the clay during the cation exchange process without destroying the crystalline structure of the clay. At high solid loading, more sulphates were adsorbed from the AMD sample by both clays. This implied that at higher solid loadings, there are more sites of adsorption and thus, the higher sulphate removal.

A further investigation on the effect of surfactant loading was done and results showed that the uptake of sulphates from AMD is dependent on the amount of surfactant percentage used during the modification process.

TABLE OF CONTENTS

LIST OF TABLES

LIST OF FIGURES

Chapter 1 : Introduction

1.1. Background

Water is a necessary natural resource, fundamental to life, the environment, food production, hygiene and sanitation, industry and power generation. Clean water is recognized around the world as an extremely important element in the fight against poverty, the cornerstone of prosperity and a limiting factor for growth [Barson, 1997]. Freshwater resources of South Africa are threatened due to the increasing population and pollution of both ground and surface water as a result of industrial and domestic activities. South Africa's water resources are mostly polluted by industrial effluents, domestic and commercial sewage, mine waters, agricultural run-off and litter [Davies et al., 1993].

Acid mine drainage arises from trapped water from abandoned mines [Davies et al., 1993] and is a recognized problem in the coal and gold mining areas of South Africa [Abdelaal, 2004]. The majority of natural life can only live and survive at, or near, pH 7 (neutral) [McGinnes, 1999] whereas AMD has pH less than 3. AMD results from the microbial oxidation of pyrite and different heavy metals such as Fe in the presence of water and air, resulting in an acidic solution that contains toxic metal ions [Rios, 2008]. The primary pollutants found in AMD are acidity, Fe, SO_4^{2-}, Mn, Mg, Al, Ni, Cu and Co [Gazea, 1998]. The acidic nature of the water increases the dissolution of minerals that contain heavy metals, therefore causing the water to be heavily contaminated with toxic heavy metals [Gazea, 1998]. The metals found within these minerals often turn into sulphate salts through precipitation. When these salts are in contact with water, they dissolve and this acidic, metal-containing mixture comprises the initial AMD discharge [McGinness, 1999]. Sulphates make water taste salty and bitter and are also a corrosive agent, thus high concentrations of SO_4^{2-} increase the rate of corrosion in metal fittings.

Conventional processes for sulphate ions removal show numerous disadvantages, such as high costs and high sludge volumes, for example; the biological sulphate removal process which is relatively expensive [Maree, 1989]. Thus, there is a need for new techniques and technologies for sulphate removal [Hameed, 2007].

This project will focus on the removal of SO_4^{2-} from AMD using barium and organically modified clay. Clay is a natural resource which is readily available in the environment and thus accessible and inexpensive.

The success of this project will help in reducing SO_4^{2-} pollution from AMD which will mean less SO_4^{2-} disposed to the environment and thus less negative effects on the environment like corrosion and pollution of the eco-system. This project will contribute to the development of a cost effective method in developing a sustainable solution for mitigating the adverse effects of AMD. Thus, this project will assist in averting the crisis by developing a cost effective method of treating AMD in combination with other measures to reduce the amount of sulphates in AMD.

Mozambican bentonite and attapulgite were used as adsorbents for sulphates from AMD. More interest was put on the study of different types of clays as adsorbents, because of their low cost and local availability. Clay minerals are naturally hydrophilic and thus are not suitable adsorbents for organic compounds. However, the surface structure of the clay can be rendered organophilic through a modification process where the inorganic cations are exchanged with organic cations and then the resulting clay is referred to as an organoclay. The most common chemicals usually used for this modification process are cationic surfactants [Su, 2001]. A number of investigations have been carried out in order to modify the clay surfaces and render them organophilic [Hameed, 2007]. Barium chloride has also been used as a modifier to remove sulphates from waste water. On contact with sulphates in the AMD, barium forms barium sulphate which is an indication of sulphates ions being removed from the AMD [Sven, 1979].

1.2. Problem Statement

Elevated concentration of SO_4^{2-} in water has harmful effects on human health. Sulphate concentrations of greater than 600 ppm causes diarrhoea to most individuals and adaptation may not occur. Exposure to high SO_4^{2-} concentrations in drinking water for long periods, usually cause people to become adapted and they may no longer experience the side effects of the high SO_4^{2-} concentrations. Higher SO_4^{2-} concentration in water causes water to taste salty or bitter. The sulphate content for Gold based AMD, which is in excess of 3000 ppm needs to be reduced to 400 ppm using a cost effective treatment method during treatment to produce better quality water for use.

1.3. Aims and Objectives

The aim of the study was to develop a method for sulphate ion removal from AMD that will have fewer drawbacks as discussed above. This study will establish the effectiveness of modified attapulgite and Mozambican bentonite as adsorbents for the removal of sulphates from AMD. This approach will aim at using the least amount of adsorbent and modifier to remove as much sulphates ions from AMD as possible.

Clay has a net negative charge and thus need to be rendered positive by modification in order to attract anions such as sulphates. This process is called modification. The higher the CEC, the more cations which can be available for ion exchange. Organically modified clays have been used in the treatment of waste water [Rajkiran, 2008], but little work has been done on the removal of sulphates from AMD using organically modified clays; hence this project will serve as an opportunity to assess their potential application for AMD remediation.

1.4. Key questions

I. Does modification of clay enhance sulphate removal?
II. How does CEC affect sulphate removal?
III. How does the concentration of $BaCl_2$ affect sulphate removal?
IV. At what temperature and solid loading can the highest removal of sulphates be achieved?
V. Which surfactant is capable of removing the highest amount of sulphates from AMD?
VI. What type of mechanism is responsible for sulphate removal?
VII. Is the reaction endothermic or exothermic?

1.5. Thesis outline

Chapter 1: The background on AMD as a source of sulphates ions is discussed. This chapter explains the effects and source of AMD and why it should be treated. The problem statement, aims and objectives of the study are outlined.

Chapter 2: This chapter discusses in detail how AMD is formed, its composition and characteristics and the effects of sulphates on the environment and human beings. Treatment techniques for AMD, uses of clay, surfactants, adsorption isotherms, kinetics and thermodynamics are also discussed.

Chapter 3: This chapter deals with the methodology used for the study. The type of equipment, materials and a detailed procedure on how the experiment was set up.

Chapter 4 and 5: The results obtained from modification of the attapulgite and Mozambican Bentonite (MB) is discussed. All parameters i.e., agitation time, effect of temperature, effect of surfactant concentration, effect of surfactant loading and solid loading are discussed. Results of XRD, SEM, XRF and FTIR characterization from the best performing modified clay are discussed in these chapters.

The thermodynamic and kinetic studies from the results obtained, adsorption isotherms, adsorption kinetics, adsorption thermodynamics and sorption activation energy are also discussed.

Chapter 6 and 7: Conclusions drawn from the results and recommendations are given in these two chapters.

Chapter 2 : Literature Review

This chapter deals with the literature on AMD formation, the effects of sulphates, AMD treatment techniques, adsorption thermodynamics and sorption kinetics.

2.1. Introduction

South Africa is a water scarce country with 98% of its water resources already allocated [Abdelaal, 2004]. South Africa's water resources are also under threat due to AMD generated from over a century of coal and gold mining [Abdelaal, 2004]. AMD has harmful effects on the environment, and therefore studies on its prediction, minimization, handling and treatment are quiet critical in order to safeguard the environment and human health [Abdelaal, 2004].

In South Africa, a number of defunct and flooded underground coal mines such as the Middelburg Colliery to the west and northwest of Witbank commenced decanting in the mid-1990s, contributing to pollution of the water resources in the upper Olifants River catchment [Motaung et al., 2008]. The Department of Water and Forestry (DWAF) took responsibility for these mines and constructed the Brugspruit Water Pollution Control Works (BWPCW) in 1997 at a cost of R26.5 million [DWAF, 2007].

Remediation of environmental contaminants is a great challenge for the modern world as an increasing global population is creating a burden on industries to supply outputs that meet demands [Haroon et al., 2013]. In the developing world this demand is often met at the expense of the environment as regulations are not usually adhered to by industries. In order to eliminate this problem, layered silicate clay minerals are used as adsorbents for the removal of environmental contaminants.

Layered silicate clay minerals are naturally occurring earth minerals, which can be value added by modifying their adsorption properties to enhance their efficiency in removing contaminants that can have detrimental environmental impact [Lee and Kim, 2002]. Naturally occurring clay minerals such as smectite can be modified by the introduction of cationic surfactants such as quaternary ammonium compounds into the clay structure to make them hydrophobic. These clays are then referred to as organoclays and are suitable for a large number of environmental remediation applications [Bonczek et al, 2002]. It has been found that the structure and chemical characteristics of the clay mineral have a strong effect on the cation exchange that is involved in the synthesis of organoclays [Xu and Boyd, 1995].

Usually the cation exchange reaction starts at the edges of the clay particle and then extends to the centre. Kinetic studies show that the reaction between the quaternary ammonium salts and the clay mineral increases with the increase of temperature [Komadel and Madejova, 2006].

2.2. AMD Formation

When sulphide ores are exposed to the atmosphere, oxidation reactions are initiated, which enhances AMD formation. When pyrite reacts with oxygen and water, a solution comprising of ferrous sulphate and sulphuric acid is produced. Further oxidation of ferrous iron produces additional acidity. Catalyses of these reactions are done by iron and sulphur oxidizing bacteria. These reactions occur at low pH levels and thus increase the rate of reaction by several orders of magnitude. The major contributor to the large surface exposure of sulphur bearing rocks is mining and milling processes.

Biological catalysis often results in oxidation reactions, which affect the sulphur compounds that often accompany coal seams. When the mine dries out, the sulphur is converted to sulphate salts in a solid, but more available form. The sulphate salts are then continuously oxidised by the activity of chemolithotrophic bacteria within the compounds in the mine and thus maintains the flow of the AMD, often over decades after the initial flush [McGinnes, 1999].

Hydrolysis and oxidation of metal sulphide minerals such as sphalerite, pyrrhotite, chalcopyrite and others release metals such as nickel, zinc, copper and lead into solution in addition to acidity and SO_4^{2-} as shown in eqn. 2-1.

$$4FeS_{2(s)} + 15O_{2(g)} + 14H_2O_{(l)} \rightarrow 4Fe(OH)_{(s)} + 8SO_4^{2-}{}_{(aq)} + 16H^+{}_{(aq)} \quad \textbf{eqn 2-1}$$

Additional oxidation of Fe^{2+} to Fe^{3+} can occur if there is enough oxygen dissolved in the water, or if there is enough atmospheric oxygen within the water (eqn. 2-2).

$$2Fe_{(s)}{}^{2+} + \tfrac{1}{2}O_{2(g)} + 2H^+{}_{(aq)} \rightarrow 2Fe_{(s)}{}^{3+} + H_2O_{(l)} \quad \textbf{eqn 2-2}$$

$Fe(OH)_3$ can be formed from the precipitation of ferric iron, which can be identified as a red-orange precipitate seen in water that has been affected by acid mine drainage. Alternatively, ferric iron can result in the production of more ferrous iron and acidity, by reacting with pyrite as shown in eqn. 2-3 and 2-4.

$$2Fe_{(s)}{}^{3+} + 6H_2O_{(l)} \rightarrow 2Fe(OH)_{3(s)} + 6H^+{}_{(aq)} \quad \textbf{eqn 2-3}$$

$$14Fe^{3+}{}_{(s)} + FeS_{2(s)} + 8H_2O_{(l)} \rightarrow 2SO_4^{2-}{}_{(aq)} + 15Fe^{2+}{}_{(s)} + 16H^{+}{}_{(aq)} \qquad \textbf{eqn 2-4}$$

The cycle of eqn. 2-2 and 2-3 is repeated when there is sufficient dissolved oxygen during the production of ferrous iron (eqn. 2-4). Eqn. 2-4 will continue to completion if there is no dissolved oxygen and elevated levels of ferrous iron will be evident in the water.

Bacteria such as *Thiobacillus ferrooxidans* can accelerate the chemical reaction of eqn. 2-2. Another producer of acidity in mine waters has been identified to be a microbe called *Ferroplasma Acidarmanus* [Beer, 2000].

2.3. AMD as a source of sulphates

Sulphide minerals responsible for AMD formation include the common iron minerals pyrite (FeS_2) and pyrrhotite, and metallic sulphides such as chalcopyrite ($CuFeS_2$), sphalerite (ZnS), galena (PbS), etc. [Madzivire, 2009]. When it rains, the exposed surfaces of sulphur bearing rocks react with water and forms acidic water which poses a threat to the environment as this water runs in river streams, ponds, lakes and dams.

AMD contains SO_4^{2-} as the principal anion and Fe, Mn and Al as the major cations. In contrast when SO_4^{2-} and HCO_3^- are the principal anions, the concentrations of Ca, Mg and Na are generally elevated compared to Fe and Al [Cravotta, 1990]. AMD is characterised by pH <3, high concentration of SO_4^{2-} (more than 3000 ppm) and high concentration of metals especially Fe and Al. This is due to the precipitation of the metals as hydroxides and SO_4^{2-} as gypsum due to the neutralisation by the carbonates that are found associated with the FeS_2 [Madzivire, 2009].

2.4. Effects of sulphates in water

The presence of sulphates in water has been considered as one of the most consequential water quality issues for mining operations and process plants, especially in countries that have problems of fresh water supply like South Africa and Australia [Bowell, 1998]. Acid mine drainage mechanisms involve the oxidation of sulphide minerals and can lead to highly acidic, metal-rich waters with high sulphate content. High concentration of sulphates in water can be potentially corrosive to surfaces. The accumulation of salts such as calcium sulphate in water limits the number of times that water can be reused and creates environmental problems if discharged [Bowell, 1998]. AMD should be treated in order to make it suitable for re-use in the mining industry, in growing agricultural crops or for discharge in the rivers and dams.

Water that is rich in sulphate has a high scaling potential. It has been estimated that 75% of gold mines in South Africa have scaling processes essentially related to saturation of water with respect to $CaSO_4$ [Bowell, 1998].

High SO_4^{2-}concentrations in industrial water causes an increase in the corrosion rate of metal fittings in distribution systems, because SO_4^{2-} promotes the growth of sulphate removing bacteria (SRB), which in turn enhances corrosion through microbially-induced corrosion (MIC), it also induces scaling in equipment, structures and pipes, deposition and fouling boilers. Furthermore, SO_4^{2-} causes acidified soils, blocking the pores of soils and retards irrigation [Silva, 2010].

Elevated SO_4^{2-} in water causes degradation of concrete structures due to gypsum formation. Water containing high SO_4^{2-} causes gypsum scaling on steam generating equipment surfaces thereby reducing the heat transfer capacity [Madzivire, 2009].

Water streams containing small amounts of AMD can disturb life in streams because the metals, SO_4^{2-} and/or other suspended solids precipitate out of the water and coat the rocks and gravel on the stream bottom. As a result, the flora and fauna that live on and under the rocks will die and be smothered away as the level of oxygen in the water will be extremely low.

2.5. AMD treatment technologies

The search for sulphate removal technologies from sulphate rich water has led to the development of the council for scientific and industrial research (CSIR) alkali barium calcium (ABC) process [Zvimba et al., 2010]. In this process, $BaCO_3$ is effectively used for the removal of sulphates from sulphate rich industrial waste waters via precipitation of barite, and have exhibited a number of advantages over the use of other chemicals [Maree et al. 2004 and Hlabela et al, 2007]. This process included a neautralization stage using calcium hydroxide, which has been reported to reduce sulphate from 4870 mg/L to 2300 mg/L, representing a 53 % reduction in sulphates (Motaung et al., 2008).

In order to address the AMD threats responsibly, the department of water affairs (DWA) of South Africa, together with a number of other departments such as department of mineral resources (DMR) have initiated a number of interventions and studies. These studies include:

a. Short-term intervention, whereby water is pumped from the Western, Central and Eastern Basins of Gauteng Province, South Africa, to prevent surface decant. AMD will then be treated to correct the pH and to remove heavy metals before being

discharged to surface water resources/river systems [Department of Water Affairs, 2012].

b. Long-Term intervention, whereby treatment as discussed in the short-term intervention above, plus removal of salts and consideration of alternative discharge/use options. The department has also recommended further research to optimise sustainable solutions in the long term and implementation of ingress control measures. Feasibility Study for a long term solution to address the AMD associated with the East, Central and West Rand underground mining basins was initiated. This study, which was concluded on the 31 July 2013, consisted of three phases, i.e. the Initiation Phase, the Prefeasibility Phase and a Feasibility Phase [Department of Water Affairs, 2012].

Furthermore, the treatment of AMD can be categorised into two broad categories which are active and passive treatment [Fripp, 2000]. Active treatment involves an addition of a neutralizing agent to the AMD source or directly into the stream that has been affected. This is a successful treatment technique but takes time and needs continuous some intermittent maintenance [Fripp, 2000].

Passive treatment is comprised of a variety of techniques which aim at raising the pH and reducing the amount of metals through a constructed treatment or containment project. Although passive treatment is more costly than active treatment, it is more uniform and uses processes that are not operation intensive and also involves some intermittent maintenance [Fripp, 2000].

2.5.1. Active treatment technologies

Previous work was done using fly ash (FA) as an adsorbent for SO_4^{2-} ions in pre-treated AMD (i.e. after removal of heavy metals). The adsorption experiments were done using a thermostatic shaker at varying temperatures and different ratios of AMD: FA. The maximum sulphate removal percentage using 10% w/v was 80% with the Temkin isotherm being the best suited for the study [Ntuli et al, 2013].

A similar study was carried out with the aim of understanding the mechanism of the removal of SO_4^{2-} from mine waters with Hendrina fly ash [Madzivire, 2009]. This study involved the application of the ettringite precipitation method to remove SO_4^{2-} to below 500 ppm.

From the results obtained from this study it was concluded that SO_4^{2-} removal depends on; the amount of FA used, the final pH achieved and the composition of the mine water. A ratio of simulated circumneutral mine water to fly ash of 2:1 achieved 71 % SO_4^{2-} removal compared to 55 % achieved with a 5:1 ratio [Madzivire, 2009].

A study carried out by [Ji, 2008] was done to examine the possibility of application of In-Adit-Sulphate-Reducing System (IASRS) as an alternative method for the improvement of the operating systems. Laboratory experiments were done using two laboratory scale IASRS models over a period of 80 days. The two models were run at temperatures of 15^{o}C and 25^{o}C, respectively. Model 2 contained twice as much COD in the beginning of the operation than model 1. The results showed sulphate removal of 23% and 27% for model 1 and model 2 respectively. Although sulphate removal was higher than that of the current operating systems, it was still considered to be very low. However, the synthetic AMD used for these experiments had a low pH of 2.8 and had a high concentration of sulphates, due to this, it was suggested that modification of the standard design would increase sulphate removal.

Chockalingam and Subramanian (2006) performed tests to investigate the behaviour of sulphate concentration in acid mine drainage. The tests were carried out in the presence of supplemented rice husk medium. The results showed a continuous decrease in sulphate concentration from 5800 mgl^{-1} to 3500 mgl^{-1} over a period of 31 days. This resulted in 40% sulphate reduction from the AMD sample. The use of the supplemented rice husk medium with the addition of carbon and nitrogen sources was beneficial to the reaction and also portrays the variation in the sulphate concentration as a function of time during the growth of nigrificans in simulated acid mine water. More experiments were done to find out whether more sulphates can be removed from simulated AMD, when the initial sulphate concentration was reduced by a factor of 2. This experiment resulted in the sulphate concentration reducing from 2100 mgl^{-1} to about 700 mgl^{-1} over a period of 21 days, and further reduced to 570 mgl^{-1} in 35 days. After 35 days, the sulphate concentration increased to about 770 mgl^{-1} after 47 days and remained unchanged thereafter.

It is worth noting that after the 35 days period, sulphate concentration reduced and about 73% bio-reduction was achieved. A similar trend in the variation of sulphate concentration to the one obtained by using simulated mine water treated with rice husk was also observed by using modified Baars medium [Chockalingam and Subramanian, 2006].

The removal of sulphate by barium carbonate was established to be effective more than 30 years ago [Kun, 1972] by a process represented by the reaction:

$$BaCO_3\,(s) + SO_4^{2-}(aq) = BaSO_4\,(s) + CO_3^{2-}(aq) \qquad \text{eqn 2-5}$$

Kun (1972) identified several problems associated with using barium carbonate for the removal of sulphates, which amongst others include the high cost of barium carbonate which is caused by the use of high concentrations of soluble barium carbonate dosed than stoichiometrically required and also, this process required a long retention time. The problem of the high cost of barium carbonate was overcome by Volman (1984), who demonstrated that the production of barium sulphate could be reduced efficiently and economically with coal under thermic conditions to produce barium sulphide. This product can either be used directly for the process or converted to barium carbonate.

2.5.2. Passive treatment technologies

2.5.2.1. Anoxic Limestone Drains (ALD)

The structure of ALD is made by constructing drainage lines of coarse limestone aggregate along gently graded slopes [Kilborn, 1999]. The limestone drain is encased within a low permeability liner and capped with clay. During operation, the limestone within the structure should not be covered with clay or organic matter and negligible air should be allowed into the drain. In order to limit the amount of oxygen, synthetic liners are usually used as encasement for the aggregate filled channels. To avoid possibilities of oxidation, AMD is introduced directly into the covered drains as close to the source as possible. Within the drain lies dissolved iron which has to be in its reduced state that is ferrous iron; Fe^{2+}. To maintain this condition, the environment within the drain has to maintain low oxygen levels. High levels of oxygen in the AMD can aid in the formation of ferric iron (Fe^{3+}) through the oxidation of ferrous iron, which can precipitate as iron-oxide/hydroxide for example, $Fe(OH)_3$. Precipitation can also be enhanced by aerobic ponds / wetlands at the outflow end of ALD's. Limestone are capable of covering up surfaces and this can cause a precipitate which can cause premature system failure and reduce the rate at which limestone dissolves. As limestone has the ability to attach itself and form a layer on surfaces, this could be drawback on an operating ALD. This problem can be limited if the contact time between the AMD and limestone is not any less than 10 hours.

The aims of an ALD are to neutralise AMD to pH levels between 6 and 8, and to maximise the efficiency of adding bicarbonate alkalinity to the water [Kilborn, 1999].

2.5.2.2. Limestone Diversion Wells (LDW)

Limestone Diversion Wells (LDW) provides a treatment option for sites that offer a suitable topographic fall. LDW's are mode of a well, for example, an in-ground metal or concrete tank which is filled with crushed limestone gravel. Part of an AMD stream with a high flow rate, is diverted through a pipeline into the well [Milavec, 1999; Ziemkiewicz and Brant, 1996].

As mentioned in section 2.4 that limestone has the ability to form a layer on surfaces, this high velocity stream will provide hydraulic force which will cause gradual reduction and abrasion of the limestone gravel, ensuring that limestone does not stick to the surfaces of the well and a fine-grained limestone slurry overflows from the top of the well back into the main body of the AMD stream. In this way, partially treated water and excess particulate alkalinity is introduced back into the waterway.

For the LDW to work efficiently a change of about 10 metre elevation change should be done between the locations where AMD is diverted into the well. The elevation has to be 10 metres, otherwise there may be insufficient water velocity to turbulently mix and abrade the limestone particles. Insufficient water velocity might result in insufficient alkalinity production and metal precipitation which could block the well, thus preventing its operation. If abnormal flows are prolonged, the production of alkalinity in the LDW might be insufficient to suitably neutralise the AMD-affected stream. The use of LDW has been both successful and unsuccessful in the field [Waters et al., 2003].

2.5.2.3. Natural wetlands

These are complex ecosystems comprising water-saturated soil and sediments with supporting vegetation that have the capacity to naturally improve water quality via a range of physical, chemical, microbial and plant-mediated processes. The processes used to improve water quality within these ecosystems include reduction, complexation, oxidation, sedimentation, adsorption, precipitation, chelation, filtration, active plant uptake of metals and microbial conversion / immobilisation mechanisms [Kilborn, 1999; Milavec, 2002; Ziemkiewicz et al., 2002].

The following factors need to be taken into consideration when determining the type, size and cost of an appropriate wetland system:

1. The load of influent acidity, redox state and pH.
2. Water flow rates and retention times.
3. The area available for a wetland.

There are two broad types of constructed wetland; namely: aerobic and anaerobic.

2.5.2.3.1. Aerobic Wetlands

Aerobic wetlands are essentially shallow ponds that lower suspended solids and provide a substrate and increased water retention times (due to reduced flow rates) for the reaction between influent alkalinity and acidity.

The acidity within the wetland is caused by the oxidation and precipitation of metals generated from AMD. Aerobic wetlands contain vegetation planted in relatively impermeable sediments for example clay. The difference between aerobic wetlands and all other passive treatment techniques is that, these wetlands do not neutralise AMD.

The water entering the wetlands must be alkaline – this often comes from a pre-treatment passive system. The wetland should provide residence time and should allow metals like iron, chromium and manganese to precipitate as their solubility depends on the redox state of the water to precipitate. The precipitates are reserved on the surfaces of the wetland or downstream. Moreover, dissolved oxygen concentrations need to have reached saturation with respect to the atmosphere early within the residence time of the water in the wetland.

2.5.2.3.2. Anaerobic Wetlands

Anaerobic wetlands are water retention ponds comprising a substrate of organic matter and/or limestone aggregate. This type of wetland reduces the level of oxygen in AMD by allowing the water to pass through organo-rich material which strips the oxygen and results in anaerobic conditions. A limestone layer might form beneath the organic material or mixed among the organic matter. A way of generating alkalinity in the wetlands is through sulphate reducing bacterial (SRB) activity. These bacteria use organic matter such as a carbon source and sulphate as an electron acceptor for growth. In the bacterial conversion of sulphate to hydrogen sulphide, bicarbonate alkalinity is produced by the following reaction:

$$2H_2O_{(l)} + SO_4^{2-}{}_{(aq)} + C_{(organicmatter)} \rightarrow H_2S_{(g)} + 2HCO_3^{-}{}_{(aq)} \qquad \text{eqn 2-6}$$

2.6. Adsorption

Adsorption is a process that occurs when a gas or liquid solute accumulates on the surface of a solid or a liquid (adsorbent), forming a molecular or atomic film (the adsorbate). Adsorption equilibria can be analyzed on the basis of step-wise and overall equilibrium constants expressions. For this purpose, the adsorption of an adsorbate "A" from liquid (or gaseous) phase onto solid adsorbent "M" can generally be expressed as:

$$M + sA \rightarrow Mas \qquad \text{eqn 2-7}$$

where "s" is the stoichiometric number of moles of adsorbate adsorbed on one mole of adsorption sites present on adsorbent.

Adsorption processes are usually carried out to remove organic or inorganic compounds from waste water [Nevskaia, 2004]. Due to its excellent adsorption ability, activated carbon is one of the most commonly used adsorbent for such experiments, but it is not economically viable because of its high initial cost and the difficult and expensive regeneration process [Ahmarruzaman, 2008]. This has led researchers to use clay as it is more economic, efficient and recyclable [Barhoumi, 2003].

Sulphate removal experiments done by Bosman et al. (2006) reduced sulphate content in a sample of AMD to 200 mgl^{-1} using barium sulphide, which resulted in a 90% sulphate removal. Silva et al. (2010) removed sulphates from an aqueous solution with co-precipitation of aluminium bearing salts. The conclusion that was drawn from the study showed that sulphate ions (sodium salts) were co-precipitated and were removed from water with aluminum-bearing colloids, formed from the hydrolysis of either $AlCl_3$ or polyaluminum chloride (PAC) and reacted under different conditions of solution pH, time and reagent/ sulphate ratios. Best results were obtained with $AlCl_3$ at a pH of 4.5 where more than 80% sulphate ions were removed [Silva et al., 2010].

2.7. Cation Exchange Capacity (CEC)

Ions that are positively charged such as magnesium (Mg^{2+}), iron (Fe^{2+}), sodium (Na^{+}), hydrogen (H^{+}), zinc (Zn^{2+}), aluminum (Al^{3+}), calcium (Ca^{2+}), manganese (Mn^{2+}), copper (Cu^{2+}) and potassium (K^{+}) are referred to as cations. Cation exchange capacity is the ability of soil to attach itself to cations. Cations are attracted to the surface of the negatively charged clay and organic matter particles in the soil through electrostatic forces. Thus, the CEC of a soil represents the total amount of exchangeable cations that the soil can adsorb.

Ethylenediamine complex of Cu^{2+} is a method that was used on different clays for the rapid determination of CEC values for clay [Bergaya, 1997]. Ethylenediamine (EDA) complexes of various metals could also be used to determine the CEC of clays [Bergaya, 1997]. This method of determining the CEC of clay was chosen because it is a fast single-step procedure and does not require sophisticated apparatus.

2.8. Clay

Clays have a wide range of applications, in various areas of science, because clay is naturally available and the propensity which allows it to be physically and chemically modified to suit practical technological needs [Rajkiran, 2008]. Clays are profitably effective to immobilise toxic environmental contaminants due to their environmental stability, inexpensive availability, and high adsorptive and ion exchange properties. Additionally, clay materials can potentially be modified using a variety of physical/chemical treatment to achieve the desired surface properties for best immobilisation performance of specific compounds [Sarkar, 2011]. Clay is an affordable natural raw material that has been widely used for many years [Sapkota, 2011]. Most of the clay minerals belong to the category of layered silicates or phyllosilicates due to the arrangement of silicate layers that are 1 nm thick and 200-300 nm wide in the lateral dimension [Lopez, 2003]. The layered silicate structure of clay is generated by 2-D arrays of silicon-oxygen tetrahedral and aluminium or magnesium-oxygen/hydroxyl octahedral units [Thomas, 2010].

Clays are classified on the basis of their crystal structure and charge per basic cell [Sapkota, 2011]. The stacking arrangement of tetrahedral (T_h) and octahedral (O_h) sheets on top of each other can form two basic types of clay structure: T_hO_h or $T_hO_hT_h$ [Sapkota, 2011]. The alternating arrangement of T_h and O_h sheets form a 1:1 structure as shown in Fig. 2-1.

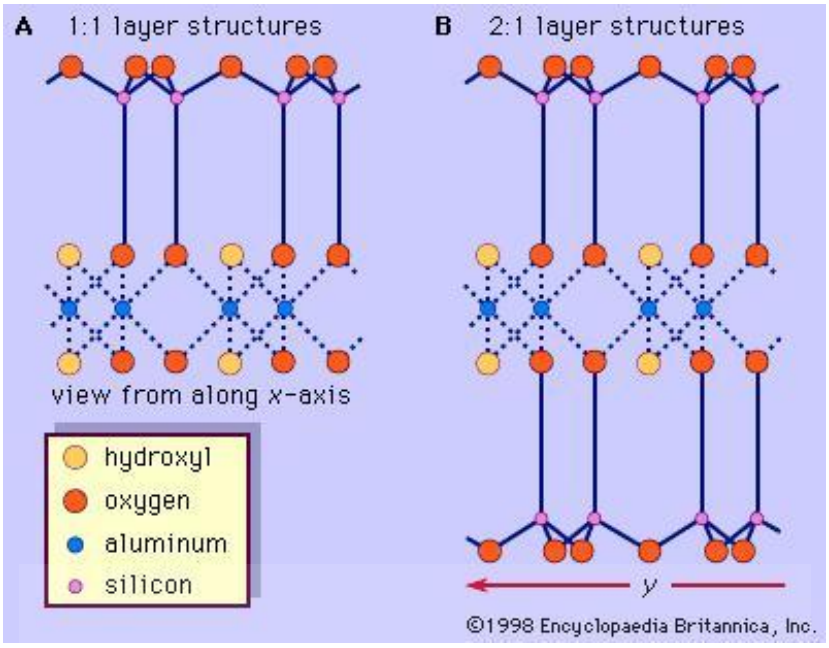

Figure 2-1: Schematic presentation of (A) 1:1 layer structures and (B) 2:1 layer structures

A 1:1 layered structure (e.g. kaolinite) is formed when only a tetrahedral sheet is linked to an octahedral sheet, whereby the oxygen atoms are shared. Hydrogen bonds between –OH of one layer and a bridging - O- of the next layer are the main bonding forces in this kind of structure [Sapkota, 2011]. The arrangement with repeating units of silica tetrahedral layers combined with one octahedron layer of alumina results in a 2:1 structure.

2.8.1. Attapulgite

Attapulgite is a type of clay consisting of double silica tetrahedral chains which are connected together by octahedral oxygen and hydroxyl groups. These groups contain ions such as Al and Mg in an inverted chain-like structure. The three-dimensional crystal structure of the clay mineral gives clay properties such as non-swelling and the needle-like mophorlogy [Ahmaruzzaman, 2008]. The unique colloidal properties of the clay are derived from the shape and size of the needles. These also aid in resistance to high concentrations of electrolytes and give high surface area and high porosity particles when activated by heat. The mineral has a moderate CEC, which ranges between 10 and 50 meq/l00 g of clay [Bish, 1993].

Attapulgite has been compared with a rather narrow range of montmorillonites, which include Southern Bentonite of which other montmorillonites have widely different properties, e.g., of swelling and inactivability with acids.

The colloidal, adsorptive and catalytic properties of attapulgite have made it widely used by many industries. Attapulgite has been used for oil well drilling wells purposes, because of its ability to build a suitable viscosity at a relatively low solid level and to maintain the desired viscosity throughout the drilling of the well [Bish, 1993].

Attapulgite is also used in the production of corrugated board and adhesives. The viscosity of the starch adhesives used, tend to be lost under shear, making it difficult to apply a constant amount of adhesive during a production run, but because of the viscous properties of attapulgite, the incorporation of attapulgite has been an effective method of counteracting the loss of viscosity of the starch. Above all, attapulgite has been widely used in liquid suspension fertilizers, emulsion paints and non-colloidal applications such as percolation adsorptive processes, floor adsorbents, carrier for agricultural chemicals, etc. Organically modified attapulgite can also be used as an adsorbent for water soluble dyes [Huang et al., 2007].

2.8.2. Bentonite

Bentonite is a rock term used to label a naturally occurring, very fine grained material largely composed of the clay mineral, montmorillonite and the lattice is negative in charge [Arthur et al., 1961]. Bentonite is a clay raw material with high CEC because of its typical layered silicate structure with CEC ranges between 70 to 110 meq/100 g of clay [Vega et al., 1995 and Arthur et al., 1961].

Bentonites are rocks whose predominant component is a smectite mineral originating from the alteration of glassy materials of igneous origin [Bergaya et al., 2006; Grim and Güven, 1978; Murray, 2007]. Alkylammonium ions can be used to render smectites organophilic through the exchange of exchangeable cations. The variety of applications of smectites is due to their properties such as thixotropy, CEC, bonding capacity, tendency to react with organic compounds, hydration, impermeability, swelling, crystal shape and size and plasticity [Odom, 1984].

Their wide versatility, natural abundance, low cost, wide range of industrial uses, and their propensity to be chemically and physically modified, are the reasons bentonites are used in numerous areas, meeting a wide range of technological needs [Abdou et al., 2013; Menezes et al., 2010; Tiwari et al., 2008].

Bentonites have high specific surface areas, in theory ranging from 700 to 850 m^2/g [Bergaya et al., 2006], and from 20 to 130 m^2/g by the N_2-BET method [Kaufhold et al., 2010]. Thus, bentonites can react with various organic compounds, such as ionic, amphoteric and nonionic surfactants, through a series of specific mechanisms [Bergaya et al., 2006; Ultracki, 2004], forming a special group of materials called organophilic clays. These are clays in which organic molecules have been incorporated, thereby changing their surface properties from hydrophilic to hydrophobic or organophilic [Bergaya et al., 2006; Groisman et al., 2004].

Bentonite clay can treat oil, sulphate, phosphate, and metals and is extremely effective at removing certain cationic components from wastewater [Abdelaal, 2004]. Bentonite has been used for a similar purpose as attapulgite for oil drilling wells purposes, but it can only be used with the help of expensive chemical treatments in areas where contaminants such as magnesium sulphate or calcium sulphate and salt are encountered [Ahmaruzzaman, 2008]. Bentonite becomes ineffective in yielding or maintaining viscosity in the presence of these contaminants, because they prevent bentonite from swelling.

The Yellow Star Quarries in the Kroonstad district was the largest bentonite deposit ever to be found in South Africa. It was estimated that this deposit contained approximately 750 000 m^3 bentonite and could be mined at 4 000 m^3/month [Waanders, 2003]. The mine was commissioned in 2007 and has an expected lifetime of over 10 years during which the clay will be mined and the project will be economically feasible [Waanders, 2003].

Previous work done by Sarkar et al., (2011) showed that bentonite and montmorillonite modified with cetylpyridinium and hexadecyl trimethylammonium (HDTMA) has the ability to effectively adsorb orange II from aqueous solutions. Bentonite has been widely studied to prepare organoclays for decolourising dye waste water [Sarkar, 2011].

2.8.3. Organically modified clay

Organically modified clay is the result of an organic modification of clay which is formed by exchanging the original interlayer cations for organo-cations [Sapkota, 2011]. The organic cations lower the surface energy and improve the wetting and intercalation by the polymer matrix, resulting in a larger interlayer spacing [Sapkota, 2011]. Organic cations may provide functional groups that can react with monomers or polymers to enhance interfacial adhesion between the clay nanomers and polymer matrix.

Generally, the organo-cations used for this purpose are quaternary alkylamonium ions. Organoclays are usually divided into two groups depending on the organic cation and sorption mechanism. The first group is the adsorptive organoclays which consist of short chain quaternary ammonium ion ($R \leq 12$), such as TMA (tetramethylammonium) and TBA (tetrabenzylammonium).

The second type of organoclays is organophilic clays which consist of a long chain quaternary ammonium ion ($R \geq 12$) such as HDTMA (hexadecyltrimethylammonium) and ODTMA (octadecyltrimethylammonium) [Groisman, 2004]. Organoclays have been used as sorbents in many industrial and environmental applications [Lee and Tiwari, 2012; Megharaj et al., 2012]. Studies have shown that modification of the clay mineral with organic cation greatly enhances the properties of the clay mineral to be used for the removal of organic/inorganic contaminants from water and wastewater.

Modification allows the formation of an organophilic surface in the clay structure [Sapkota, 2011]. During the modification of the clays, excess surfactant cations attach to the clay mineral surface giving a positive surface charge to the resultant organically modified clay mineral [Sarkar, 2011]. Organic surfactants which have previously been used to modify clay include primary, secondary, tertiary and quaternary alkylammonium cations which are water soluble [Sapkota, 2011]. To obtain organically modified clay, most cation exchange reactions are performed in aqueous suspension. Alkylammonium cations in organo-silicates improve the wetting ability between the organically modified clay and the polymetric matrix by reducing the surface energy of the clay. This will result in a larger intergallery spacing which is dependent on the size of the organic cations for example, alkylammonium cations which are used for modification [Sapkota, 2011]. The cation exchange reaction is directly affected by the length of the alkyl chain the number of alkyl tails on the surfactant molecules [Tjong, 2006]. Previous work done on the adsorption of dye using organically modified clays showed that organically modified clays can adsorb anionic dyes not only by hydrophobic binding, but also by electrostatic attraction [Khenifi, 2007].

2.8.4. Modifiers

Surfactants are widely used and find a very large number of applications because of their remarkable ability to influence the properties of surfaces and interfaces [Laurier, 2000]. For this research, surfactants were used to modify the types of clay used so that the clay could be able to adsorb sulphates from AMD.

The types of modifiers used were Hexadecyltrimethylamonium bromide (HDTMA), tetradecyltrimethylamonium bromide (TDTMA) and $BaCl_2$.

2.8.4.1. HDTMA bromide

Hexadecyltrimethylammonium (HDTMA) bentonite based organoclays were used for the removal of textile dyes, benzene, tannins, phenols, nitrate, dibenzofuran, hexavalent chromium, acid orange 10 and Pb(II) ions, nitrobenzoic acid, arsenic, BTEX, and phenol [Muhammad et al., 2013] and has never been used for sulphate treatment.

Previous work on the preparation and use of clinoptilolite modified with HDTMA was done to remove phenol and study the effect of positively charged ions on the phenol sorption performance. The study showed that HDTMA modification of clinoptilolite enhanced phenol removal in comparison with natural clinoptilolite. This was due to the enhanced hydrophobic surface properties of HDTMA-modified clinoptilolite [Wanga, 2011].

HDTMA was again used to modify the surface of a lignocellulosic polymer, coconut coir pith. The coconut coir pith was used as an adsorbend for the removal of sulphates from aqueous solutions [Namasivayam and Sureshkumar, 2007]. Removal of sulphate ions from aqueous solution by HDTMA modified coir pith was found to be effective with up to 70% sulphate removal [Namasivayam and Sureshkumar, 2007]. Work done by Li et al. (2003) showed that HDTMA-modified palygorskite and sepiolite can effectively be used to remove anionic contaminants such as nitrate and chromate from waste water. A suggestion was then made that the surfactant molecules formed admicelles on the surface of palygorskite and enhanced anion adsorption [Li et al., 2003]. Table 2-1 shows the physical properties of HDTMA as presented on the material safety and data sheet (MSDS).

Table 2-1: Physical properties of HDTMA

Physical state	Solid
Appearance	Crystalline solid. Crystalline powder.
Molecular mass	364.45 g/mol
Colour	White.
Odour	Almost odourless.

2.4.8.2. TDTMA bromide

It has been shown that bentonite modified by tetradecytrimethylammonium (TDTMA) provides a considerable ion uptake capacity [Saljoghi, 2012]. The main advantage of this procedure is firstly that natural bentonite is very cheap and abundant and secondly this adsorbent can remove toxic compounds such as NO_3^-, NO_2^-, PO_4^{3-} and SO_4^{2-} from aquaculture systems [Saljoghi, 2012]. Table 2-2 shows the physical properties of TDTMA as presented on the MSDS.

Table 2-2: Physical properties of TDTMA

Physical state	White Powder
Molecular formula	$C_{17}H_{38}BrN$
Molecular weight	336.41 g/mol
Density	775.0 g/m^3

2.4.8.3. $BaCl_2$

Barium chloride is a toxic compound used in waste water treatment and many manufacturing processes. Barium hydroxide and barium chloride is effective when used to remove soluble sulphate from industrial and municipal wastewater. Sulphates present in waste water can be removed by the addition of barium chloride. When barium chloride contacts the sulphates in the waste water, it forms barium sulphate. The use of barium chloride is rather expensive and toxic to use and in some instances has been substituted by cheaper materials, like iron and aluminium salts [Sven, 1979]. Table 2-3 shows the physical properties of $BaCl_2$ as presented on the MSDS.

Table 2-3: Physical properties of $BaCl_2$

Physical state	White Powder
Molecular formula	$BaCl_2.\ 2H_2O$
Molecular weight	244.26 g/mol
Odour	Almost odourless

2.8.5. Adsorption Isotherms

Information on the capacity of an adsorbent can be provided through an equilibrium study on adsorption. Characterization of an adsorption isotherm is done by certain constant values. These constant values express the affinity of the adsorbent, the adsorbent surface properties and can also be used to compare the adsorptive capacities of the adsorbent for different pollutants.

Commonly known adsorption systems can be used to analyse the equilibria data and experimental data of adsorption isotherms can be described using several mathematical models. The Freundlich, Langmuir and Temkin models are commonly employed to analyse adsorption.

2.8.5.1. Langmuir isotherm

This adsorption isotherm is meant for an ideal adsorption process. The Langmuir isortherm takes into consideration that the active centres across the adsorbent surface are homogenously spread. In this regard, the active centres of the adsorbent have the same exact energy level and monolayer adsorption and the adsorption on an active centre has no influence on the adsorption on other active centres [Langmuir, 1916].

The Langmuir isotherm can be represented as:

$$q_e = \frac{q_m.b.C_2}{1+b.C_2} \qquad \text{eqn 2-8}$$

$$C_e/q_e = 1/q_m b + C_e/q_m \qquad \text{eqn 2-9}$$

where q_e is the amount adsorbed at equilibrium (mol·kg^{-1}), C_e is the equilibrium concentration (mol·ℓ$^{-1}$), b is a constant related to the energy or net enthalpy of adsorption (ℓ·mol^{-1}) and q_m is the maximum adsorption capacity (mol·kg^{-1}). A plot of $\frac{C_e}{q_e}$ vs. C_e should be linear if the isotherm fits the experimental data.

2.8.5.2. Freundlich isotherm

The Freundlich isotherm model describes the adsorption process and adsorption characteristics for a homogenous surface [Adamson and Gast, 1997]. The isotherm assumes there is an infinite supply of unreacted sorption sites. It is not only applicable to homogenous surfaces, but also on heterogeneous surfaces which interact amongst adsorbed molecules. The isotherm model suggest that the relationship between sorption energy and completion of the sorption centres of the adsorbent decreases exponentially, this implies that the Freundlich isotherm can be used to describe heterogeneous systems [Zeldowitsch, 1934]. The following equation best represents the isotherm model:

$$q_e = K_F C_e^{1/n_F} \qquad \text{eqn 2-10}$$

where K_F is the Freundlich constant (l g^{-1}) related to the bonding energy and can be defined as the adsorption or distribution coefficient. It represents the quantity of metals adsorbed onto adsorbent for unit equilibrium concentration. $1/n_F$ is the heterogeneity factor and it is a measure of the deviation from linearity of adsorption. The n_F value indicates the degree of non-linearity between solution concentration and adsorption as follows:

If the value of $n_F = 1$, the adsorption is linear; $n_F < 1$, the adsorption process is chemical and if $n_F > 1$, the adsorption is a favourable physical process.

The linearised form of the Freundlich sorption isotherm is:

$$\log q_e = \log K_F + {}^{1}\!/\!_{n} \log C_e \qquad \text{eqn 2-11}$$

A plot of $logq_e$ vs. $logC_e$ should give a linear equation if the isotherm fits the experimental data.

$$y = A + B.x;\ y = \log(q_e)\ ;\ x = \log(C_e)\ ;\ A = \log(K_F)\ ;\ B = \frac{1}{n}$$

The constants K_F and n were obtained from the slope and intercept of the plot of $log(q_e)$ versus $log(Ce)$.

2.8.5.3. Temkin isotherm

This adsorption isotherm takes into consideration interactions between the adsorbent and adsorbate. It ignores the values of concentration and accounts for heat of adsorption of the molecules, implying that it is a function of temperature.

This isotherm assumes that heat of adsorption decreases linearly rather than logarithmic with coverage [Aharoni and Ungarish, 1977].

The derivation of the Temkin isotherm is characterized by even distribution of binding energies. The constants can be determined from the slope and intercept a plot of q_e (quantity sorbed) against lnC_e. The following equations best describes the model:

$$q_e = {}^{RT}\!/\!_{b} \ln\left(A_T C_e\right) \qquad \text{eqn 2-12}$$

$$q_e = {}^{RT}\!/\!_{b_T} \ln A_T + {}^{RT}\!/\!_{b} \ln C_e \qquad \text{eqn 2-13}$$

$$B = {}^{RT}\!/\!_{b_T} \qquad \text{eqn 2-14}$$

$$q_e = B \ln A_T + B \ln C_e \qquad \text{eqn 2-15}$$

where A_T is the Temkin isotherm equilibrium binding constant (L/g), b_T is the Temkin isotherm constant, T is the temperature at 298 K, R is the universal gas constant (8.314 J/mol/K) and B is the constant related to heat of sorption (J/mol).

2.8.5.4. Dubinin–Radushkevich isotherm model

Dubinin–Radushkevich isotherm is generally applied to express the adsorption mechanism [Gubay et al., 2007] with a Gaussian energy distribution onto a heterogeneous surface [Dabrowski, 2001]. The model has often successfully fitted high solute activities and the intermediate range of concentrations data well.

$$q_e = (q_s)\exp\left(-K_{ad}\in^2\right) \quad \text{eqn 2-16}$$

$$\ln q_e = \ln q_s - K_{ad}\in^2 \quad \text{eqn 2-17}$$

where q_e is the amount of adsorbate in the adsorbent at equilibrium (mg/g), q_s is the theoretical isotherm saturation capacity (mg/g), K_{ad} is the Dubinin–Radushkevich (DRK) isotherm constant (mol^2/kJ^2) and $\in$ is the Dubinin–Radushkevich isotherm constant.

The Dubinin method can be used to distinguish between the chemical and physical adsorption of metal ions. Molecules are removed from their locations in the sorption space to the infinity using free energy (E) per molecule of adsorbate. This can be represented by the following relationship [EL-Kamash et al., 2005]:

$$E = \left[\frac{1}{\sqrt{2B_{DR}}}\right] \quad \text{eqn 2-18}$$

where B_{DR} is denoted as the isotherm constant. Meanwhile, the parameter can be calculated as:

$$\varepsilon = RTln\left[1+\frac{1}{C_e}\right] \quad \text{eqn 2-19}$$

where R represents the gas constant (8.314 J/mol K), T is the absolute temperature (K) and C_e is the adsorbate equilibrium concentration (mg/L). The Dubinin-Radushkevich isotherm model is temperature dependent and thus, when adsorption data at different temperatures are plotted as a function of logarithm of amount adsorbed (lnq_e) vs the square of potential energy, all suitable data will lie on the same curve, named as the characteristic curve [Dada,

2012]. The eqn 2-17 is linearized to eqn 2-18 which is used in the plot of DRK. The constant such as q_s, and K_{ad} are determined from the appropriate plot using eqn 2-19 above.

The Dubinin–Radushkevich equation cannot be used on adsorption isotherms of many microporous carbonaceous materials, as the fittings are unsatisfactory, which affects the accuracy of the results.

Attention is paid on the impact of temperature on the obtained values of the structural parameter and the volume of micropores caused by the presence of submicropores.

2.8.5.5. Flory–Huggins isotherm model

This isotherm model derives the degree of surface coverage characteristics of adsorbate onto adsorbent [Horsfallm and Spiff, 2005], and can express the feasibility and spontaneous nature of an adsorption process. The isotherm equation is given by:

$$\log \theta / C_o = \log K_{FH} + \lambda \log(1-\theta) \qquad \text{eqn 2-20}$$

where $\theta = \left(1 - C_e / C_o\right)$ is the degree of surface coverage and K_{FH} is the equilibrium constant.

The equilibrium constant, $K_{FH,}$ that is used for the calculation of spontaneity free Gibbs energy (ΔG^0) [Vijayaraghavan et al, 2006].

2.8.5.6. Hill isotherm model

The Hill equation [Hill, 1910], originates from the non-ideal competitive adsorption (NICA) model [Koopal et al, 1994]. The model was used to describe the binding of different species onto homogeneous substrates. The model assumes that the ligand binding ability on one site of a macromolecule has the ability to influence other binding sites on the same macromolecule, implying that adsorption is a cooperative phenomenon [Ringot et al, 2007]. The isotherm model can be represented by the following linear equation:

$$\log q_e / q_H - q_e = n_H \log(C_e) - \ln(a_R) \qquad \text{eqn 2-21}$$

where q_e is the amount adsorbed at equilibrium ($mol \cdot kg^{-1}$), C_e is the equilibrium concentration ($mol \cdot \ell^{-1}$) and a_R is the isotherm constant.

2.8.5.7. Koble–Corrigan isotherm model

Koble–Corrigan isotherm [Koble, 1952] is a three-parameter equation, which represents equilibrium data by incorporating both Langmuir and Freundlich isotherm models represented by the following equation:

$$1/q_e = 1/AC_e^n + B/A \qquad \text{eqn 2-22}$$

where *A*, *B* and *n* are the isotherm constants which are evaluated from the linear plot using a trial and error optimization from the equation.

2.8.5.8. Khan isotherm model

Khan isotherm [Khan et al, 1997] is a generalized model suggested for the pure solutions. As given in the following equation:

$$Q_e = (Q_m b_K C_e)/(1 + b_K C_e)^{a_K} \qquad \text{eqn 2-23}$$

where b_K represents the model constant while a_K represents the model exponent. The model's maximum uptake values can be well determined at relatively high correlation coefficients and minimum chi-square values [Khan et al, 1996].

2.5.8.9. Radke–Prausnitz isotherm model

The correlation of Radke–Prausnitz isotherm is usually predicted well by the high root mean square error (RMSE) and chi-square values represented in the following equation:

$$q_e = a_{RP} r_R C^{\beta} R / a_{RP} + r_R C_e^{\beta} R^{-1} \qquad \text{eqn 2-24}$$

β represents the models exponent, a_{RP} and r_R are the model constants as represented in the following equation [Vijayaraghavan et al, 2006].

2.5.8.10. Sips isotherm model

Sips isotherm [Sips, 1948] is used for predicting heterogeneous adsorption systems while avoiding the limitation of the rising adsorbate concentration [Dubinin and Radushkevich, 1947]. This model is a combination of Langmuir and Freundlich expressions and reduces to the Freundlich isotherm at low adsorbate concentrations, while at high concentrations it predicts a monolayer adsorption capacity characteristic of the Langmuir isotherm. Operating conditions such as temperature, pH and concentration govern the equation parameters [Pérez-Marín et al, 2007]. The isotherm model is given by the following equation:

$$q_e = (q_m . b . C_e^{1/n})/(1 + b . C_e^{1/n}) \qquad \text{eqn 2-25}$$

where q_e is the amount adsorbed at equilibrium (mol·kg^{-1}), C_e is the equilibrium concentration (mol·ℓ$^{-1}$), b is a constant related to the energy or net enthalpy of adsorption (ℓ·mol^{-1}) and q_m is the maximum adsorption capacity (mol·kg^{-1}).

2.5.8.11. Toth isotherm model

Toth isotherm model [Toth, 1971], is another empirical equation developed to improve the experimental data of Langmuir isotherm fittings. This model is suitable for describing heterogeneous adsorption systems and also satisfying both high and low-end boundaries of the concentration [Vijayaraghavan et al, 2006].

An asymmetrical quasi-Gaussian energy is distributed from its correlation with most of its sites having adsorption energies lower than the peak or mean value [Ho et al, 2002]. The isotherm model is given by the following equation:

$$q_e = q_m C_e / \sqrt[n]{\left(K_T + C_e^{\,2}\right)} \qquad \text{eqn 2-26}$$

where q_e is the amount adsorbed at equilibrium (mol·kg^{-1}), C_e is the equilibrium concentration (mol·ℓ$^{-1}$), and q_m is the maximum adsorption capacity (mol·kg^{-1}).

2.8.6. Adsorption Kinetics

The study of adsorption kinetics in water treatment is significant as it provides valuable insights into the reaction pathways and into the mechanism of sorption reactions. In addition, the kinetics describes the solute uptake rate that in turn controls the residence time of sorbate uptake at the solid–solution interface [Gürses et al., 2006]. Adsorption kinetics also gives information on the type of removal mechanism used during the adsorption process. Therefore, it is important to be able to predict the rate at which pollutant is removed from aqueous solutions in order to design appropriate sorption treatment plants. The aim of the present work is to investigate both the adsorption mechanism and adsorption kinetics of sulphates onto clay.

2.8.6.1. Intra-particle diffusion Weber-Morris model

The Morris-Weber equation can be used to formulate the intra-particle diffusion model. A plot of the amount adsorbed (q_t) and the square root of the time should be linear to fit the model and can be represented as:

$$\mathbf{q_t = K_p . t^{0.5} + I_d} \qquad \text{eqn 2-27}$$

$$y = A + B.x; y = q_t; x = t^{0.5}; A = I_d; B = K_p$$

where K_p is the initial rate of the intra-particle diffusion (mol-kg^{-1}.min$^{-0.5}$) and I_d is the constant with the same units as q_t.

The intercept of a plot of q_t versus $t^{0.5,}$ can be used to determine the two parameters. I_d, which can be obtained from the intercept of the plot, is used to study the relative significance of the two transport mechanisms of the solute which are external mass transfer and intra-particle diffusion. I_d values equal to 0 imply that the intra-particle diffusion is considered as the rate limiting step. I_d values greater than 0 imply that the rate limiting steps are both the intra-particle diffusion and external mass transfer. Ions of the layer of the liquid surrounding the particle become highly resistant with an increase in I_d values.

The diffusion coefficient of ions inside the adsorbent material can be determined by the Weber-Morris model [Apiratikul and Pavasant, 2008]. By considering k_p a constant it is possible to calculate the diffusion coefficient expressed as:

$$\mathbf{D_e = \pi \left(\frac{D_p . k_p}{12 . q_e}\right)^2} \qquad \textbf{eqn 2-28}$$

where *De* is the effective diffusion coefficient ($m^2 \cdot min^{-1}$) and d_p is the mean diameter of particles (m^{-1}).

2.8.6.2. Pseudo-first order kinetic model

Pseudo-first order kinetic model is one of the most widely used models for the adsorption of a solute from aqueous solution. The pseudo-first-order kinetic model is represented by:

$$\frac{dq_t}{dt} = K_1(q_e - q_t) \qquad \textbf{eqn 2-29}$$

where q_t ($mol \cdot kg^{-1}$) is the amount of metal ions adsorbed on the adsorbent at time *t* (min), q_e ($mol \cdot kg^{-1}$) is the amount adsorbed at equilibrium and k_1 (min^{-1}) is the rate constant of first-order adsorption [Ho and McKay, 1998].

After integration between boundary conditions (t = 0 to t and q_t = 0 to q_e), the equation becomes:

$$\log(q_e - q_t) = \log(q_e) - \frac{K_1 . t}{2.303} \qquad \textbf{eqn 2-30}$$

where q_e and k_1 can be determined from the intercept and slope of the plot, respectively. A plot of q_e vs. *t* should give a linear equation if the model fits the experimental data [Ho and McKay, 1998].

$$y = A + B.x;\ y = \log(q_e - q_t)\ ;\ x = t;\ A = \log(q_e)\ ;\ B = \frac{K_1}{2.303}$$

2.8.6.3. Pseudo second order kinetic model

The pseudo-second-order kinetic model is also one of the most widely used kinetic models and is based on the sorption capacity of the solid phase and is expressed as:

$$\frac{dq_t}{dt} = K_2(q_e - q_t)^2 \qquad \text{eqn 2-31}$$

where K_2 (kg·mol^{-1}·min^{-1}) is the rate constant of second-order model [Ho and McKay, 1998].

For boundary conditions (t = 0 to t and q_t = 0 to q_e), this equation becomes:

$$\frac{t}{q_t} = \frac{1}{K_2.q_e^2} + \frac{1}{q_e}.t \qquad \text{eqn 2-32}$$

$$y = A + B.x;\ y = \frac{t}{q_t};\ x = t;\ A = \frac{1}{(K_2.q_e)\text{^}2};\ B = \frac{1}{q_e}$$

$$q_t = \frac{q_e^2 K_2.t}{1 + q_e.K_2.t} \qquad \text{eqn 2-33}$$

The plot of t/q_t versus t should give a straight line if the pseudo second-order kinetic model is applicable, and q_e and k_2 can be determined from the slope and intercept of the plot, respectively.

2.8.6.4. Elovich kinetic model

Elovich kinetic model is closely related to second order model and has been successful in describing the second order kinetic model, assuming that the solid surfaces of the actual solid are energetically heterogeneous. The semi-empiral equation of this model does not propose any definite mechanism for adsorbate-adsorbent relationship, but can describe the chemisorption process. The linear form of this equation [Demibras et al., 2008; Ho and McKay, 1998] is given by:

$$\boldsymbol{q_t = \frac{1}{\beta}\ln(\alpha\beta) + \frac{1}{\beta}\ln(t)} \qquad \text{eqn 2-34}$$

where, α is the initial adsorption rate (mg/g·min), and the parameter β is related to the extent of surface coverage and activation energy for chemisorption (g/mg).

2.8.7. Sorption activation energy (Ea)

It is known that the temperature dependence of the rate of most chemical reactions can be fit successfully with Arrhenius equation. The activation energy (Ea) of the sorption of sulphate anion is evaluated by using the linearized Arrhenius equation in the following form [Cao et al., 2014]:

$$lnK = lnA.\frac{Ea}{RT}$$ eqn 2-35

Where *Ea* is the sorption activation energy (KJ/mol); k is the sorption rate constant; A is the Arrhenius constant; R (8.314 J/ (K mol)) and T (K) were the ideal gas constant and Kelvin temperature, respectively. Chemical bond force involves chemical sorption and is a much stronger force than that involved in physical sorption. The rate for activated chemical sorption varies with temperature according to finite activation energy from 8.4 to 83.7 kJ/mol [Li et al., 2009]. The energy requirement for physical sorption usually is no more than 4.2 KJ/mol since the forces involved in physical sorption are weak [Aksu, 2002 and Aksu & Karabayır, 2008].

2.8.8. Adsorption Thermodynamics

Thermodynamic considerations of an adsorption process are necessary to conclude whether the process is spontaneous or not. The Gibbs free energy change, G^o, is an indication of spontaneity of a chemical reaction and therefore is an important criterion for spontaneity. Both energy and entropy factors must be considered in order to determine the Gibbs free energy of the process [Hong et al., 2009]. Reactions occur spontaneously at a given temperature if G^o is a negative quantity. Gibbs free energy can be calculated using the following equation:

$$\Delta \boldsymbol{G^0 = -RTlnK_{Do}}$$ eqn 2-36

Where ΔG° is the standard free energy change (J/mol), R is the universal gas constant, 8.314 J/mol.*K* and *T* is absolute temperature (K). K_{D0} can be obtained from the slope of the *ln* (q_e/c_e) *vs* q_e plot. Enthalpy and entropy can be calculated using the following Van't Hoff equation:

$$lnK_{D0} = {}^{\Delta S^0}/_{R} - {}^{\Delta H^O}/_{RT}$$ eqn 2-37

where entropy (ΔS^0) and enthalpy (ΔH^O) are obtained from the intercept and slope respectively of *ln* K_{D0} *vs 1/T*. A positive value of entropy indicates affinity of the adsorbent for the adsorbate, whilst a positive value of enthalpy indicates that the adsorption reaction is endothermic [Gupta, 1998].

2.8.9. Characterisation of clay and AMD

2.8.9.1. X ray fluorescence (XRF)

X-ray fluorescence (XRF) is an analytical technique used for qualitative and quantitative elemental analysis of materials. It gives a measure of film thickness, composition of the material, determines the elemental concentration of solids and solutions by weight and identifies the specific and trace elements in complex sample matrices. Elements in the sample are subjected to high intensity X-rays. Fluorescent X-rays are then emitted from the sample at unique energy levels with regard to the elements.

A complete XRF analytical system is made up of an X-ray source, a sample and a detection system. The source will irradiate the sample and the detector will measure the emitted fluorescence radiation from the sample. An X-ray tube is usually used as the source in most XRF systems.

2.8.9.2. X-ray diffraction (XRD)

X-ray diffraction is a technique used to identify the molecular and atomic structure of a crystal. A beam of incident X-rays, caused by the crystalline atoms, diffracts into many specific directions. The dual wave/particle nature of X-rays is used in XRD to give information about the structure crystalline materials. The intensities and angles of these diffracted beams are measured to enable the crystallographer to produce a three-dimensional picture of the density of electrons within the crystal. The mean positions of the atoms in the atoms in the crystal can be determined, as well as their entropy, chemical bonds and other information.

Based on the compounds diffraction pattern, XRD can be used to identify and characterize compounds. When the monochromatic X-ray beam is focused on a material, the X-rays are scattered from the atoms of the material. When a crystalline material is subjected to the X-rays, the X-rays then undergo constructive and destructive interface, this process is called diffraction. Bragg's Law below can be used to describe the diffraction of X-rays by crystals.

$$n\lambda = 2d \sin\boldsymbol{\theta} \qquad \textbf{eqn 2-38}$$

The size and shape of the unit cell of the material used in the XRD determines the directions of possible diffractions, whilst the kind and arrangement of atoms in the crystal structure determines the intensities of the diffracted waves. Although not all materials are not single crystals; they are composed of polycrystalline aggregate or powder, which are tiny crystallites in all possible orientations.

The X-ray beam is able to see all atomic planes when a powder with randomly oriented crystallites is placed in an X-ray beam. Possible diffraction peaks will be detected from the sample if the experimental angle is changed.

The most common geometry that is used in diffraction instruments is the parafocusing or sometimes called Bragg-Brentano. The advantages of this geometry are high beam intensity and high resolution analysis, but require very precise alignment and carefully prepared samples. In addition, this geometry requires that the distance between the source and sample be equal and constant to the distance between the sample and detector distance. Errors in alignment can lead to difficulties in identifying the phase and improper quantification. A sample placed in the wrong position can lead to unacceptable errors in sample displacement.

Factors such as sample roughness, positioning and flatness constraints prevent in-line sample measurement. High powered X-ray sources aid in increasing X-ray flux on the sample, which increases the detected diffraction signals from the sample, therefore XRD systems with high power are recommended to increase the detected diffraction signals from the sample. These sources also have large excitation areas, which are often disadvantageous for the diffraction analysis of small samples or small sample features.

2.8.9.3. Scanning electron microscope (SEM)

The SEM is a technique used to generate a variety of signals at the surface of solid samples. This device uses a beam of high-energy electrons focused on the sample to reveal information about the external morphology, crystalline structure and chemical composition of the material making up the sample. The signals that reveal this information are derived from the interactions between the electron and the sample. Usually, the special variations of these properties are displayed in a two dimensional image. Data are collected over a selected area of the surface of the sample. SEM can generate images ranging from a width of 5 microns to 1 cm.

To obtain this, conventional SEM techniques with magnification ranging from approximately 20X to 30 000X and spatial resolution 50 to 100 nm. SEM can also perform analyses of selected point locations on the sample; this approach is very useful in semi-quantitatively or qualitatively determining the crystal orientations, chemical compositions and crystalline structure. The chemical compositions and crystal orientations can be determined using energy dispersive spectroscopy (EDS) and electron backscatter diffraction (EBSD).

SEM and the electron probe micro-analysis (EPMA) are very similar in design and function, considerable overlap in capabilities exists between the two techniques.

2.8.9.4. Fourier-Transform infrared (FTIR) spectroscopy

In infrared (IR) spectroscopy, infrared radiation is passed through a sample. Some of the infrared radiation is absorbed by the sample and some of it is passed through (transmitted). The resulting spectrum represents the molecular absorption and transmission, creating a molecular fingerprint of the sample. The sample analysis process entails the emission of infrared radiation from a black body source. Molecular structures are unique and cannot produce the same infrared spectrum. This makes infrared spectroscopy useful for several types of analysis. The beam enters the interferometer where the spectral encoding takes place. Identification and determination of the amount of components in a mixture, the quality or consistency of a sample and unknown materials is done using this technique.

2.8.9.5. Ultra violet visible spectroscopy

In an ultraviolet-visible light (UV-Vis) spectroscopic technique, light absorption as a function of wavelength provides information about electronic transitions occurring in the material. The fraction of light transmitted is described by the Beer-Lambert law [Zhebo et al., 2013]. Conventional spectrometers use a technique whereby a sample, which is held in a small square–section cell, is radiated by electromagnetic radiation. Scanning of radiation across the UV-Vis is done over a period of time starting from 30 s. Radiation of the same frequency and intensity is simultaneously passed through a reference cell containing only the solvent. The radiation transmitted is then detected by photocells and the difference between the intensity of the radiation passing through the sample and the reference cells is recorded by the spectrometer.

A photomultiplier or photodiode can detect the radiation passing through the sample or reference cell by converting photons of radiation into tiny electrical currents; or a semiconducting cell that emits electrons when radiation is incident on it, followed by an electron multiplier similar to those used in mass spectrometers.

2.8.9.6. Zeta Potential

Zeta potential is a technique used to measure the magnitude of the electrostatic or charge repulsion/attraction between particles, and is one of the fundamental parameters known to affect stability. Information on the causes of aggregation, dispersion or flocculation, can be obtained from the measure of zeta potential.

These can be applied to improve the formation of emulsions, dispersions and suspensions. The net electrical charge contained within the region bounded by the slipping plane causes the zeta potential, which also depends on the location of that plane. Thus it is widely used for quantification of the magnitude of the charge. Electric surface potential and Stern potential in the double layer are not equal to the zeta potential, because these are defined at different locations [Kirby, 2010] and such assumptions of equality should be applied with caution. Nevertheless, zeta potential is often the only available path for characterization of double-layer properties.

The zeta potential is an instrument used to indicate the stability of colloidal dispersions. The amount of electrostatic repulsion between adjacent, similarly charged particles in dispersion is indicated by the magnitude of the zeta potential.

During analysis of small particles or molecules, a high zeta potential indicates stability, which means that the dispersion or solution will resist aggregation. A small zeta potential indicates that attractive forces may cause dispersion to break and flocculate and attractive forces may exceed repulsion.

This means that colloids with high zeta potential (negative or positive) are electrically stabilized while colloids with low zeta potentials tend to coagulate or flocculate [Greenwood and Kendall, 1999].

Chapter 3 : Materials and methods

This chapter deals with the methodology that was followed for the removal of sulphates from AMD using modified clays. The CEC of each clay was determined using the copper bis-ethylenediamine complex method. Two types of clay, which are attapulgite and Mozambican bentonite, were each modified with HDTMA, TDTMA and barium chloride. The modified clay samples were used for adsorption studies and sulphate analysis was done on the spent liqour samples. For each clay studied, the modified clay that showed the highest sulphate removal during adsorption studies was used for further studies.

3.1. Equipment

Adsorption experiments were done using a thermostatic shaker (Labotec OrbiShaker) and a UV Visible spectrophotometer (PG Instruments T60) was used to analyze for sulphate ions. pH was measured using Metler Toledo dual meter (Sevenduo pH/conductivity meter with a Metler Toledo InLab Pro ISM pH electrode probe). Malvern Zetasizer Nano Series was used for the measurement of zeta potential and XRF (Rigaku ZSK Primus II) was used to determine the elemental compositions of the clay minerals. Fourier-Transform infrared (FTIR) spectroscopy (Thermoscientific Nicket IS10) was used to characterise the clays before and after the adsorption experiments. Scanning Electron Microscope (SEM model Tescan Vega 3 XMU) was used to study the morphology of the adsorbents.

3.2. Materials

Tetradecyltrimethylammonium bromide (TDTMA) 95.0% and Hexadecyltrimethyl ammonium bromide (HDTMA) 95.0% were supplied by Sigma Aldrich and were used for clay modification. Original AMD was supplied by a local gold mine in the West Rand with a pH value of 3.3. Glycerol (≥99.0%) and ethanol (95.0%) were supplied by Sigma Aldrich and were used for the conditioning reagent preparation. Sodium chloride (≥99.0%) supplied by Sigma Aldrich was used for preparation of the conditioning reagent and activation of the clay minerals. Barium chloride (≥99.0%) and sodium sulphate (≥99.0%) were supplied by Sigma Aldrich and were used for sulphate precipitation, modification of clay and preparation of calibration standards respectively. Potassium iodide (99.0%), HCl (37.0%), starch and sodium thiosulphate ($Na_2S_2SO_3$) 99.0% were used for titration. $CuCl_2$ (99.0%) and ethylene-diamine (98.0%) were supplied by Sigma Aldrich and used for the formation of the copper complex $[Cu(en)_2]^{2+}$.

3.3. Procedure

3.3.1. Determination of the Cation Exchange Capacity

The copper bis-ethylene diamine complex method was used to determine the cation exchange capacity (CEC) of the clays. A quantity of 50 ml of 1 M $CuCl_2$ solution was mixed with 102 ml of 1 M ethylene diamine solution to allow the formation of the $[Cu(en)_2]^{2+}$ complex.

A slight excess of the amine ensured complete formation of the complex. The solution was diluted with reverse osmosis water to 1 L to give a 0.05 M solution of the complex. 5 ml of the complex solution was diluted to 25 ml with reverse osmosis water, and 0.5 g clay was added to the solution and was agitated for 30 min in a thermostatic shaker at 200 rpm and 25^{o}C and then centrifuged.

The concentration of the complex remaining in the centrifugate was determined by mixing 5 ml of the liquid with 5 ml of 0.1 M HCl to destroy the $[Cu(en)_2]^{2+}$ complex, followed by adding 0.5 g KI per ml and then titrating iodometrically with 0.02 M $Na_2S_2O_3$ in the presence of starch as an indicator. The CEC was calculated using eqn 3-1 [Bhattacharyya and Gupta, 2007].

$$\text{CEC } (\text{meq}/100\text{ g}) = MSV\,(x - y)/1000m \qquad \textbf{eqn 3-1}$$

Where M is the molar mass of the complex (mol.g), S is the concentration of the thiosulphate solution (mol.ml^{-1}), V the volume (ml) of the complex taken for iodometric titration, m the mass of adsorbent taken (g), x is the volume (ml) of thiosulphate required for blank titration (without the adsorbent), and y is the volume (ml) of thiosulphate required for the titration (with the adsorbent).

3.3.2. Effect of surfactant concentration on sulphate removal

In order to predict the correct amount of surfactant to use on each clay, attapulgite was modified with HDTMA and TDTMA. Due to cost implications, only 100, 150 and 200% CEC was used.

3.3.2.1. *Organic Modification*

Organic modification of clay was done as illustrated in the following flow diagram:

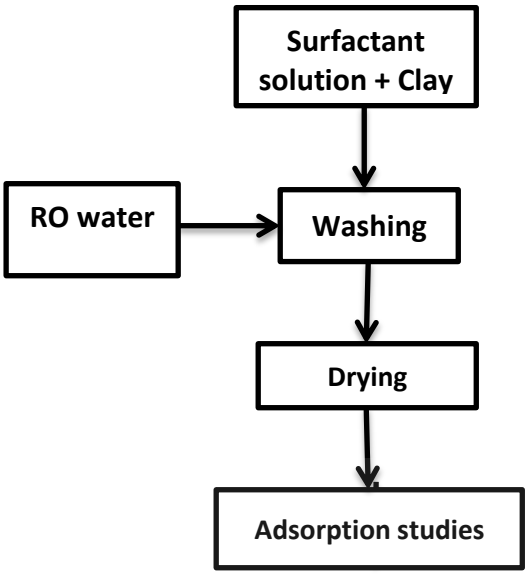

Figure 3-1: Flow diagram for organic modification

Table 3-1 shows the amount of each reagent used for organic modification (TDTMA and HDTMA) for attapulgite and MB at different surfactant loadings in terms of CEC.

Table 3-1: Organic modification of attapulgite and MB

Surfactant	HDTMA	TDTMA	HDTMA	TDTMA
CEC (%)	Mass (g/100 g attapulgite)		Mass (g/100 g MB)	
100	1.84	1.70	18.22	16.82
150	2.75	2.55	27.33	25.23
200	3.67	3.40	36.44	33.64

Appropriate mixing of the clay and surfactant was done according to Table 3-1 in 1 L of RO water, using an overhead stirrer for 24 h. The modified clay was washed with RO water to remove the superficially held adsorbate and dried at 150^{o}C before being used for adsorption studies.

3.3.2.2. Barium Modification

Barium modification of clay was done as illustrated in the following flow diagram:

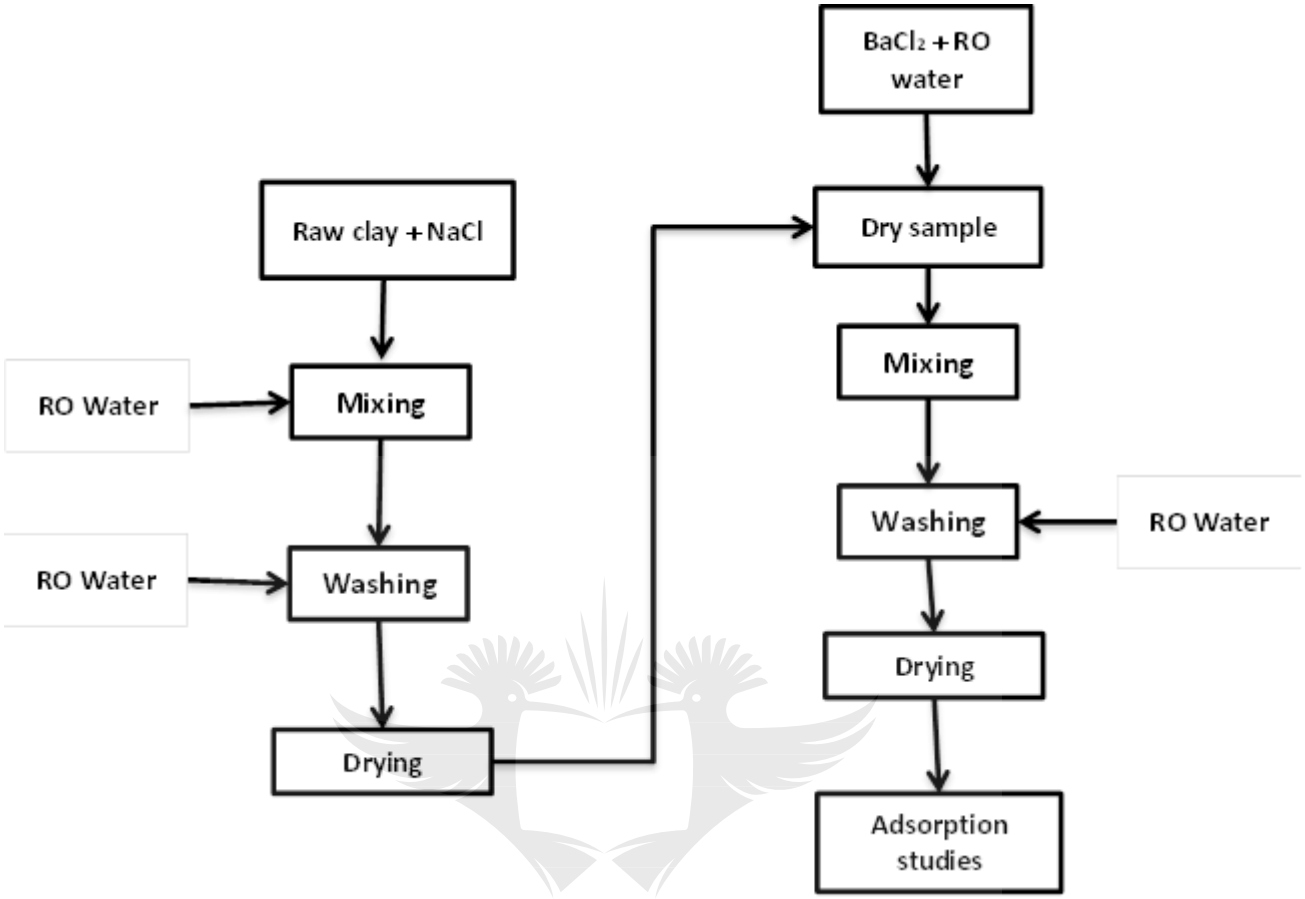

Figure 3-2: Flow diagram for barium modification

3.3.2.2.1. Modification using 1 M barium chloride

Raw clay was first activated by preparing 1 L of 1 M NaCl solution which was mixed with 100 g raw clay for 24 h using an overhead stirrer. The mixture was washed with RO water, decanted and dried at 150^{o}C. The dried sample was mixed with 1 L of 1 M $BaCl_2$ solution and stirred for 24 h using an overhead stirrer. The sample was washed with RO water and dried at 150^{o}C before being used for adsorption studies.

3.3.2.2.2. Modification using 2 M barium chloride

Samples of the modified clay which gave a higher sulphate removal when modified with $BaCl_2$ were subjected to further studies involving the effect of $BaCl_2$ concentration on sulphate removal. 1 L of 1 M NaCl solution was prepared and mixed with 100 g MB for 24 h. 1 L of 2 M $BaCl_2$ solution was prepared and mixed with 100 g of activated clay for 24 h. The samples were washed with RO water and dried at 150^{o}C before being used for adsorption studies.

3.3.3. Determination of sulphate content using the turbidimetric method

3.3.4.1. Preparation of conditioning reagent

30 mL of HCl was mixed with 300 ml RO (reverse osmosis) water. The solution was mixed with 100 ml 95% ethanol, 75 g NaCl and stirred using an overhead stirrer. While still stirring, 50 ml of glycerol was added and stirring continued for 20 min.

3.3.4.2. Standard sulphate solution from Na_2SO_4

147.9 mg anhydrous Na_2SO_4 was dissolved in 1.0 L RO water to make 100 ppm standard solution. Calibration standards of 10, 20, 30, 40 and 50 ppm were prepared by appropriate dilution of the 100 ppm stock solution.

3.3.4.3. Formation and measurement of barium sulphate turbidity

The wavelength of the UV-Vis was set to 420 nm. A sample blank was run using the procedure of formation of barium sulphate turbidity and measurement of barium sulphate turbidity without the addition of barium chloride.100 mL sample was placed into a 250 mL Erlenmeyer flask and mixed with 5.0 mL of conditioning reagent using a magnetic stirrer. While the solution was being stirred, a spatula full of $BaCl_2$ crystals was added and timing was commenced. Stirring continued for 1.0 min at constant speed. Immediately after the stirring period ended, the solution was poured into the absorbance cell. Turbidity was measured after 2.0 min.

3.3.4. Sulphate removal.

During sulphate removal, a maximum of 10% w/v clay to AMD was used to ensure effective mass transfer. 10% w/v of modified clay to AMD was used to determine which modified clay was able to remove the highest amount of sulphates. 10 g of each modified clay was agitated with 100 ml of AMD in a thermostatic shaker at 200 rpm and 25^{o}C. Sampling was done every 2, 4, 6, 22 and 24 h. The samples were centrifuged and the centrifugate was analysed for sulphates using a UV- Visible spectroscopy.

3.4. Measurement of Zeta Potential

Raw and modified samples of attapulgite and MB were analysed for Zeta potential. 2 g of the dry samples were mixed with 5.0 mL distilled water and transferred into a dip cell then analysed 3 times, then the average zeta potential (mV) was recorded. The instrument was operated at 25^{o}C.

3.5. XRD, XRF, FTIR and SEM analysis

A sample of modified clay which had removed the highest amount of sulphates from AMD was further characterised, because it was a more promising clay for the purpose of this study. The operating parameters of the equipment are tabulated in Appendix 1.

3.5.1. Sample preparation

- ***XRF-*** 12 g milled sample was pressed into a powder briquette by a hydraulic press at an applied pressure of 25 ton.
- ***XRD-*** A 10 g milled sample was placed on a sample holder and flattened using a glass plate.
- ***SEM-*** A 5 g milled sample was mounted on an aluminium stub using a double sided carbon tape. The sample was coated with carbon before analysis was commenced.

3.6. Effect of solid loading and agitation time

Samples of the modified clay that removed the highest amount of sulphates were subjected to further studies as mentioned previously. Dry samples of modified clay at 2, 6 and 10% w/v clay to AMD were agitated in a thermostatic shaker at 25^{o}C and 200 rpm. Sampling was done every 2, 4, 6, 22 and 24 h. The samples were centrifuged and the centrifugate was used for sulphate analysis.

3.7. Effect of temperature

Samples of the modified clay that removed the highest amount of sulphates were studied for the effect of temperature on sulphate removal. Dry samples of modified clay at 10% w/v clay to AMD were agitated in a thermostatic shaker at 25, 35 and 45^{o}C and 200 rpm. Sampling was done every 2, 4, 6, 22 and 24 h. The samples were centrifuged and the centrifugate was used for sulphate analysis.

Chapter 4 : Attapulgite

4.1. Introduction

This chapter addresses the characteristics of modified attapulgite and also assess its potential for application in the removal of sulphate from AMD.

4.2. Experimental

Modified attapulgite was used for the sorption experiments. The effects of agitation time, solid loading, temperature and surfactant loading on the removal of sulphates from AMD were investigated. Adsorption isotherms, kinetics and thermodynamic parameters were calculated from the data obtained. The materials, equipment and methods used are described in Chapter 3.

4.3. HDTMA Modification

4.3.1. The trend of CEC before and after modification with HDTMA

Table 4-1 represents the results of the CEC before and after attapulgite modification using HDTMA.

Table 4-1: Comparison of CEC before and after modification of attapulgite using HDTMA

Surfactant loading (% CEC)	CEC before modification (meq/100g)	CEC after modification (meq/100g)
100	10.08	0.247
150	10.08	0.044
200	10.08	0.003

A reduction in the CEC value indicates that the cation exchange sites of the clay were reduced, hence modification took place. The results as shown in Table 4-1show a decreasing trend of CEC as the surfactant loading increases. This is because; clay is naturally organophobic and is rendered organophilic by the addition of a surfactant. As the amount of surfactant is increased, the available sites for cation exchange decrease.

4.3.2. The effect of surfactant loading on sulphate removal

In order to identify which surfactant loading to use for optimal sulphate removal, different percentages of CEC were tested using 10% w/v modified attapulgite to AMD with different loadings of HDTMA at 25^{o}C. Sulphate removal (%) was calculated using equation 4-1.

$$removal(\%) = \frac{C_o - C}{C_o} \times 100 \qquad \text{eqn 4-1}$$

where C_o is the initial concentration and C is the final concentration of sulphates.

Figure 4-1 and Fig 4-2 shows the effect of HDTMA attapulgite modification and contact time on sulphate removal.

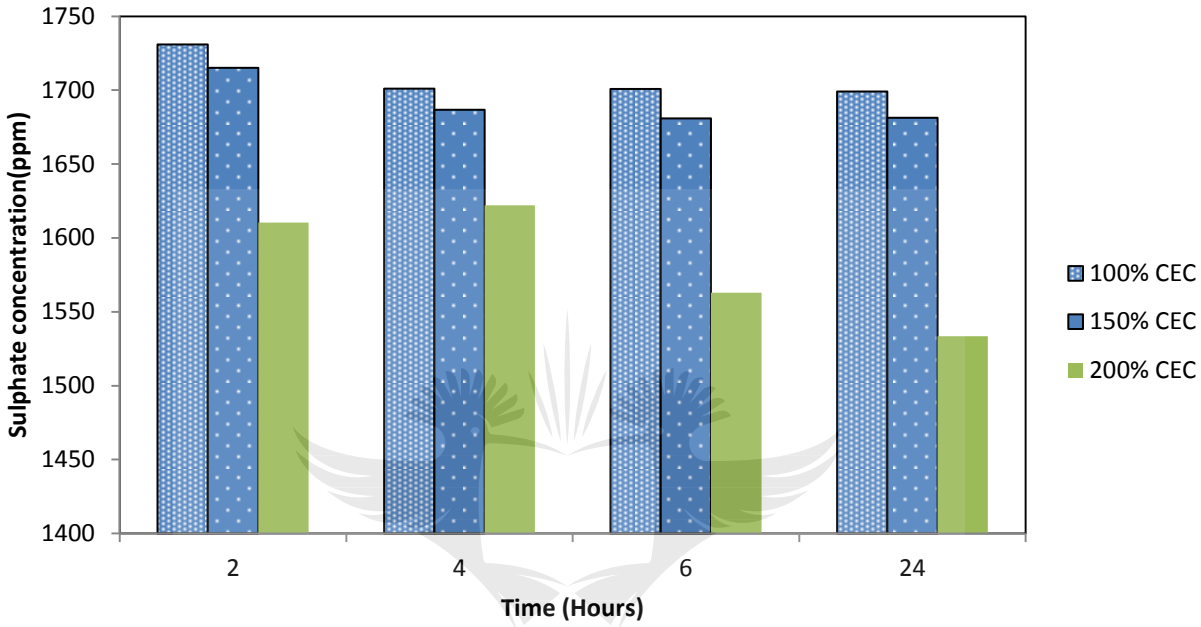

Figure 4-1: Effect of HDTMA loading and contact time on residual sulphate concentration using 10% w/v attapulgite to AMD.

The concentration of sulphates was reduced from 1811 ppm to 1699, 1681 and 1533 ppm after 24 h when using 100, 150 and 200% CEC respectively. This was supported by the drop in CEC values as presented in Table 4-1.

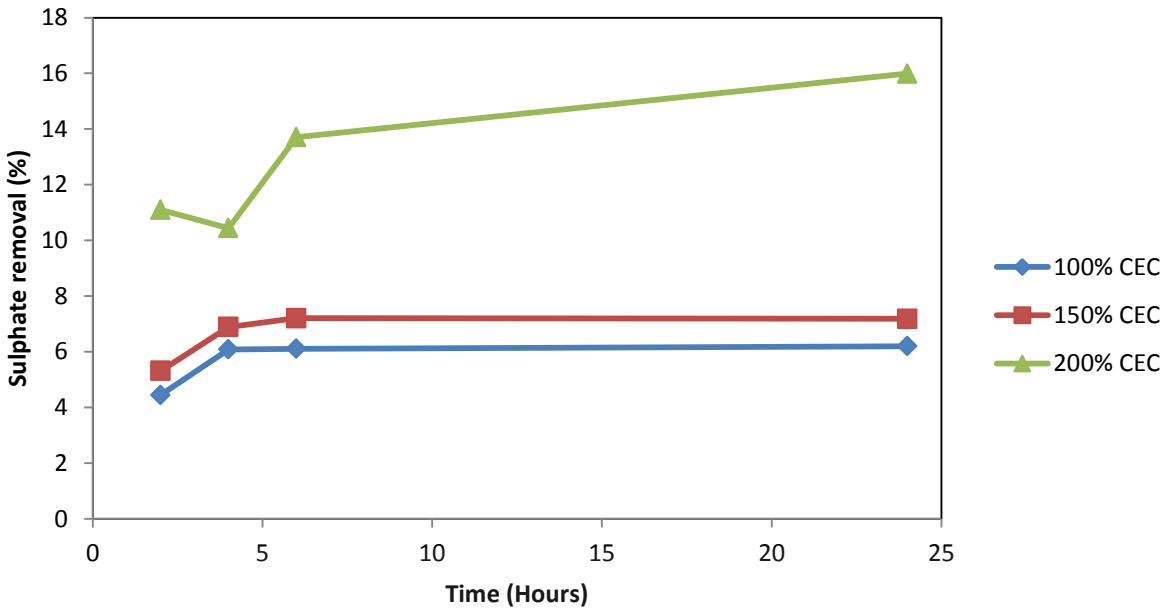

Figure 4-2: The effect of HDTMA loading and contact time on sulphate removal using 10% w/v attapulgite to AMD.

An increment in surfactant loading enhanced sulphate removal with the lowest amount of sulphates removed being 4.4% and the highest being 16.0%. This is because at higher concentrations of the surfactant, the clay becomes more organophilic, which then allows the clay to adsorb sulphates.

4.3.3. Effect of agitation time

Further experiments were done using 200% CEC, 10% w/v and 25^{o}C as it had shown better removal of sulphates compared to other concentrations of HDTMA. Figure 4-3 shows the effect of agitation time on sulphate removal and concentration.

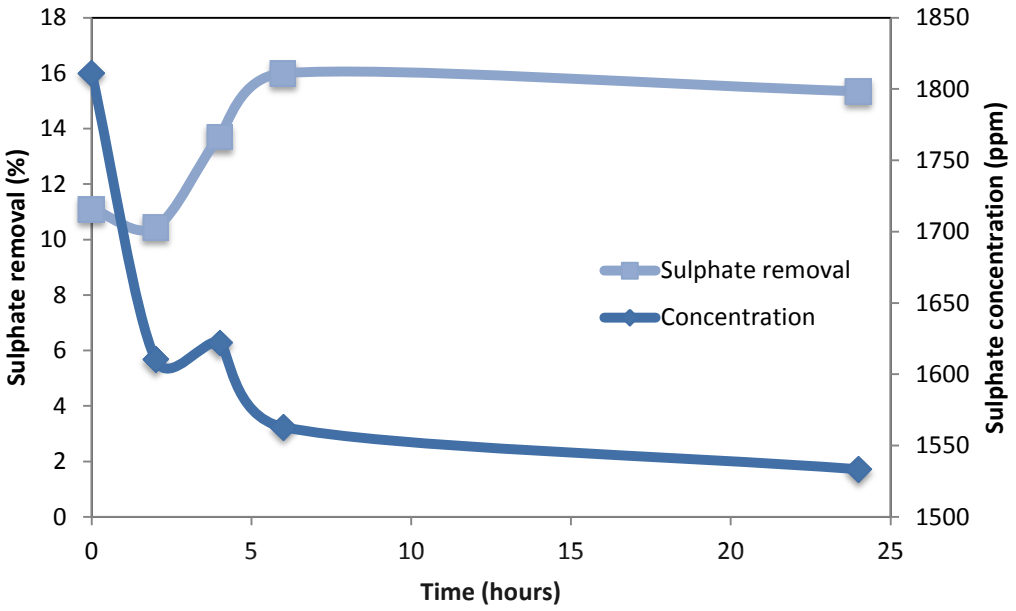

Figure 4-3: Effect of agitation time on sulphate removal and residual concentration using HDTMA modified attapulgite.

Sulphate concentration reached the lowest point (from1811 ppm to 1522 ppm) after 22 h of mixing and then the reaction underwent adsorption-desorption process thereafter. There was a maximum sulphate removal of only 16.0% from the AMD sample after 22 h of agitation.

4.4. TDTMA Modification

4.4.1. The trend of CEC before and after TDTMA modification

Table 4-2 shows the CEC before and after modification of attapulgite using different loadings of TDTMA.

Table 4-2: Comparison of CEC before and after modification of attapulgite using TDTMA

Surfactant loading (% CEC)	CEC before modification (meq/100g)	CEC after modification (meq/100g)
100	10.08	0.456
150	10.08	0.388
200	10.08	0.318

Modification with TDTMA showed a decrease in the CEC value, implying the cation exchange capacity of the clay increased with an increase in surfactant loading.

4.4.2. The effect of TDTMA loading on sulphate removal

In order to determine the sulphate removal efficiency of the modified attapulgite at different CEC percentages, the experiment was done at 25°C and 10% w/v clay to AMD was used. Figure 4-4 shows the effect of surfactant loading on sulphate removal.

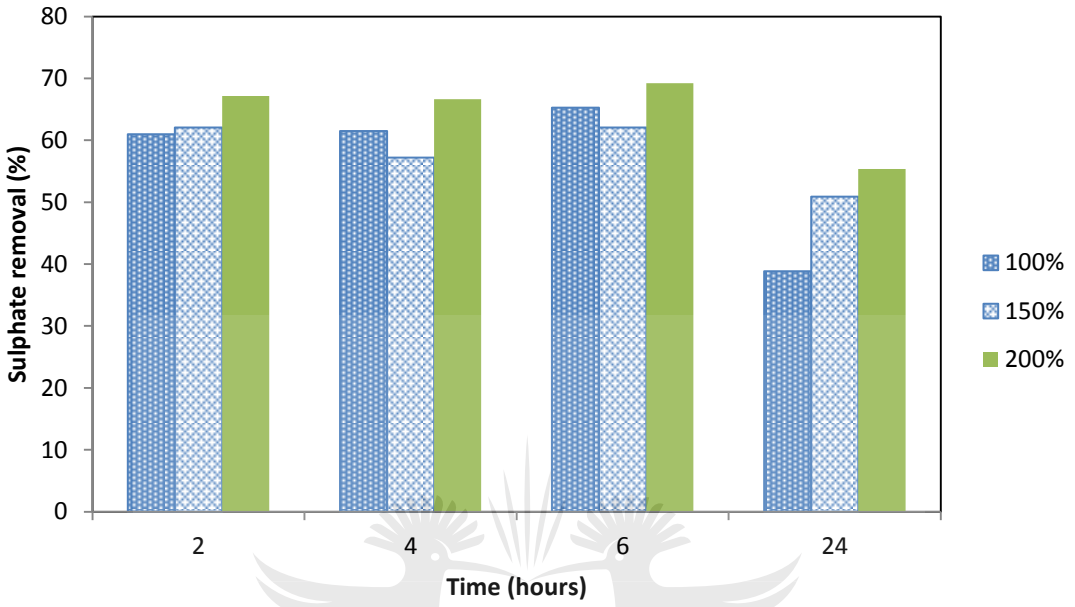

Figure 4-4: Effect of TDTMA loading on sulphate removal

An increase in TDTMA loading enhanced sulphate removal as supported by the drop in the CEC value in Table 4-2. The increasing and decreasing trend in sulphate removal with time is due to the adsorption-desorption process.

4.4.3. The effect of agitation time

Further experiments were done using 200% CEC, 25°C and 10% w/v as it had shown better removal of sulphates compared to other concentrations of TDTMA. Figure 4-5 shows the effect of agitation time on sulphate removal and concentration.

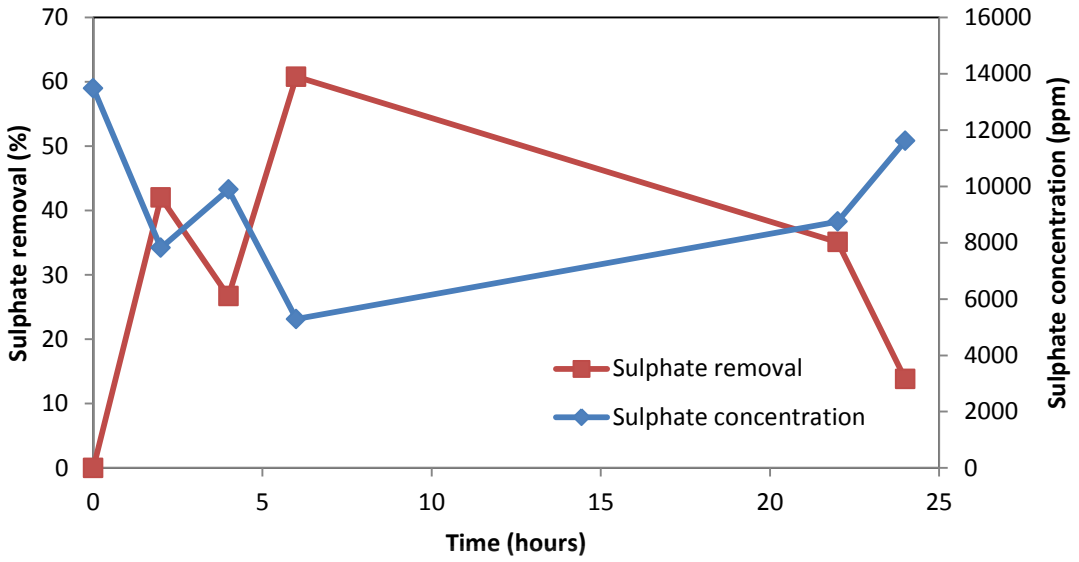

Figure 4-5: Effect of agitation time on sulphate removal and residual concentration using TDTMA modified attapulgite

Sulphate concentration reached the lowest point of 160 ppm after 6 h of mixing. Fig. 4-6 shows an increasing and decreasing concentration of sulphates with time, which implies that there was an adsorption-desorption process. A maximum sulphate removal of 69.2% was reached after 6 hours of agitation. Sulphate concentration dropped after 6 hours of agitation, implying that this is a reversible reaction. It is worth noting that higher sulphate removal was achieved when using TDTMA modified clay than HDTMA in all experiments. This is an indication that interaction between HDTMA and water is very weak [Pálková et al., 2015]. This is also brought about by the length differences in the carbon chain within the structures. HDTMA has a longer carbon chain as compared to TDTMA. It has been reported by Gonzalez-Garcia et al., 2004, that adsorption is decreased at longer carbon chains.

4.5. $BaCl_2$ Modification

To investigate the effect of $BaCl_2$ modification on attapulgite, 1 and 2 M $BaCl_2$ modified clay was mixed with AMD at 10% w/v and 25^{o}C. Fig. 4-6 shows the effect of agitation time on sulphate concentration.

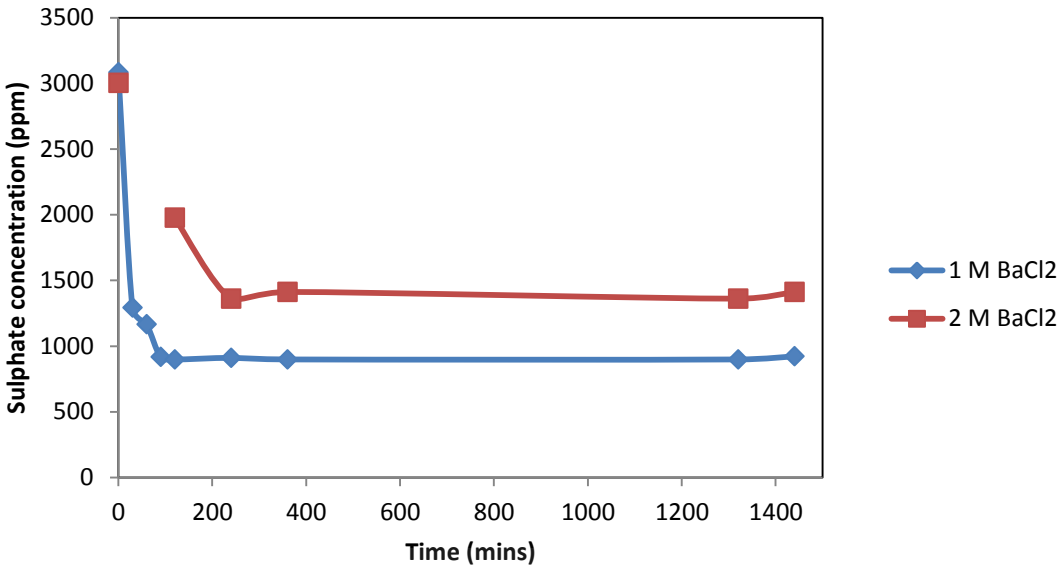

Figure 4-6: Effect of agitation time on residual sulphate concentration using $BaCl_2$ modified attapulgite

There was a stable concentration of sulphates ranging from 899 to 923 ppm over a period of 24 h for 1 M $BaCl_2$. This resulted in a sulphate removal of 70.8% (Fig. 4-7). This shows that the sulphate removal at different agitation times was rapid in the initial stages and gradually decreased until the equilibrium was reached [Namasivayam and Sangeetha, 2008]. The residual sulphate concentration was higher when the concentration of $BaCl_2$ was doubled from 1 M to 2 M. This is because when the concentration of $BaCl_2$ is doubled, more Cl^- are attached to the surface of the clay, thus making the clay surface more negatively charged and creating competition for the sulphate ions.

Figure 4-7 shows the effect of agitation time on sulphate removal efficiency using barium modified attapulgite.

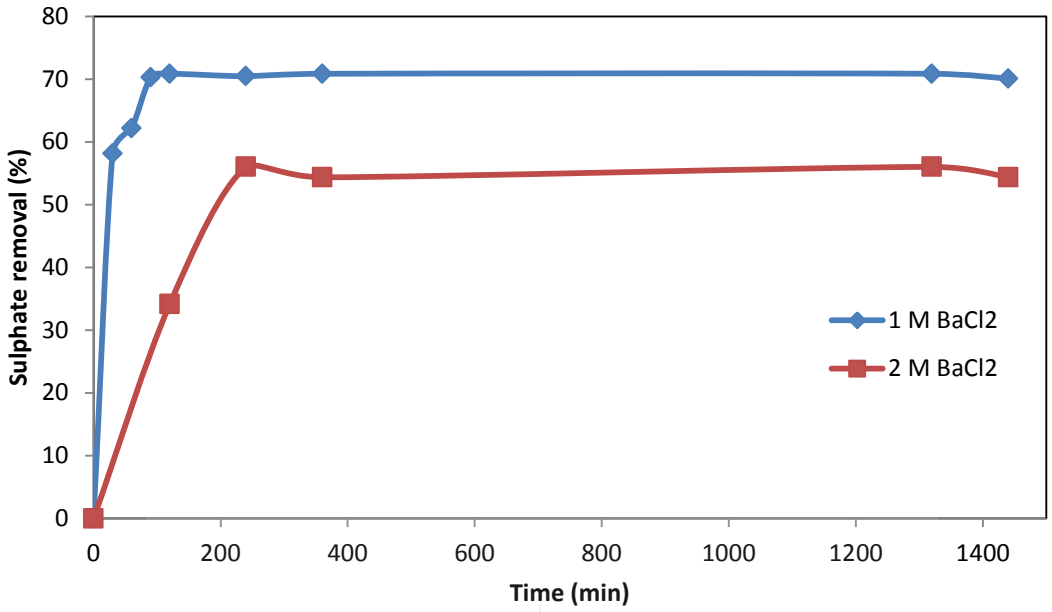

Figure 4-7: Effect of agitation time on sulphate removal using $BaCl_2$ modified attapulgite

The amount of sulphates removed was between 70.1 and 70.8% which was reached during the first 2 h of agitation when attapulgite was modified with 1 M $BaCl_2$. This indicates that the sorption capacity was increased when the clay was barium modified. An increase in $BaCl_2$ concentration resulted in a drop in sulphate removal, with the highest of 56.0% removed from the AMD sample.

Table 4-3 shows the data obtained during the first 2 h of agitation when using 1 M barium modified attapulgite.

Table 4-3: First 2 h data using 1 M barium modified attapulgite

Time (mins)	SO_4^{2-} Concentration (ppm)	SO_4^{2-} removal (%)
0	3084.0	0
30	1291.0	58.12
60	1166.0	62.17
90	916.7	70.28
120	899.2	70.84

4.6. Solid loading

Barium modified attapulgite was used for further studies on the effect of solid loading on the removal of sulphates from AMD, as it showed higher removal of sulphates than the other surfactants.

Experiments were carried out at 25°C at different solid loadings i.e. 2%, 6% and 10% w/v clay to AMD, and analysed to find out the solid loading required to achieve a higher percentage of sulphates removal from AMD. Fig. 4-18 shows the effect of solid loading on sulphate concentration.

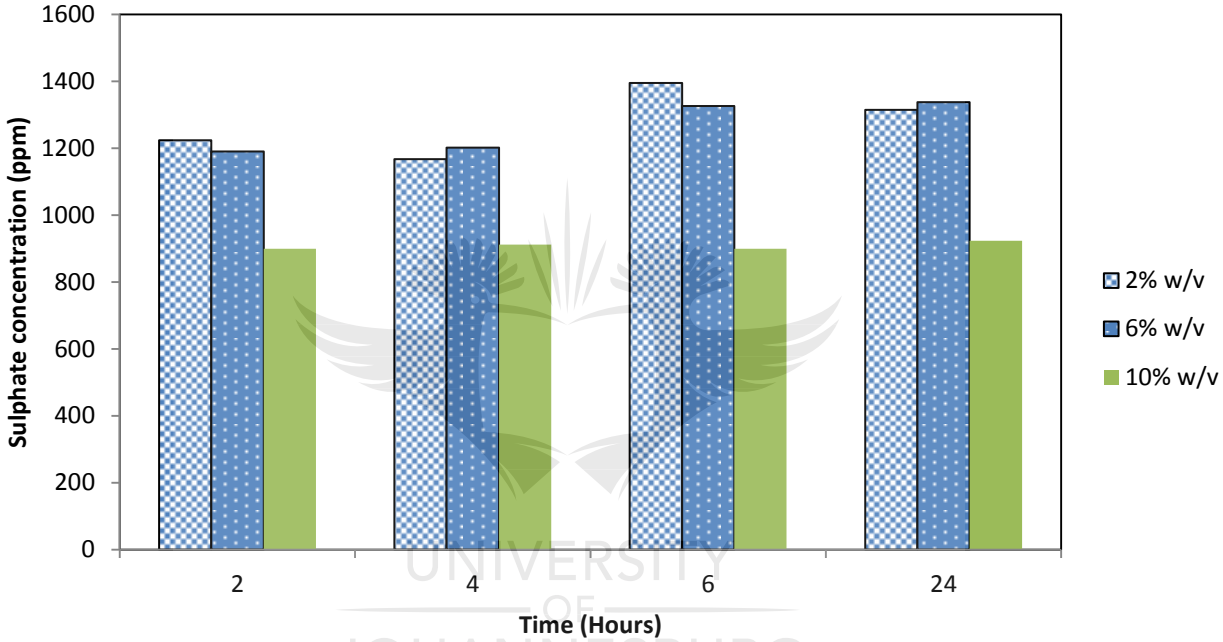

Figure 4-8: Effect of Solid loading on sulphate concentration using $BaCl_2$ modified attapulgite

It was observed that at higher solid loading (10%); the concentration of sulphates was greatly reduced, reaching the lowest of 899 ppm within the first 2 h of agitation.

Fig. 4-9 shows the effect of solid loading on sulphate removal from AMD.

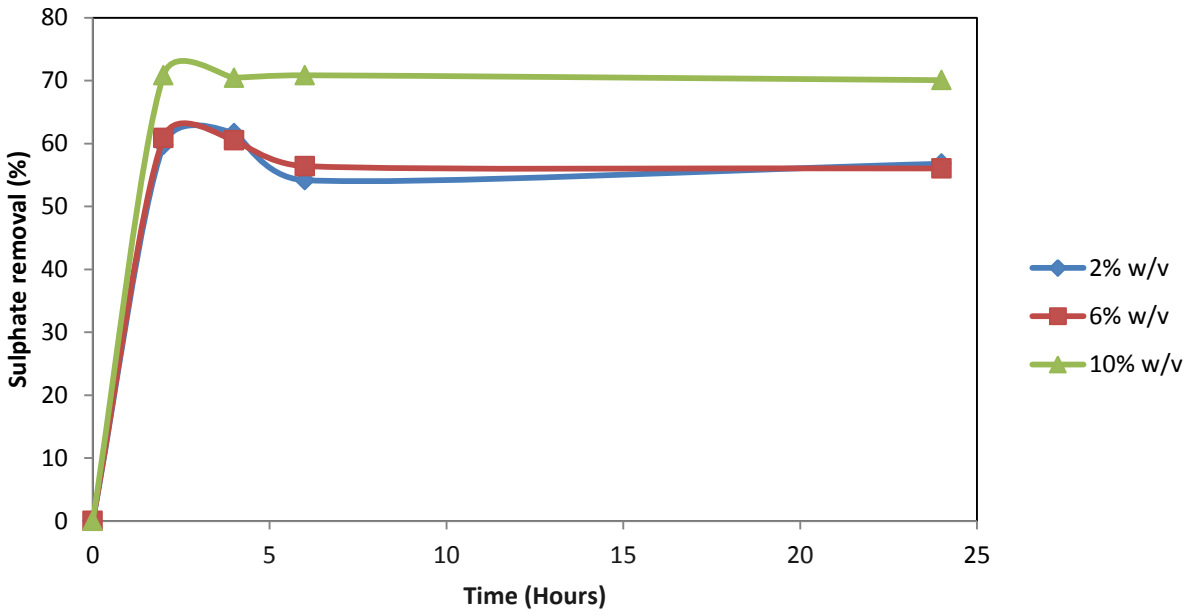

Figure 4-9: Effect of solid loading on sulphate removal using $BaCl_2$ modified attapulgite

A maximum of 70.1% sulphates was removed after 24 h of mixing, while only 56.0% was removed using 2 and 6% solid loading within the same time and conditions. This means that at higher solid loadings, there are more sites of adsorption and thus, the higher sulphate removal obtained [Namasivayam and Sangeetha, 2008].

4.7. Effect of temperature

Figure 4-10 and Figure 4-11 show the effect of temperature on sulphate removal.

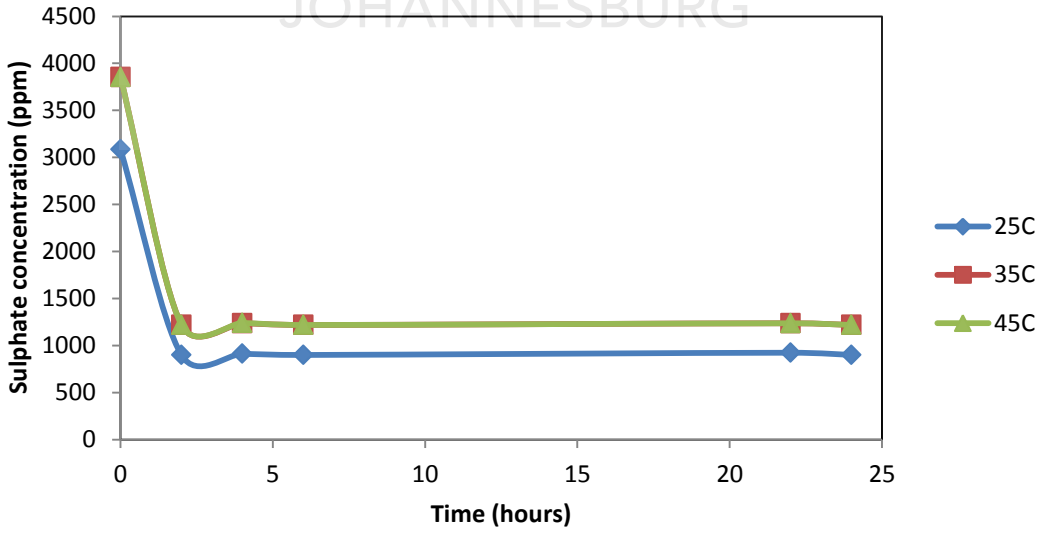

Figure 4-10: Effect of temperature on residual sulphate concentration using $BaCl_2$ modified attapulgite

Although the lowest residual concentration of sulphates was obtained at 25°C and the residual concentration remained high when the temperature was increased from 35°C and 45°C, the difference in sulphate removal percentage (Fig. 4-11) was too little (≈2%) when the temperature was varied.

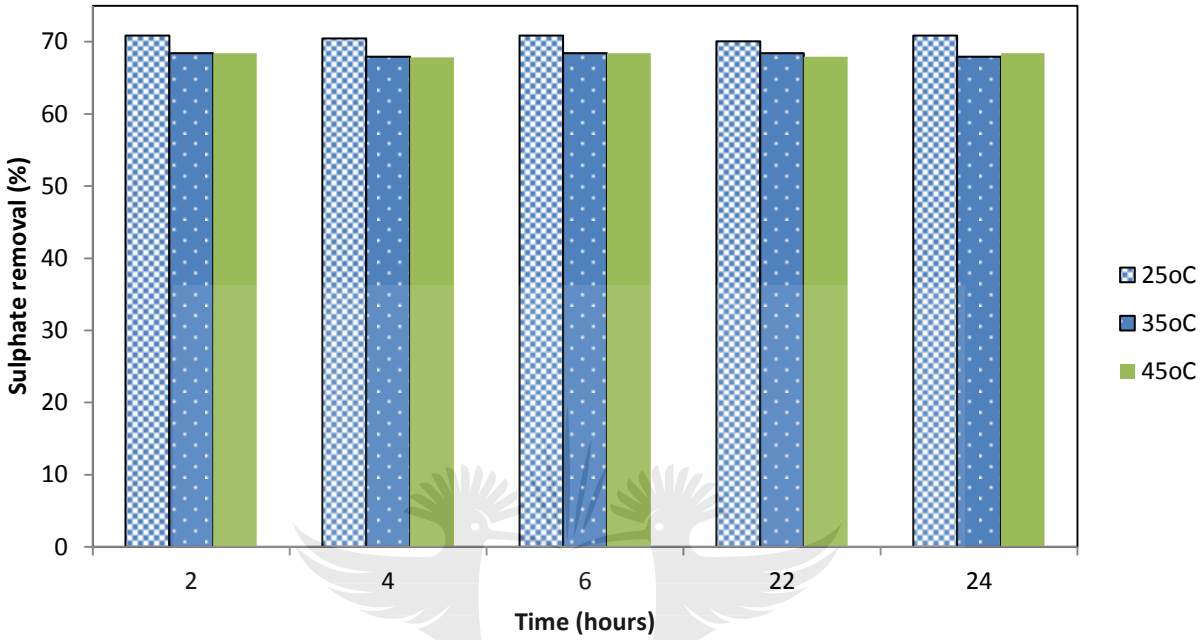

Figure 4-11: Effect of temperature on sulphate removal using $BaCl_2$ modified attapulgite

The removal of sulphates from AMD using attapulgite dropped slightly with temperature increments. The small difference in sulphate removal with temperature implies that this reaction can be run at room temperature without any need for energy input.

4.8. Measurement of Zeta Potential

The zeta potential of raw attapulgite and attapulgite modified with 1 M $BaCl_2$, 200% CEC TDTMA and 200% CEC HDTMA was measured. Table 4-4 shows the zeta potential of the attapulgite samples.

Table 4-4: Zeta potential results for the attapulgite samples

Sample	Zeta potential (mV)
Raw attapulgite	-11.8
Barium modified	0.140
TDTMA modified	-9.57
HDTMA modified	-2.45

The raw sample of attapulgite had a net negative charge. After modification, the zeta potential values moved towards the positive side, implying that modification of attapulgite made it more organophilic. Barium modified attapulgite had the most positive value of zeta potential; hence it removed the highest amount of sulphates from AMD. Zeta potential values of ±30 mV are considered to be a suitable threshold for stability; hence aggregation of the clay samples is not expected during adsorption [Barnes, 1992].

4.9. Characterization

Characterization of attapulgite was done on raw attapulgite, modified attapulgite and sulphate loaded attapulgite using XRD, XRF, FTIR and SEM.

4.9.1. XRD analysis

Figure 4-12 shows the XRD spectrum of raw attapulgite, modified attapulgite and sulphate loaded barium modified attapulgite, as it showed better removal of sulphates from AMD. The operating parameters of XRD are given in the methodology.

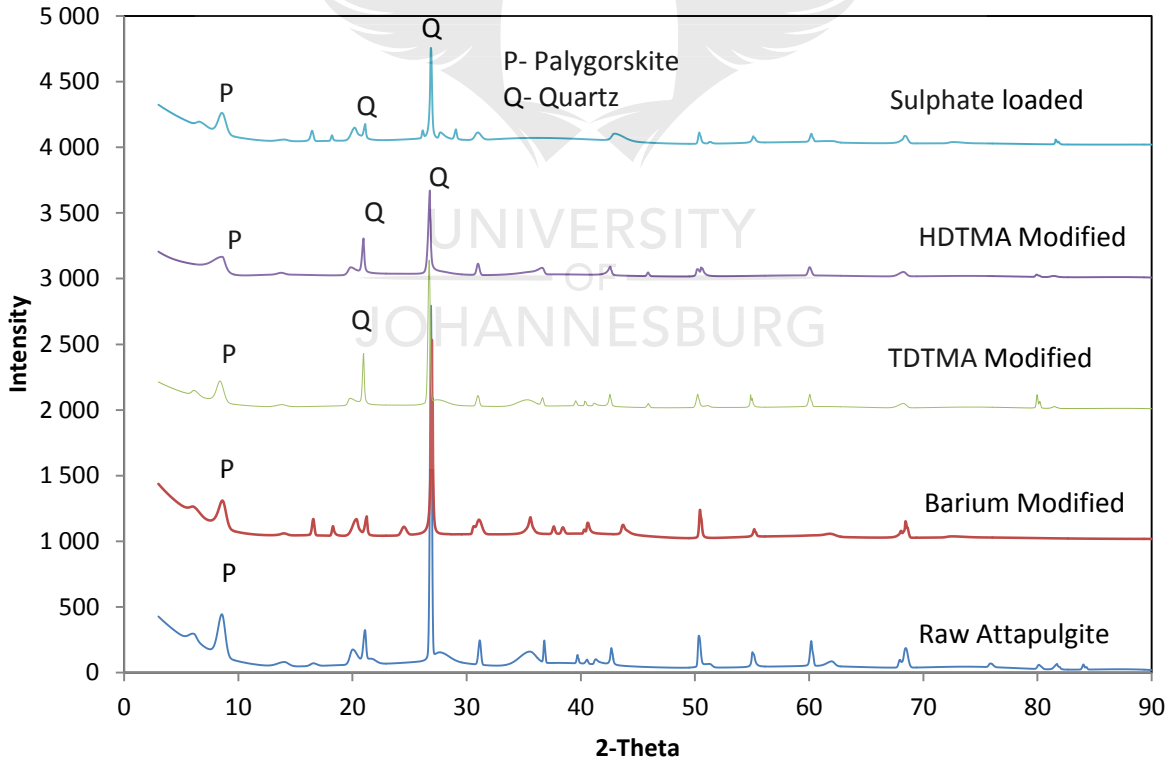

Figure 4-12: XRD spectrum for attapulgite at different stages.

The main constituent of raw attapulgite is quartz (56%) and palygorskite (40%), with the main peak of palygorskite at 8.56^{o} with the basal spacing of 10.3 Å. After modification with barium, TDTMA and HDTMA the peak shifted to 8.61^{o}, 8.38^{o} and 8.60^{o} with basal spacing of 10.26 Å, 10.54 Å and 10.27 Å respectively as reported by previous researchers Gan et al., (2009), Xiping et al., (2008) and Jeffrey & Peter, (2008). This is an indication that the surfactants are just adsorbed on the surface of the clay during the cation exchange process without destroying the crystalline structure of the clay [Xiping et al., 2008].

The diffraction peaks due to quartz, detected in the raw sample are noticeable at all the stages of the modification and have been gradually reduced during the modification process.

4.9.2. XRF analysis

Table 4-5 shows the chemical composition of raw attapulgite, barium modified and sulphate loaded attapulgite modified with barium.

Table 4-5: XRF results for attapulgite (ATT) at different stages

Component	Raw ATT	1M Barium modified	2M Barium modified	SO_4^{2-} loaded
		Weight (%)		
F	0.264	0.127	0.206	0.157
Na	0.188	1.14	0.709	1.12
Mg	13.6	9.64	6.51	9.28
Al	10.3	8.13	5.3	7.37
Si	64	48.3	35.5	46.5
P	0.0159	0.0154	0.0235	0.0116
S	0.282	1.14	0.387	3.07
Cl	0.0351	7.09	13.6	6.78
K	0.617	0.446	0.314	0.456
Ca	4.39	3.02	2.08	3.478
Ti	0.594	0.342	0.223	0.349
V	0.0637	-	-	-
Cr	0.0723	0.0581	0.052	0.0574
Mn	0.0712	0.0563	0.0566	0.157
Fe	5.37	4.14	2.953	4.54
Ni	0.0155	0.0128	0.0183	0.0151
Cu	0.0053	0.0081	-	0.0074
Zn	0.0058	-	0.0208	0.0066
Rb	0.0045	0.0029	-	0.0028
Sr	0.0216	0.0127	0.012	0.0124
Zr	0.0228	0.0156	0.0101	0.0168
Nb	0.0018	-	-	-
I	-	0.0477	-	-
Ba	0.0435	16.3	32.0	16.6

The major constituent of attapulgite was silicon dioxide, as supported by the XRD results presented earlier. After the modification with barium there was a high increase in Cl and Ba due to the NaCl and $BaCl_2$ used to modify the clay. There was an increase in sulphur ions from the raw attapulgite to the sulphate loaded attapulgite, which indicates that sulphates were adsorbed from the AMD sample onto the attapulgite surface. When the concentration of $BaCl_2$ was increased to 2 M, it was evident that Cl^- were doubled, which caused sulphate removal to drop [Fig. 4-7], due to the increased negative charge on the clay surface.

It is worth noting that XRF is a semi quantitative analysis technique hence results are relative to the total constituent of the material analysed.

4.9.3. FTIR analysis

Figure 4-13 shows the FTIR spectra of raw attapulgite, modified and sulphate loaded attapulgite modified with barium as it gave higher sulphate removal from AMD.

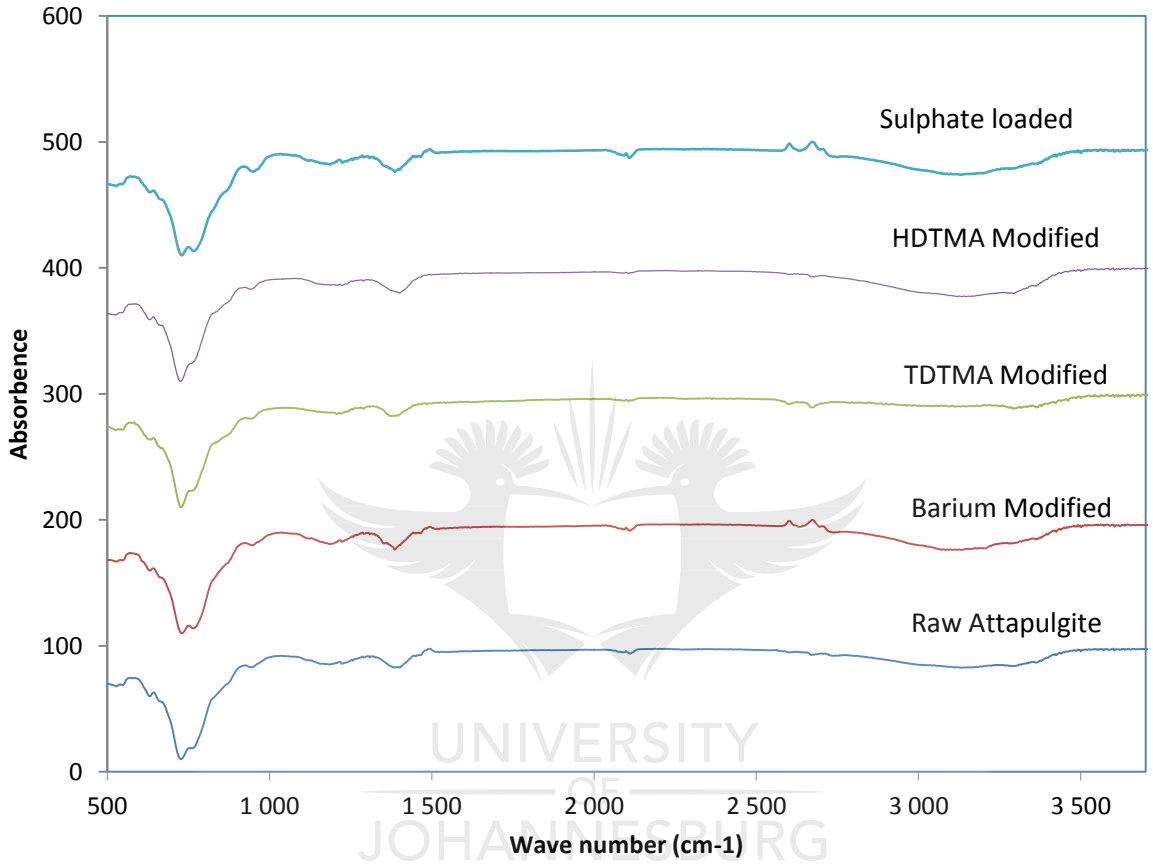

Figure 4-13: FTIR Spectra for attapulgite at different stages

Modification of attapulgite is evident by the appearance of absorption bands between 2800 and 2965 cm^{-1} due to the attachment of the modifiers to silicon [Wright and Hunter, 1947]. The absence of the same bands on the HDTMA spectra gives evidence that HDTMA methyl groups were not able to attach strongly to attapulgite; hence it removed the lowest amount of sulphates from AMD. These bands were sharper on barium modified attapulgite, hence barium modified attapulgite removed the highest amount of sulphates from AMD.

The pronounced wide absorption band in the 3000–3700 cm^{-1} region was observed and that is characterized by OH groups. The peak in wave number of 1025 cm^{-1} is assigned to Si–O vibration in the layer that is observed in natural and modified samples [Karimi and Salem, 2011].

4.9.4. SEM analysis

The morphology of attapulgite was analysed using SEM. Figure 4-14 shows the morphology of the clay at different stages and the Energy Dispersive Spectroscopy (EDS) for sulphate loaded attapulgite which was modified with barium, as it gave higher removal of sulphates from AMD.

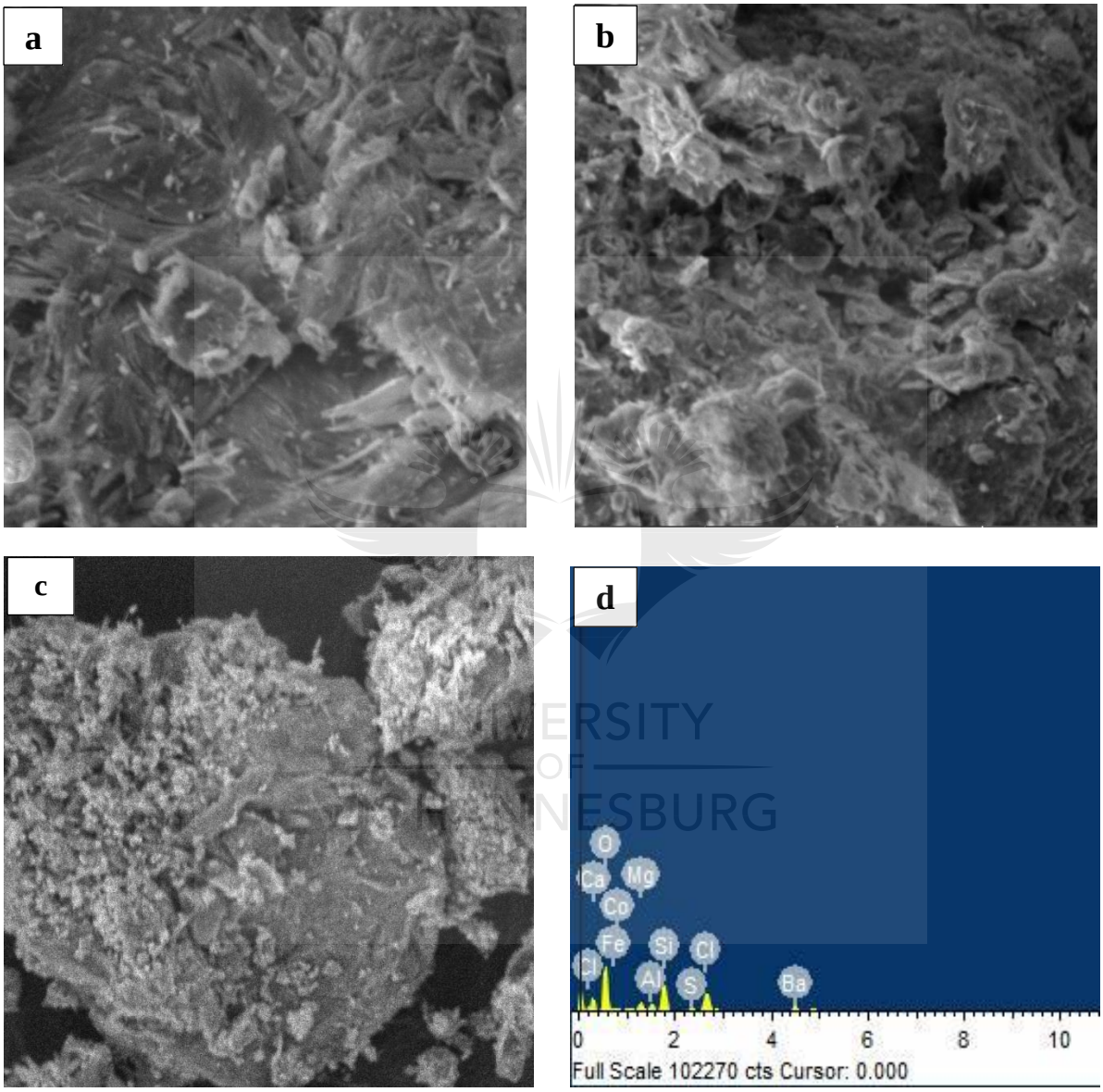

Figure 4-14: SEM images of attapulgite at different stages. (a): raw attapulgite, (b): barium modified, (c): sulphate loaded barium modified, (d): sulphate loaded barium modified EDS.

It was noticed that raw attapulgite was rod-shaped, with a lot of fibres as reported by Xiping et al., 2008. Comparing Fig. 4-14a and Fig. 4-14b, it was noted that the rod-shaped modified attapulgite showed better inter-particle spacing than the raw sample [Han et al., 2010]. The EDS for barium modified attapulgite shows that the sample contains mainly of Ba (41.6%) and SiO_2 (26.8%), which is also supported by the XRF results presented previously.

The high amount of Ba results from the adsorption of the surfactant on the surface of the clay [Xiping et al., 2008]. Trace amounts of sulphur were also detected (2.5%), which result from the adsorption of sulphates from AMD, which is also supported by the XRF results where there was an increase in sulphates in the sulphate loaded sample. The sulphates can be identified as the lighter shades on Figure 4-14c.

4.10. Thermodynamic and kinetic studies

4.10.1. Adsorption isotherms

The data obtained at 25^{o}C; between 0-2 h of agitation for barium modified attapulgite was used for further studies, because equilibrium was reached thereafter. Figure 4-15 shows the plots of Temkin, Langmuir and Freundlich adsorption isotherms, which have to be linear to fit the isotherm models respectively

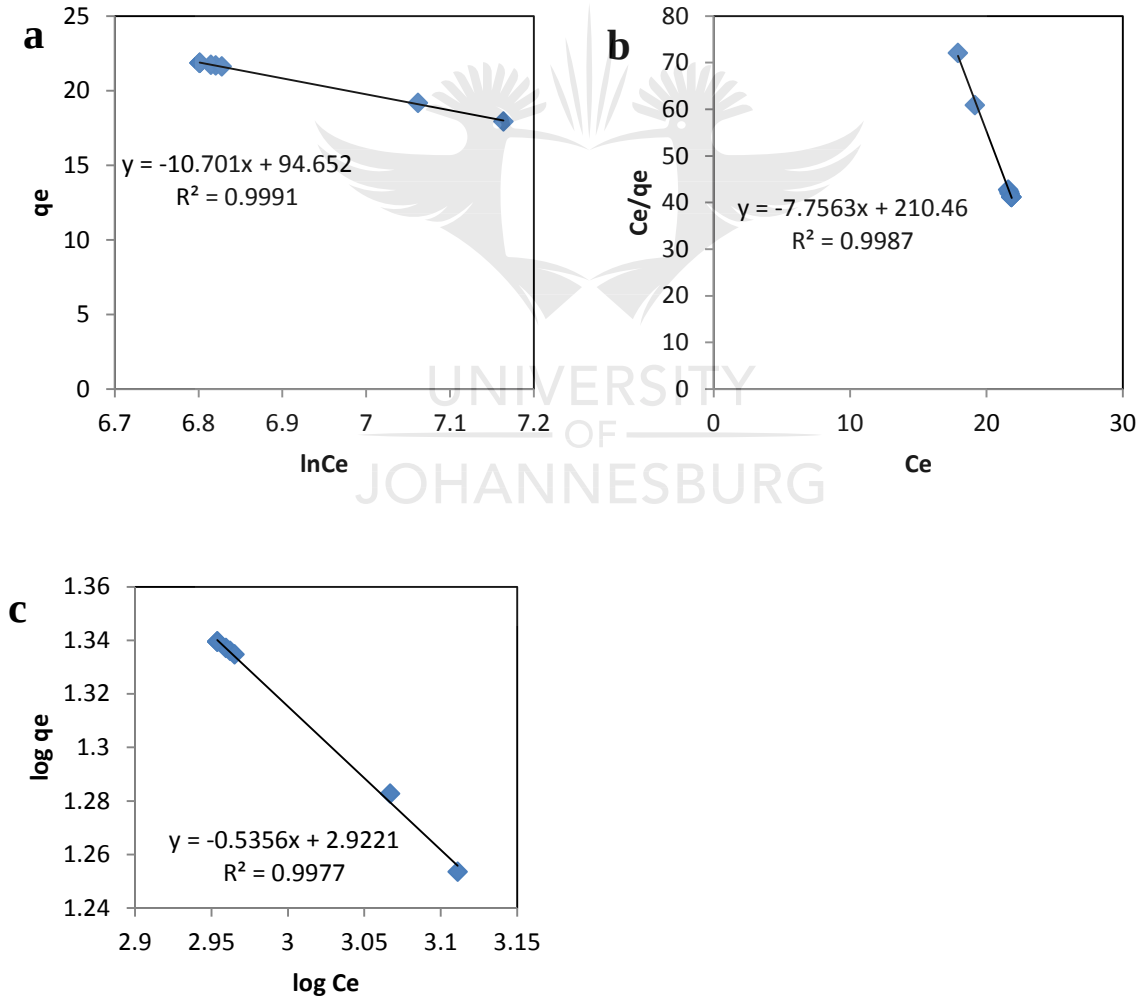

Figure 4-15: Adsorption isotherm models of barium modified attapulgite. (a): Temkin isotherm, (b): Langmuir isotherm, (c): Freundlich isotherm.

The high values of R^2 (close to 1) suggest that the experimental data exhibit a very good mathematical fit to all the models, but best fits the Temkin isotherm model. Table 4-6 shows parameters and correlation coefficients of Langmuir, Freundlich and Temkin adsorption isotherms for sulphate loaded barium modified attapulgite.

Table 4-6: Parameters and correlation coefficient of Langmuir, Freundlich and Temkin

Langmuir			Freundlich			Temkin		
q_m (mg/g)	b (L/g)	R^2	K_f	n	R^2	A_t(L/g)	B(J/mol)	R^2
0.129	0.0369	0.9987	835.8	-1.867	0.9977	25.096	10.701	0.9991

The Temkin constant *B* is related to heat of sorption and indicates how much heat was required during the adsorption process. The Temkin adsorption isotherm assumes that the heat of adsorption decreases linearly with the sorption coverage due to adsorbent-adsorbate interactions [Jusoh et al., 2011].

4.10.2. Adsorption kinetics

Figure 4-16 is a plot of $log(q_e - q_t)$ *vs t* which has to be linear if the pseudo first order model is applicable.

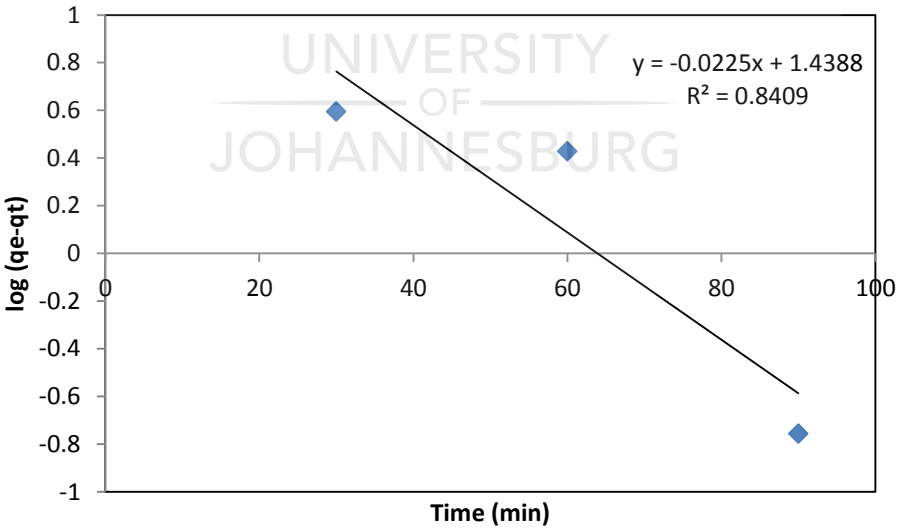

Figure 4-16: Plot for first order kinetic model for barium modified attapulgite

The square regression value of 0.84 indicates that the data does not clearly fit the first order kinetic model.

A plot of t/q_t versus t should be linear if the pseudo second-order kinetic model is applicable, and q_e and K_2 can be determined from the slope and intercept of the plot, respectively using equation 2-29 for pseudo second order kinetic model. Figure 4-17 shows a plot for second order kinetic model for barium modified attapulgite.

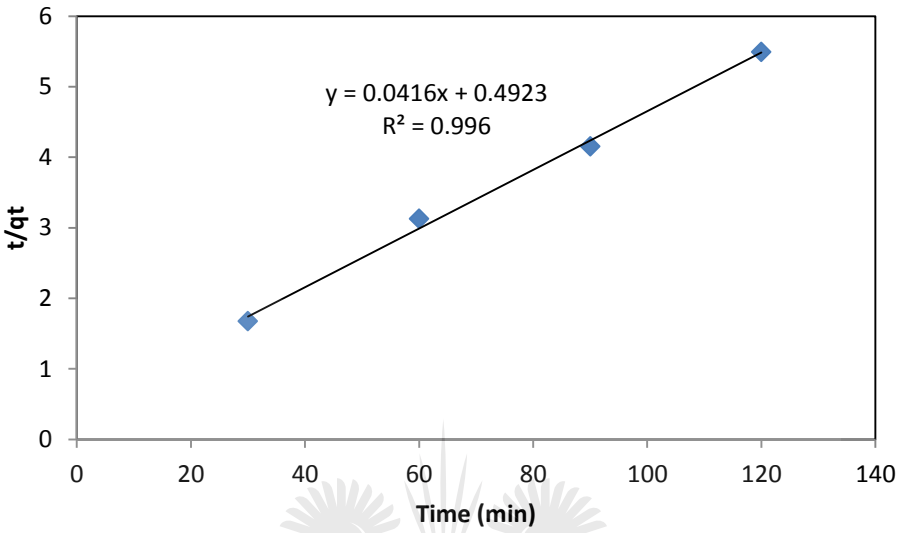

Figure 4-17: Plot for Second order kinetic model for barium modified attapulgite

An R^2 value of 0.996 was obtained, which indicates that the data fits the second order kinetic model. Further, the value of q_e was calculated to be 24.0 mol.kg^{-1} using eqn 2-30. The small difference of the q_e calculated from the equation 2-30 and the experimental q_e value of 21.9 mol.kg^{-1} indicates that the data fits the pseudo second order kinetic model. This model implies that the rate-limiting step is the surface adsorption that involves chemisorption, where the removal from a solution is due to physicochemical interactions between the two phases [Wang et al., 2007].

4.10.3. Adsorption thermodynamics

Table 4-7 shows the thermodynamic parameters for sulphate removal. Gibbs free energy (ΔG^o) was calculated using eqn. 2-36 and enthalpy (ΔH^o) and entropy (ΔS^o) were calculated using the Van't Hoff eqn. 2-37.

Table 4-7: Thermodynamic parameters for sulphate removal

Temperature (K)	K_{Do}	ΔG^o(KJ/mol)	ΔS^o(J/mol)	ΔH^o(J/mol)
298.15	0.1559	4607	6.174	1274.3
308.15	0.1195	5443		
318.15	-0.0926	-		

The positive value of entropy (ΔS^o) indicates the affinity of attapulgite for the sulphate ions and some structural changes in adsorbate and adsorbent interface [Gupta, 1998]. The low value of enthalpy energy (1274.3 J/mol) indicates that the reaction did not require a lot of heat to reach equilibrium. This is supported by the small difference in sulphate removal when the temperature was increased and the positive value of Gibbs free energy (ΔG^o) indicating that the reaction was not thermodynamically spontaneous.

4.10.4. Sorption Activation energy

The slope of a plot of lnK_2 *vs* $1/T$ (Fig 4-18) was used to calculate the sorption activation energy as presented in equation 2-35.

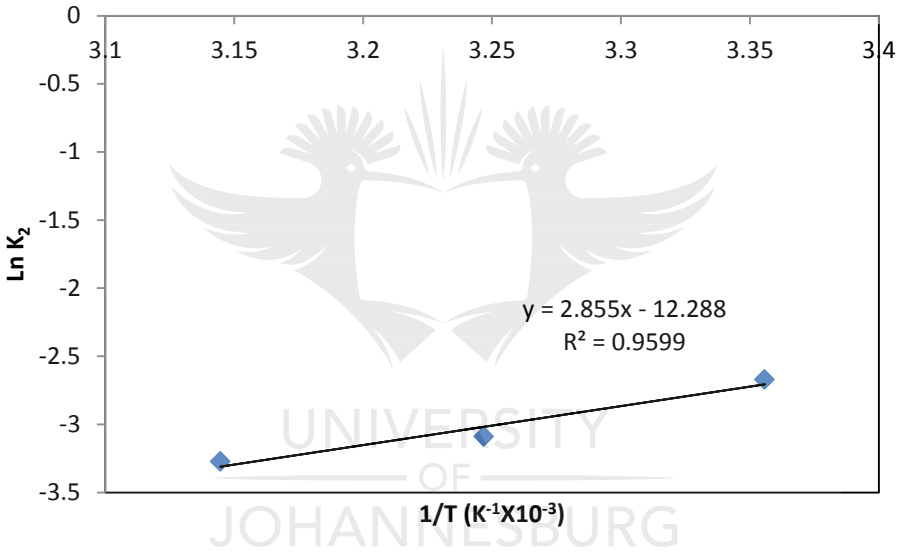

Figure 4-18: Arrhenius plots for the sorption of sulphate on AMD

Values of activation energy between 8.4 and 83.7 kJ/mol indicate chemisorption [Li et al., 2009]. The value of the activation energy (23.7 kJ/mol), which is calculated from the slope of corresponding ln K_2 vs 1/T, indicates chemisorption mechanism [Cao et al., 2014].

4.11. Conclusions

An increase in surfactant loading enhanced sulphate removal, as more sulphates were adsorbed when using higher concentrations of surfactants than lower concentrations. The order of the effectiveness of the utilised modifier surfactants to modify attapulgite for effective sulphate removal is Barium > TDTMA > HDTMA. At higher solid loading, more sulphates were adsorbed onto the clay surface.

The measurement of zeta potential provided evidence that modification of attapulgite made the clay more organophilic as supported by literature.

The difference in sulphate removal with temperature between 25 and 45^{o}C was not statistically significant, indicating that the reaction was not affected by temperature in this temperature range. XRD analysis showed that the surfactants were only adsorbed on the surface of the clay during the cation exchange process without destroying the crystalline structure of the clay. FTIR analysis confirmed that modification did take place. The experimental data best fitted the Temkin isotherm model and the second order kinetic model.

Chapter 5 : Mozambican Bentonite

5.1. Introduction

This chapter addresses characteristics of modified Mozambican Bentonite and its effect on the removal of sulphates from AMD.

5.2. Experimental

Modified Mozambican bentonite was used for the sorption experiments. The effects of agitation time, solid loading, temperature and surfactant loading on the removal of sulphates from AMD were investigated. Adsorption isotherms, kinetics and thermodynamic parameters were calculated from the data obtained. The materials and equipment used are described in Chapter 3 (Methodology).

5.3. TDTMA Modification

Modification was done using 200% CEC and experiments were done at 25^{o}C using 10% w/v clay to AMD. Figure 5-1 shows the effect of agitation time on sulphate concentration.

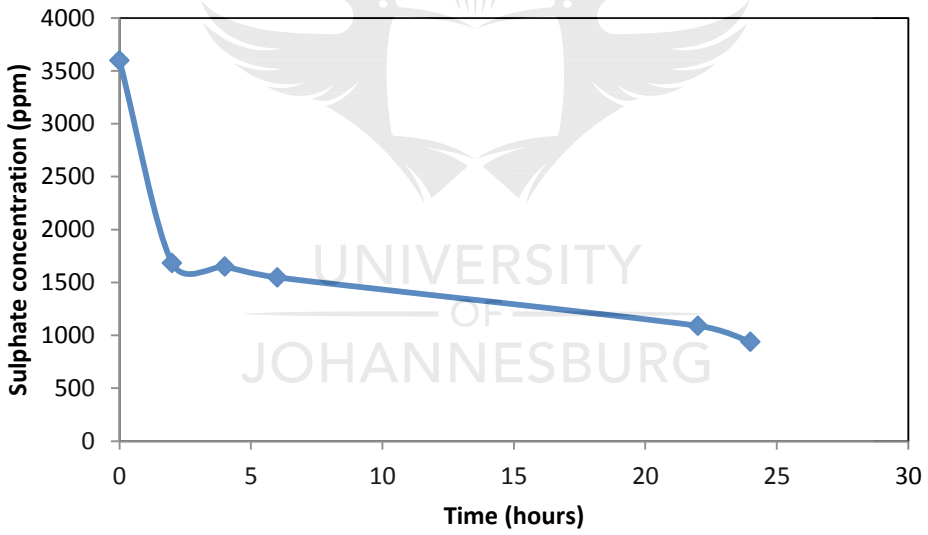

Figure 5-1: Effect of agitation time on residual sulphate concentration using TDTMA modified MB

Sulphate concentration reached its lowest point (from 3598.3 ppm to 937.3 ppm) after 24 h of mixing. The sulphate concentration decreased further with time, indicating that the reaction takes time to reach equilibrium.

Figure 5-2 shows the effect of agitation time on sulphate removal efficiency.

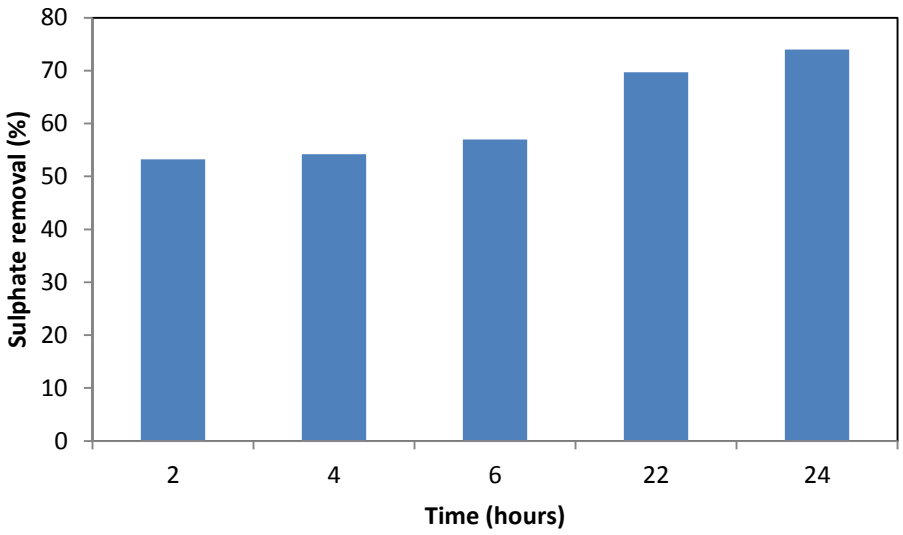

Figure 5-2: Effect of agitation time on sulphate removal using TDTMA modified MB

After 24 h of agitation, there was 73.9% sulphate removal. More sulphates were removed during longer periods of agitation. This implies that the adsorption of sulphates on the clay surface was time dependent.

5.4. HDTMA Modification

Modification was done using 200% CEC and experiments were done at 25^{o}C using 10% w/v clay to AMD. Figure 5-3 shows the effect of agitation time on sulphate concentration.

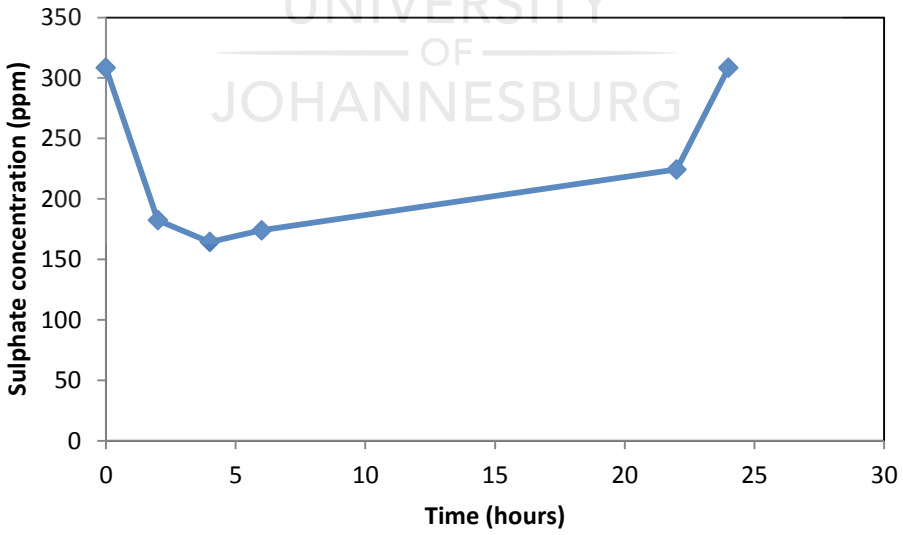

Figure 5-3: Effect of agitation time on sulphate concentration using HDTMA modified MB

Sulphate concentration reached its lowest point (from 308.4 ppm to 164.3 ppm) after 4 h of mixing.

It was observed that the sulphate concentration continued to rise again after 6 h and back to its original concentration after 24 h. The results show that the binding of sulphates onto the clay surface when using HDTMA as a surfactant, is a reversible process also shown in Fig. 5-4.

Figure 5-4 shows the effect of agitation time on sulphate removal efficiency.

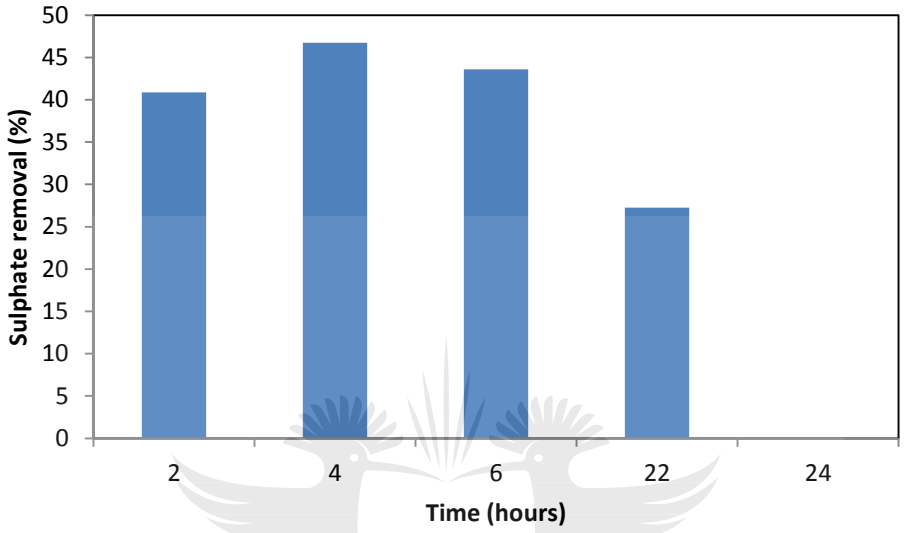

Figure 5-4: Effect of agitation time on sulphate removal using HDTMA modified MB

There was a maximum sulphate removal of 46.7% after 4 h of agitation, which is very low when compared to the maximum sulphate removal, achieved using TDTMA.

5.5. $BaCl_2$ Modification

Modification was done using 1 and 2 M $BaCl_2$. The experiments were done at 25^{o}C using 10% w/v clay to AMD. Figure 5-5 shows the effect of agitation time on sulphate concentration using the two concentrations of $BaCl_2$.

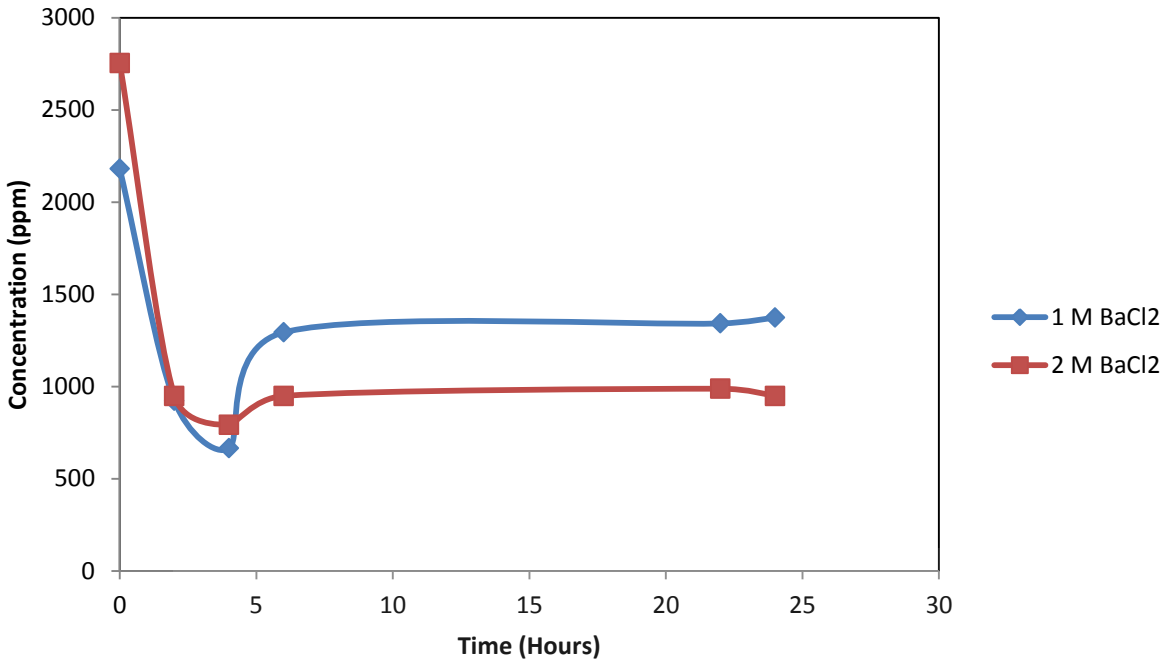

Figure 5-5: Effect of agitation time on residual sulphate concentration using $BaCl_2$ modified MB

Sulphate concentration reached the lowest point (from 2181 ppm to 664 ppm) after 4 h of mixing with 1 M $BaCl_2$ and reached the lowest point (from 2752.9 ppm to 792.1 ppm) after 4 h of mixing with 2 M concentration. This resulted in 69.5% and 71.2% sulphate removal using 1 M and 2 M concentration respectively.

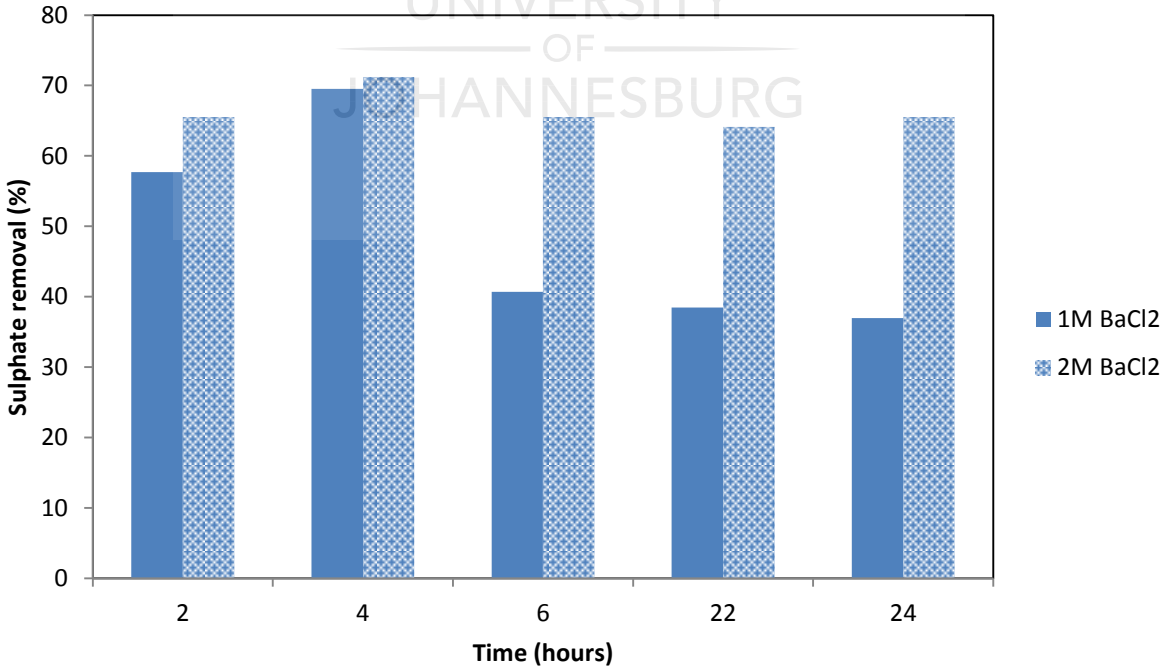

Figure 5-6: Effect of agitation time on sulphate removal using $BaCl_2$ modified MB

The amount of sulphates removed decreased from 6 h of agitation onwards as the sorption process starts going through adsorption and desorption cycles.

5.6. Measurement of Zeta Potential

Raw MB and MB modified with 1 M $BaCl_2$, 200% CEC TDTMA and 200% CEC HDTMA were taken for measurement of zeta potential. Table 5-1 shows the zeta potential data.

Table 5-1: Zeta potential for MB samples

Sample	Zeta potential (mV)
Raw MB	-9.69
Barium modified	-5.98
TDTMA modified	37.2
HDTMA modified	32.3

The raw sample of MB had a net negative charge as supported by literature. After modification, the zeta potential values moved towards the positive side, implying that modification of MB made it more organophilic, hence attracting sulphate anions. TDTMA modified MB had the most positive value of zeta potential, hence it removed the highest amount of sulphates from AMD. Zeta potential values of ±30 mV are considered to be a suitable threshold for stability [Barnes, 1992]. Therefore, clays modified with TDTMA and HDTMA at 200% CEC will aggregate in solution reducing the surface area available for adsorption.

5.7. Solid loading

Mozambican bentonite modified with TDTMA was used to carry out further experiments on solid loading, the effect of temperature and CEC, because it had shown a better ability to remove sulphates from AMD. Experiments were conducted at different solid loadings i.e. 2%, 6% and 10% w/v clay to AMD and 25^{o}C, then analysed. Figure 5-7 shows the effect of solid loading on sulphate removal.

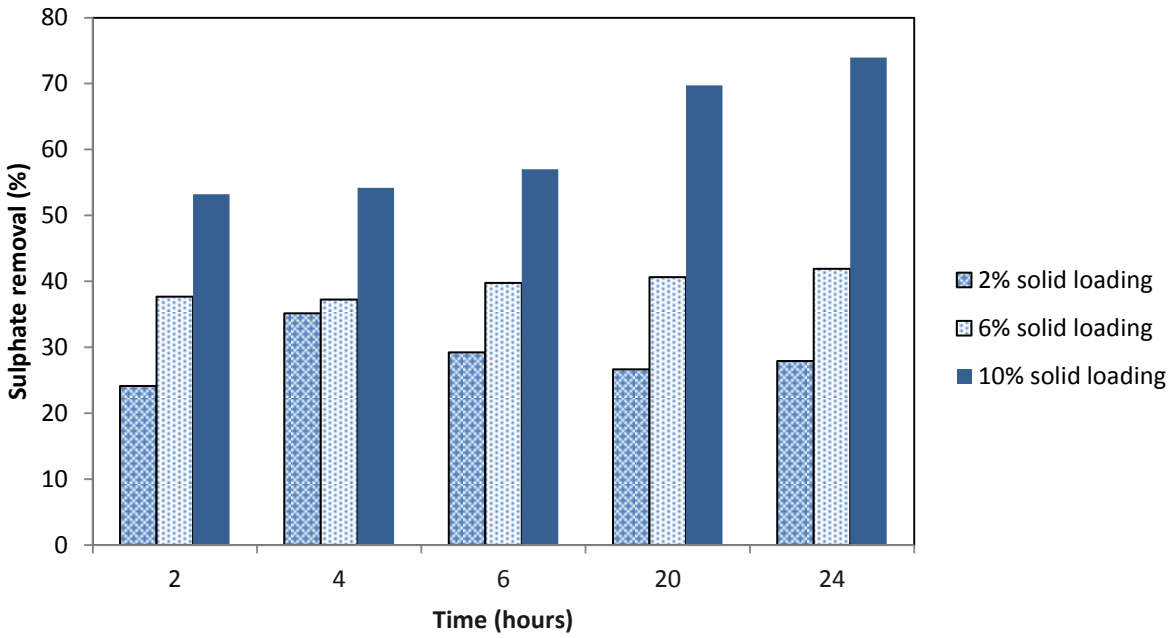

Figure 5-7: Effect of solid loading on sulphate removal using TDTMA modified MB

It was observed that at higher solid loading (10%), more sulphates were adsorbed by the clay. A maximum of 73.9% sulphates were removed after 24 h of mixing, while only 27.9% and 41.9% were removed using 2 and 6% solid loading respectively using the same time and conditions. This means that at higher solid loadings, there are more adsorption sites and thus, the higher sulphate removal [Namasivayam and Sangeetha, 2008]. It was also observed that at 2% solid loading, sulphate removal dropped after 4 hours of agitation and then increased again after 20 hours of agitation. This implies that the binding of sulphates onto the clay surface when using TDTMA modified MB, is a reversible process at lower surfactant loadings.

5.8. Effect of temperature

Samples of MB modified with TDTMA using 200% CEC and 10% w/v clay to AMD were further studied for the effect of temperature on sulphate removal. Figure 5-8 shows the effect of temperature on sulphate removal.

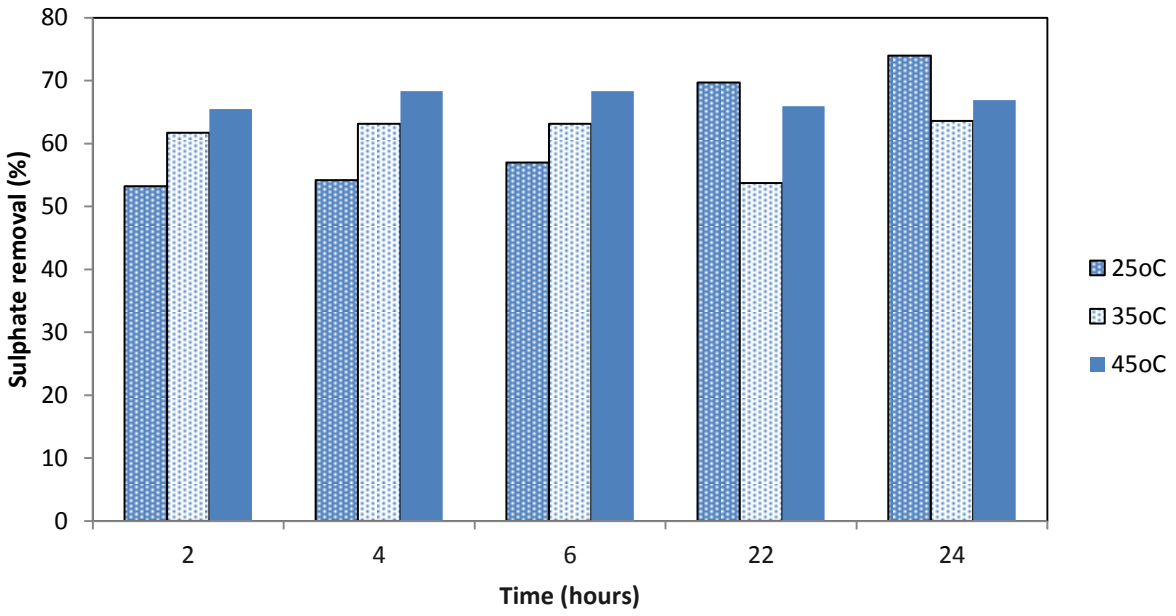

Figure 5-8: Effect of temperature on sulphate removal using TDTMA modified MB

At different temperatures, sulphate removal is consistent for the first 6 hours, then the trend changes for 35°C and 45°C, but remains the same for 25°C. For temperatures at 35°C and 45°C, the sample starts to undergo adsorption-desorption cycles after long hours of agitation.

5.9. Effect of TDTMA loading

Figure 5-9 shows the effect of TDTMA loading on sulphate concentration.

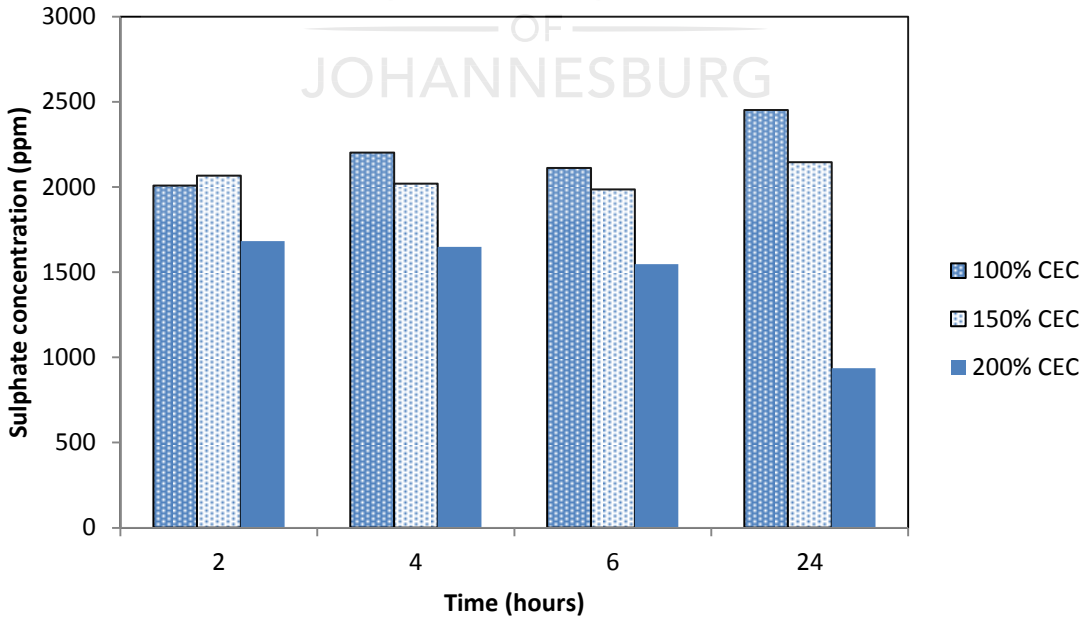

Figure 5-9: Effect of TDTMA loading on sulphate concentration using MB

An increment of surfactant loading from 100% CEC to 200% CEC decreased sulphate concentration from 3598 ppm to a minimum of 937 ppm during adsorption studies.

Figure 5-10 shows the effect of surfactant loading on sulphate removal.

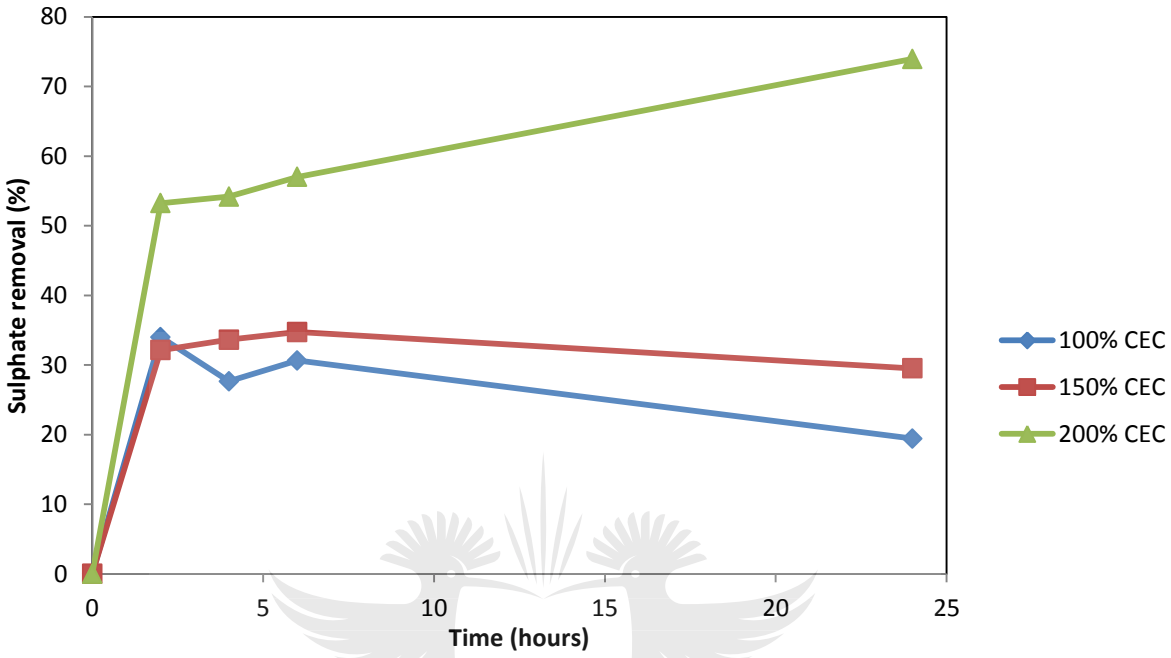

Figure 5-10: Effect of TDTMA loading on sulphate removal using MB

At CEC lower than 200%, sorption was reversible; hence less sulphates were removed from the AMD sample. This is because there were not enough sites of adsorption on the clay surface. At 200% surfactant loading, more sulphates (73.9%) were removed from the AMD sample.

5.10. Characterization

5.10.1. XRF analysis

Table 5-2 shows the chemical composition of raw MB, TDTMA modified MB and sulphate loaded MB modified with TDTMA.

Table 5-2: XRF results for MB at different stages

Component	Raw MB	TDTMA modified	SO_4^{2-} loaded
		Wt%	
F	0.308	0.199	0.237
Na	0.792	1.03	0.204
Mg	3.16	2.86	2.05
Al	11.8	9.72	11.0
Si	79.2	70.9	75.6
P	0.0114	0.0125	0.0122
S	0.0343	0.0671	1.21
Cl	0.787	0.449	0.163
K	0.164	0.164	0.163
Ca	0.402	0.413	0.290
Ti	0.247	0.236	0.256
Mn	0.0102	0.0169	0.0285
Fe	2.76	2.59	2.93
Ni	0.00420	0.00610	0.00650
Zn	0.0286	0.0267	0.0288
Br	0.00420	11.1	5.46
Sr	0.00720	0.00700	0.00260
Y	0.0943	0.0139	0.0128
Zr	0.0573	0.0482	0.0579
Ba	0.145	0.0986	0.247

The major constituent of MB was silica. The Na content in MB is high due to ion exchange during activation. After the modification with TDTMA there was an increase in bromine due to the adsorption of TDTMA bromide onto the clay surface. There was an increase in sulphur ions from the raw MB to the sulphate loaded sample. This indicates that sulphates were adsorbed from the AMD sample to the MB surface. It is worth noting that XRF is a semi quantitative analysis technique hence results are relative to the total constituent of the material analysed.

5.10.2. XRD analysis

Figure 5-11 shows the XRD spectrum for raw MB, barium modified, TDTMA modified, HDTMA modified and TDTMA modified sulphate loaded MB as it showed the highest removal of sulphates from AMD.

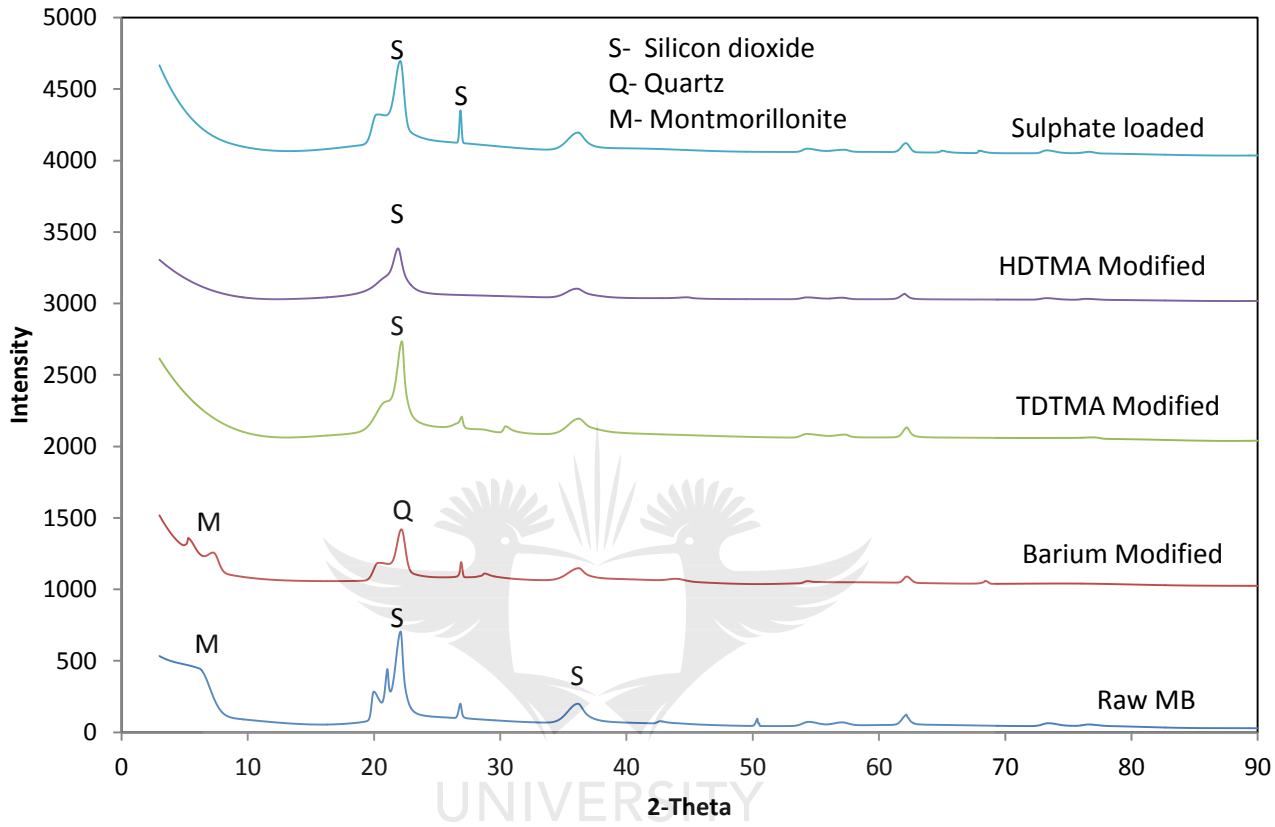

Figure 5-11: XRD of MB at different stages

The major constituents of raw MB were silicon dioxide (48%) and is closer to what was reported by Vega et al., 1995 and montmorillonite (48%) as supported by the XRF results. The main peak for SiO_2 was at 21.05^o and basal spacing of 4.22 Å and the main peak for montmorillonite was at 6.15^o with basal spacing of 14.36 Å, as reported by previous researchers (Silva et al., 2014). The new peak on the sulphate loaded sample at 26.8^o is formed by the adsorption of sulphates onto the clay surface.

5.10.3. FTIR analysis

Figure 5-12 shows the FTIR spectra of raw MB, modified MB and solid loaded MB modified with TDTMA as it showed the highest sulphate removal from AMD.

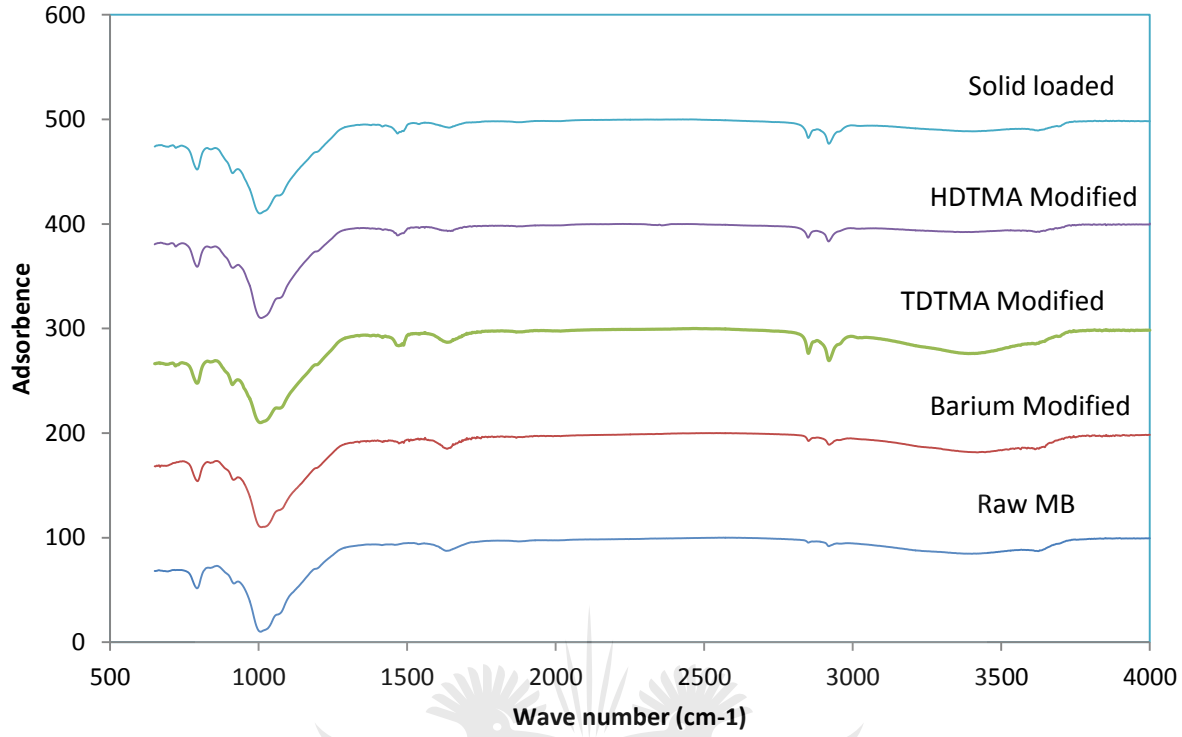

Figure 5-12: FTIR of MB at different stages

The bands at 2852 and 2921 cm^{-1}, which are not visible on the raw sample, are evidence of organification by a physical adsorption effect as the methyl groups and of the surfactants and barium attach to the clay sample [Wright & Hunter, 1947 and Xiping et al., 2008]. The peaks are stronger on the TDTMA modified sample, which explains why TDTMA modified MB removed the highest amount of sulphates from AMD. The new peaks that formed at around 1400 cm^{-1} on the TDTMA and HDTMA modified clay can be assigned to the crystal water of the organoclays [Xiping et al., 2008].

The band at 1077 cm^{-1} is related to Si–O (Si,Al) bridges vibrations and the bands at 913 cm^{-1} to Al–OH (octahedral coordination of Al) vibrations [Mozgawa et al., 2009]. It is possible to suppose that the growing content of sorbed ions causes a probable partial transfer of quartz grains of colloidal sizes to the solution as a suspension. This causes a relative decrease on 1077 cm^{-1} band and increase in 913 cm^{-1} band intensities [Hrachová et al., 2007., Madejova., 2003., Xuea et al., 2007]. Attachment of the modifiers on the clay surface are visible on the FTIR on bands in the range from3000-4000 cm^{-1}.

5.10.4. SEM analysis

The morphology of MB was analysed using SEM. Figure 5-13 shows the morphology of the raw and modified clay MB and the Energy Dispersive Spectroscopy (EDS) for the sulphate loaded MB which was modified with TDTMA, as it showed higher removal of sulphates from AMD.

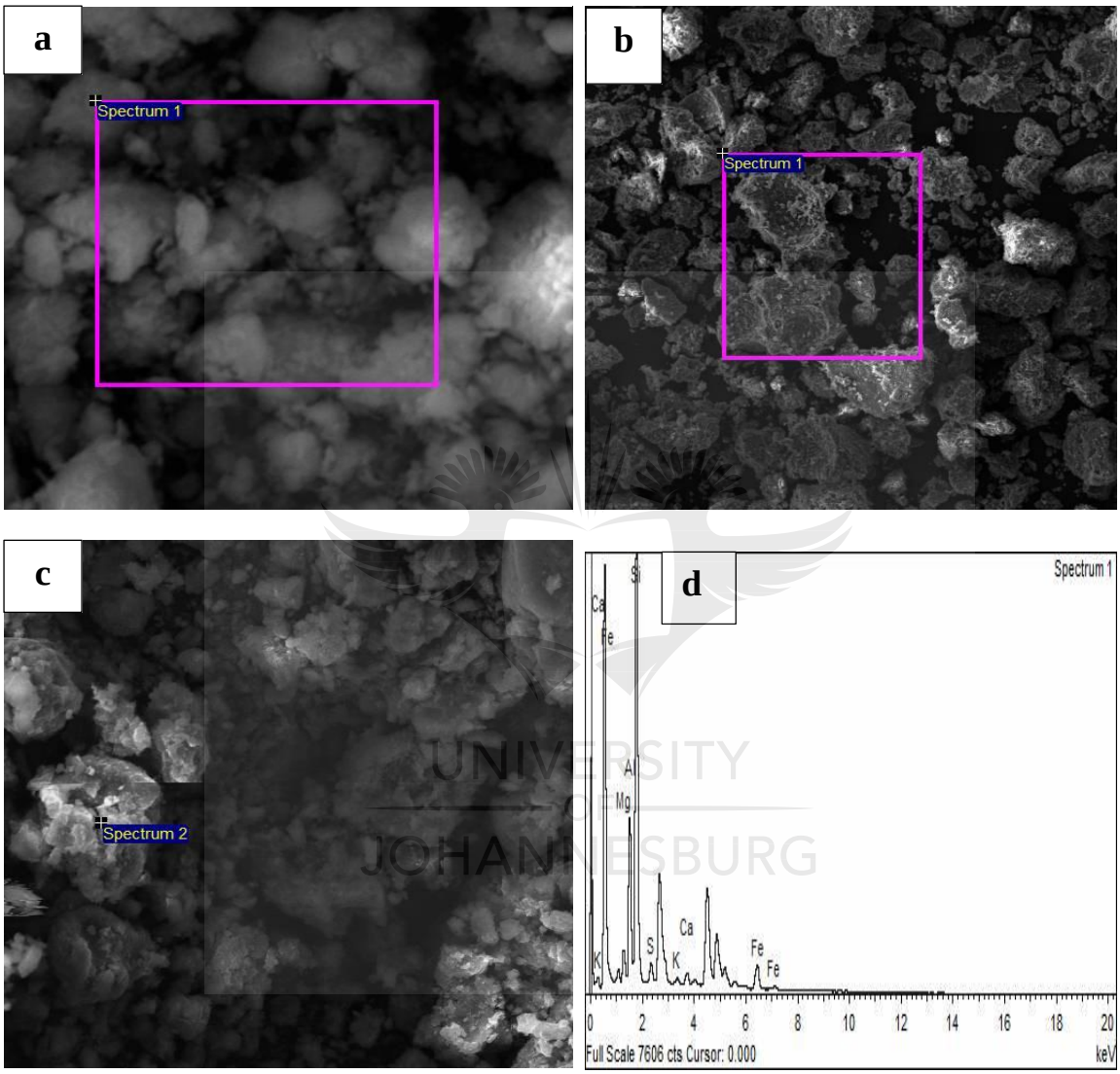

Figure 5-13: SEM Morphology of MB. (a): raw MB, (b):TDTMA Modified, (c):TDTMA Modified sulphate loaded, d:sulphate loaded EDS

The morphology of raw MB, Fig. 5-13a, shows that the clay is clogged together in a ball-like structure, the biggest constituent composition being SiO_2 and Al_2O_3 as reported by previous researchers [Muhammad et al., 2013]. Comparing Fig. 5-13a and Fig. 5-13b, it is notable that the organically modified MB showed better dispersion than raw MB, because of the effect of long hydrophobic alky group of the surfactant TDTMA [Xiping et al., 2008]. Increased porosity is the result of an increase of the distances between clay layers, upon incorporation

of the molecule of the surfactant, which enables water molecules to more easily penetrate into the inner part of the composite [Stojiljkovic et al., 2013]. Adsorption of sulphates on the surface of the clay is identified as the lighter shade on Fig. 5-13c. The TDTMA modified MB EDS, Fig. 5-13d, showed that the main constituent of MB is SiO_2 (85%) which was comparable with data from XRD and XRF, where the main constituent of the sample was also confirmed as SiO_2. Trace amounts of sulphur of 4.3% were detected during analysis.

5.11. Thermodynamics and kinetic studies

5.11.1. Adsorption isotherms

Figure 5-14 shows the plots of Temkin, Langmuir and Freundlich adsorption isotherms obtained at 25^{o}C, which have to be linear to fit the isotherm models respectively.

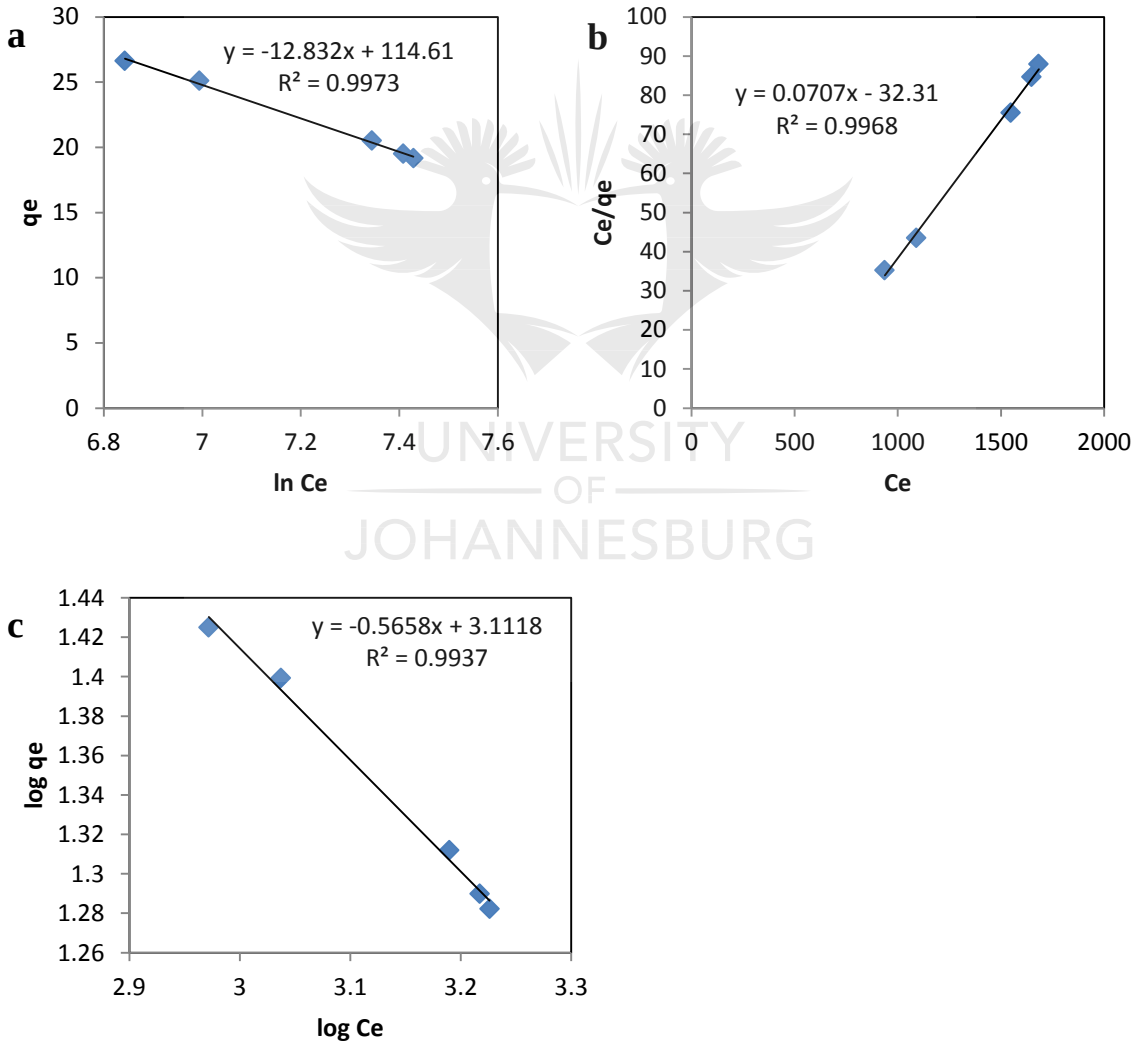

Figure 5-14: Adsorption isotherm models of barium modified attapulgite. (a): Temkin isotherm, (b): Langmuir isotherm, (c): Freundlich isotherm.

The high values of R^2 (close to 1) suggest that the experimental data exhibit a very good mathematical fit to all the models, but best fits the Temkin isotherm model.

Table 5-3 shows parameters and correlation coefficient of Langmuir, Freundlich and Temkin adsorption isotherms for sulphate loaded TDTMA modified MB.

Table 5-3: Parameters and correlation coefficient of Langmuir, Freundlich and Temkin

Temperature (C)	Langmuir			Freundlich			Temkin		
	q_m (mg/g)	b (L/g)	R^2	K_f	n	R^2	A_t(L/g)	B(J/mol)	R^2
25	14.14	0.00219	0.9968	1293	-1.767	0.9937	75.67	12.83	0.9973
35	12.21	0.00163	0.9995	3726	-1.410	0.9991	61.04	14.84	0.9999
45	16.13	0.00255	0.9999	788.0	-2.030	0.9998	90.42	11.87	0.9997

The Temkin constant *B* is related to heat of sorption and indicates how much heat was required during the adsorption process. The Temkin adsorption isotherm assumes that the heat of adsorption decreases linearly with the sorption coverage due to adsorbent-adsorbate interactions [Jusoh et al., 2011].

5.11.2. Adsorption kinetics

Figure 5-15 is a plot of $log(q_e - q_t)$ *vs t* which has to be linear if the pseudo first order model is applicable.

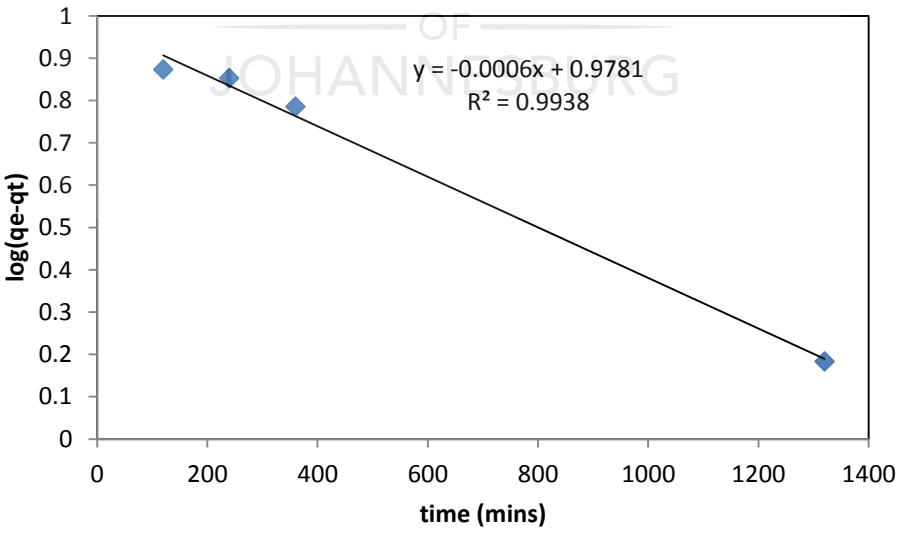

Figure 5-15: First order kinetics model plot

A high square regression value of 0.9938 was obtained from the plot, however, a value of 9.5 mol.kg^{-1} was calculated as q_e from eqn 2-29, which was compared with the experimental q_e value of 26.6 mol.kg^{-1}. The difference in the two values indicates that the first order kinetic model does not adequately model the experimental data.

The plot of t/q_t versus t should give a straight line if the pseudo second-order kinetic model is applicable, and q_e and K_2 can be determined from the slope and intercept of the plot, respectively using eqn 2-30 for pseudo second order. Figure 5-16 shows the plot for the second order kinetic model.

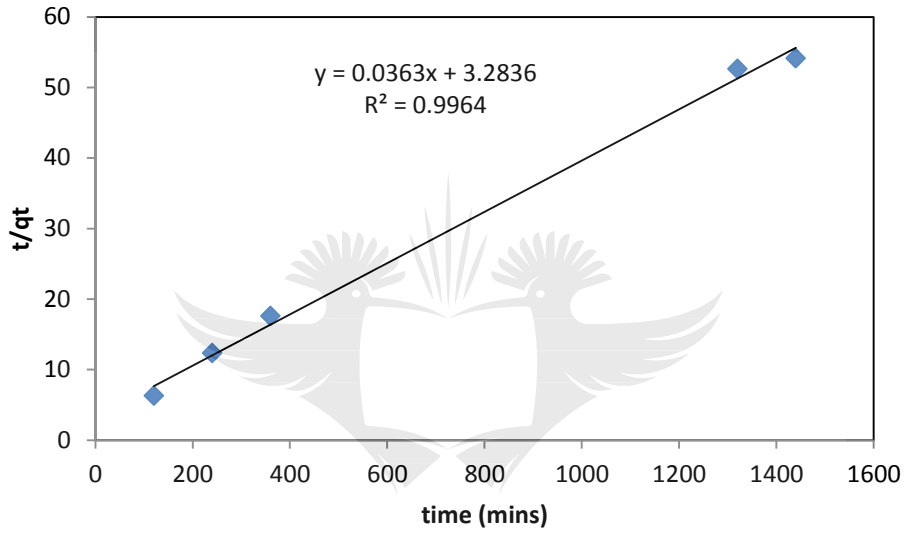

Figure 5-16: Second order kinetics model plot

An R^2 value of 0.9964 was obtained from the second order kinetic plot. The value of q_e was calculated to be 27.5 mol.kg^{-1} from eqn 2-29. The small difference of q_e values obtained from eqn 2-29 and the experimental q_e of 26.6 mol.kg^{-1} indicates that the data fits the pseudo second order kinetic model. This model implies that the rate-limiting step is the surface adsorption that involves chemisorption, where the removal from a solution is due to physicochemical interactions between the two phases [Wang et al., 2007].

5.11.3. Adsorption thermodynamics

Figure 5-17 shows the variation of q_e with increase in temperature.

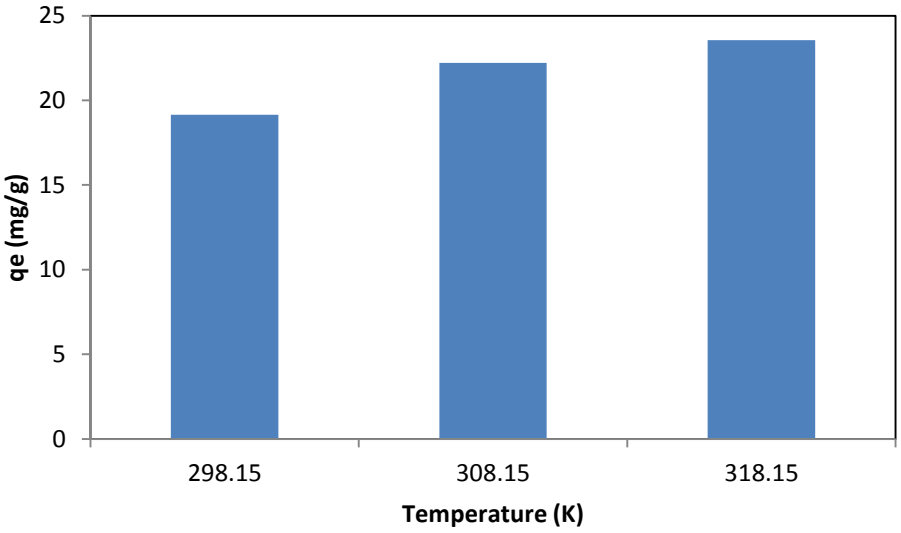

Figure 5-17: Variation of q_e with increase in temperature

There was an increase in q_e values with increase in temperature indicating that the adsorption of sulphate ions on AMD becomes more favourable at higher temperature, indicating an endothermic process. Similar results have also been reported with the use of coconut coir pith as an adsorbent for sulphate ions [Namasivayam and Sangeetha, 2008].

Table 5-4 shows the thermodynamic parameters for sulphate removal. Gibbs free energy (ΔG^o) was calculated using eqn. 2-36 and enthalpy (ΔH^o) and entropy (ΔS^o) were calculated using eqn. 2-37.

Table 5-4: Thermodynamic parameters for sulphate removal

Temperature (K)	K_{Do}	ΔG^o(KJ/mol)	ΔS^o(J/mol)	ΔH^o(J/mol)
298.15	0.1219	5217	1.955	1049
308.15	0.1148	5543		
318.15	0.1257	5483		

The positive value of entropy (ΔS^o) indicates the affinity of the activated MB for the sulphate ions and some structural changes in adsorbate and adsorbent interface [Gupta, 1998]. The positive value of enthalpy energy (1049 J/mol) indicates that the reaction was endothermic and the positive value of Gibb's free energy (ΔG^o) indicates that the reaction was not thermodynamically spontaneous.

5.11.4. Sorption activation energy

The slope of a plot of lnK_2 *vs* $1/T$ (Fig. 5-18) was used to calculate the sorption activation energy as presented in equation 2-35.

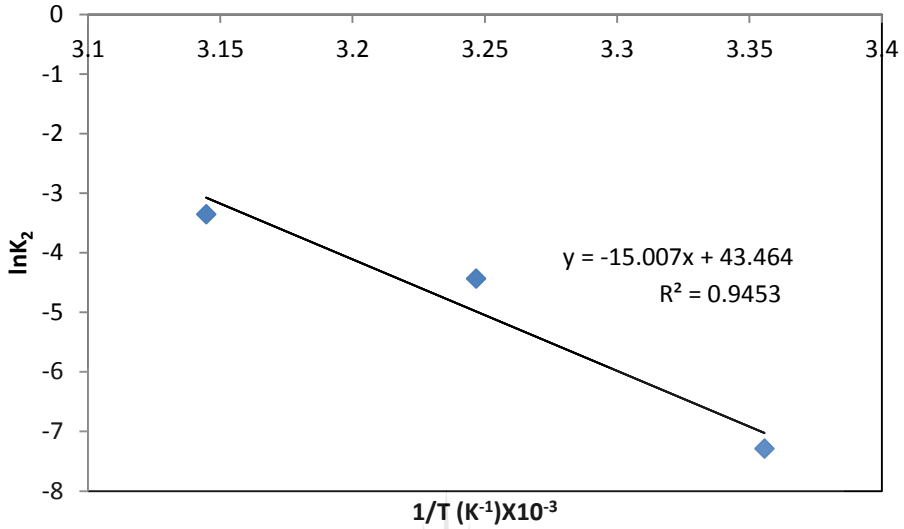

Figure 5-18: Arrhenius plots for the sorption of sulphate on AMD

Activation energy values of less than 4.2 kJ/mol are associated with physical sorption [Aksu, 2002 and Aksu & Karabayır, 2008]. The negative value of the activation energy (-124.8 kJ/mol) obtained from the experimental data therefore suggests physisorption mechanism [Cao et al, 2014].

5.12. Conclusions

The order of the effectiveness of the utilised surfactants to modify MB was TDTMA > Barium > HDTMA. The surface of MB was rendered more organophilic through the modification process, as the values of zeta potential became more positive after modification. At higher solid loading, more sulphates were adsorbed onto the clay surface. Sulphates were dominantly removed from the AMD sample at higher temperatures during the first 6 h of agitation then the reaction started to undergo an adsorption-desorption process, assuming that this was not a thermodynamically spontaneous reaction. An increment in surfactant loading enhanced sulphate removal, as more sulphates were adsorbed when using higher concentrations of surfactants than lower concentrations. The experimental data best fitted the Temkin isotherm model. The small difference between the experimental and calculated values of q_e, suggested that the experimental data fits the second order kinetic model. The value of the activation energy indicated a physisorption mechanism.

Chapter 6 : Conclusions

Modification of both attapulgite and MB enhanced sulphate removal from the AMD. After barium modification of attapulgite, 70.8% sulphates were removed whilst modification of MB using TDTMA resulted in 74.0% sulphate removal. This was higher when compared to previous work done using rice husks and Hendrina FA, which removed 40 and 71% sulphates respectively, but lower when compared to work done by Ntuli et al., 2014 using FA as an adsorbent; however 50% w/v AMD to FA was used during this experiment. The removal of sulphates using modified MB was a good indication that the surfactants used rendered the surface of the clay positive, thus attracting sulphate anions. Higher CEC percentages resulted in an increase in sulphate removal for both clay samples used. This implies that at higher surfactant loadings, there are more anion exchange sites which aid in sulphate removal. An increase in solid loading for both clays resulted in higher sulphate removal.

A new peak formed on the XRD spectra of the MB sulphate loaded sample was an indication that sulphates were adsorbed onto the clay surface following exposure to AMD during adsorption studies. XRF analysis of MB also gave evidence that sulphates were attached to the clay surface, as sulphate ions increased from 0.03% to 1.2%.

XRF characterization of attapulgite showed that there was an increase in sulphate ions from 0.3% to 3.1% after adsorption experiments, which indicates that sulphates were adsorbed onto the clay surface during adsorption studies.

The process of sulphate removal using MB was endothermic, as higher recovery of sulphates was obtained at higher temperatures. However, for attapulgite temperature had an insignificant effect on sulphate removal from AMD, as the sulphate concentration in the liquor did not change much when the temperature was varied. A thermodynamic and kinetic study of both clays showed that the data for both clays fitted the second order kinetic model and Temkin adsorption isotherm model. The value of the activation energy (23.7 kJ/mol) for barium modified attapulgite indicates a chemisorption mechanism; while physisorption was evident by the value of -124.8 kJ/mol for TDTMA modified MB.

Chapter 7 : Recommendations

From the results obtained from organic and barium modification of both clays, it is recommended that organic modification of clay should be utilised other than $BaCl_2$ as $BaCl_2$ is toxic and a more expensive method requiring high quantities. More research should be done on different modifiers in order to achieve a higher sulphate removal whilst using the least amount of clay. This can also be done by utilising a reactor and a catalyst to speed up the reaction. Studies on how the sulphate loaded clay can be re-used should also be explored. This will help to avoid huge clay dumps in the environment and also in understanding the environmental impacts of clays generated from AMD treatment.

References

Abdelaal, A.M (2004) Using a natural coagulant for treating wastewater. Eighth International Water Technology Conference, IWTC8 2004, Alexandria, Egypt 2004, 781-792 pp.

Ahmaruzzaman, M (2008) Adsorption of phenolic compounds on low-cost adsorbents: a review. Advances in Colloid and Interface Science. 143, 48–67 pp.

Aksu, Z (2002) Determination of the equilibrium, kinetic and thermodynamic parameters of the batch biosorption of nickel(II) ions onto Chlorella vulgaris. Process Biochemistry (38) 89-99 pp.

Aksu, Z., Karabayır, G (2008) Comparison of biosorption properties of different kinds of fungim for the removal of Gryfalan Black RL metal-complex dye, Bioresource Technology 99, 7730-7741 pp.

Arthur G, Clelyi and Robert W. Doehler (1961) Sypnosium on Industrial applications of bentonite. Clays and Clay minerals, 272-283 pp.

Bae, J.A., Song, D., Jeon, Y (2000) Adsorption of anionic dye and surfactant from water onto organomontmorillonite. Separation Science and Technology. 353 pp.

Barhoumi, M., Beurroies, I., Denoyel, R., Said, H., Hanna, K (2003) Coadsorption of phenol and nonionic surfactants onto clays. 223, 63–72 pp.

Barnes, H.A., (1992), Recent advances in rheology and processing of colloidal systems, The 1992 IChemE Research Event, IChemE, Rugby, 24-29 pp.

Barson, M.S., Van Niekerk, P.H. & van Rooyen, J.A (1997) Overview of Water Resources Availability and Utilization in South Africa. 151 pp.

Baskaralingam, P., Pulikesi, M., Elango, D., Ramamurthi, V., Sivanesan, S (2006) Adsorption of acid dye onto organobentonite. Journal of Hazardous Materials, 138–144 pp.

Beer, J (2000) Effects of Coal-Mine Drainage on Stream Water Quality in the Allegheny and Monongahela River Basins— Sulfate Transport and Trends, 23 pp.

Bergaya, F (1997) CEC of clays: Measurement by adsorption of a copper ethylenediamine complex. Applied Clay Science 12, 275-280 pp.

Bhattacharyya, G. and Gupta, S. (2007) Adsorptive accumulation of Cd(II), Co(II), Cu(II), Pb(II), and Ni(II) from water on montmorillonite: Influence of acid activation, Journal of Colloid and Interface Science 310, 411–424 pp.

Bish, D. (1993) Mineralogy of clay and zeolite dusts (exclusive of 1: 1 layer silicates). 139-184 pp.

Bonczek, J.L., Harris, W.G., and Nkedi-Kizza, P (2002) Monolayer to bilayer transitional arrangements of hexadecyltrimethylammonium cations on Na-montmorillonite, Clays and Clay Minerals 50 (1) 11–17 pp.

Bosman, D.J., Clayton, J.A., Maree J.P. and Adlem, C.J., (2006) Removal of sulphate from mine water with barium sulphide, Mine Water and the Environment, International Mine Water Association, 149-161 pp.

Bowell, R.J (1998) A review of sulfate removal options for mine waters. IMWA Proceedings 329-339 pp.

Cao, W., Dang, Z., Yuan, B., Shen, C., Kan, J., Xue, X (2014) Sorption kinetics of sulphate ions on quaternary ammonium-modified rice straw, Journal of Industrial and Engineering Chemistry, 20, 2603–2609 pp.

Chang, I.S., Shin, P.K., Kim, B.J (2000) Biological treatment of acid mine drainage under sulfate reducing conditions with solid waste materials as substrate.

Chockalingam, E. and Subramanian S (2006) Studies on removal of metal ions and sulphate reduction using rice husk and Desulfotomaculum nigrificans with reference to remediation of acid mine drainage. Chemosphere, 62(5) 699-708 pp.

Christensen, B., Laake, M., Lien, T. (1990) Treatment of acid mine water by sulfate reducing bacteria: Results from a bench scale experiment.

Cravotta, C.A., Brady, K.B.C., Smith, M.W. and Beam, R.L. (1990) Effectiveness of the addition of alkaline materials at surface coal mines in preventing or abating acid mine drainage.

Dabrowski, A. (2001). Adsorption- from theory to practice. Advanced Colloid Interface Science, 93, 135-224 pp.

Dada, A.O., Olalekan, A., Olatunya, A., Dada, O. (2012) Langmuir, Freundlich, Temkin and Dubinin-Radushkevich Isotherms Studies of Equilibrium Sorption of Zn2+ Unto Phosphoric Acid Modified Rice Husk. Journal of Applied Chemistry, 3(1) 38-45 pp.

Davies, B.R., O'keeffe, J.H. and Snaddon, C.D. (1993). A Synthesis of the Ecological Functioning, Conservation and Management of South African River Ecosystems. Water Research Commission, Pretoria. Report TT62/932.

Demabas, E., Kobya, M., Sulak, M.T. (2008). Adsorption kinetics of a basic dye from aqueous solutions onto apricot stone activated carbon. Bioresource Technology, 99, 5368-5373 pp.

Department of Water Affairs (2012) Feasibility Study for a Long-Term Solution to Address the Acid Mine Drainage Associated with the East, Central and West Rand Underground Mining Basins, Inception Report Study Report No. 1 [P RSA 000/00/16112] Aurecon Report No.: 6163, 1-122 pp.

Dubinin, M., Radushkevich, L. (1947) The equation of the characteristic curve of the activated charcoal, Proc. Acad. Sci. USSR Phys. Chem. Sect. 55, 331–337 pp.

DWAF (2007) Best Practice Guideline No. H4: Water Treatment (Pretoria: Department of Water Affairs and Forestry).

EL-Kamash, A., Kaki, A., EL-Geleel, M.A., (2005). Modeling batch kinetics and thermodynamics of zinc and cadium ions removal from waste solutions using synthetic zeolite. American Journal of Hazardous Material, B127, 211-220 pp.

Fripp, J., Ziemkiewicz, F., Charkavork, H., (2000) Acid Mine Drainage treatment. EMRRP Technical Notes Collection (ERDC TN-EMRRPSR-14), U.S. Army Engineer Research and Development Center, 1-7 pp.

Gan, F., Zhou, J, Wang, H., Du, C., Chen, X., (2009). Removal of phosphate from aqueous solution by thermally treated natural palygorskite. Water Research, 43, 2907-2915 pp.

Gazea, B., Adam, K. and Kontopoulos A. (1996) A review of passive systems for the treatment of acid mine drainage. Minerals Engineering, 9(1) 23-42 pp.

Gonzalez-Garcıa, C.M., Gonzalez-Martın, M.L., Gonzalez, J.F., Sabio, E., Ramiro, A., Ganan, J. (2004) Nonionic surfactants adsorption onto activated carbon. Influence of the polar chain length, Powder Technology 148, 32–37 pp.

Greenwood, R., Kendall, K (1999) Electroacoustic studies of moderately concentrated colloidal suspensions. Journal of the European Ceramic Society 19 (4) 479–488 pp.

Groisman, L., Rav-Acha, C., Gerstl, Z., and Mingelgrin, U. (2004) Sorption and detoxification of toxic compounds by a bifunctional organoclays. Journal of Environmental Quality, 33(5) 1930–1936 pp.

Gunay, A., Arslankaya, E., Tonsun, I., (2007). Lead removal from aqueous solution by natural and pretreated clinoptilolite: adsorption equilibrium and kinetics. Journal of Hazardous Materials, 146,362-371 pp.

Gupta, V.K. (1998). Equilibrium uptake, sorption dynamics, process development and column operations for the removal of copper and nickel from aqueous solution and wastewater using activated slag, a low-cost adsorbent. Industrial & Engineering Chemistry Research 37,192-20 pp.

Gurses, A., Dogar, C., Yalcın, M., Acıkyıldız, M., Bayrak, R., Karaca, S. (2006) The adsorption kinetics of the cationic dye, methylene blue, onto clay, Journal of Hazardous Materials B131, 217–228 pp.

Hameed, B.H. (2007) Equilibrium and kinetics studies of 2,4,6-trichlorophenol adsorption onto activated clay. Colloids and Surfaces A: Physicochemical and Engineering Aspects. 307, 45–52 pp.

Hameed, B.H. (2007) Equilibrium and kinetics studies of 2,4,6-trichlorophenol adsorption onto activated clay. Colloids and Surfaces A: Physicochemical and Engineering Aspects. 307, 45–52 pp.

Han, Y., Huifang, C., Dajun, C. (2010) Morphology and mechanical properties of polyacrylonitrile/attapulgite nanocomposite. Journal of Materials Science, 45(9) 2372-2380 pp.

Haroon, H., Waseem, A., and Mahmood, Q. (2013) Treatment and reuse of wastewater from beverage industry," Journal of Chemical Society of Pakistan, 35, 5–11 pp.

Hill A.V. (1910) The possible effects of the aggregation of the molecules of haemoglobin on its dissociation curves, J. Physiol. (London) 40, iv–vii pp.

Hlabela P., Maree J., Bruinsma D., (2007) Mine Water Environ. 26 (1) 14–22 pp.

Ho, Y.S., McKay, G. (1998). A comparison of chemisorption kinetic models applied to pollutant removal on various sorbents. Transactions of the Institution of Chemical Engineers 76B, 332-339 pp.

Ho, Y.S., Porter, J.F., Mckay, G. (2002) Equilibrium isotherm studies for the sorption of divalent metal ions onto peat: copper, nickel and lead single component systems, Water Air Soil Pollut. 141, 1–33 pp.

Hong, S., Wen, C., Hea, J., Gana, F., Ho, Y. (2009) Adsorption thermodynamics of Methylene Blue onto bentonite, Journal of Hazardous Materials 167, 630–633 pp.

Horsfall, M., Spiff, A. (2005) Equilibrium sorption study of Al3+, Co2+ andAg2+ in aqueous solutions by fluted pumpkin (Telfairia occidentalis HOOK) waste biomass, Acta Chim. Slov. 52, 174–181 pp.

Hrachová, J., Komadel, P., Fajnor, V.S. (2007) Infuence of C atom concentration for acetylene production in a CH_4/N_2 afterglow, Vacuum 61, 3361 pp.

Huang, J., Liu, Y., Jin, Q., Wang, X., Yang, J. (2007) Adsorption studies of a water soluble dye, Reactive Red MF-3B, using sonication-surfactant-modified attapulgite clay. Journal of Hazardous Materials,1-2(143) 541–548 pp.

Jeffrey, E. and Peter J. (2008) Synchrotron powder X-ray diffraction study of the structure and dehydration behavior of palygorskite, American Mineralogist, 93, 667–675 pp.

Ji, S.W. and Kim, S.J. (2008) Lab-scale study on the application of In-Adit-Sulfate-Reducing System for AMD control. Journal of Hazardous Materials, 160(2–3): 441-447 pp.

Jusoh, A., Hartini, W., Ali, N. and Endut, A. (2011) Study on the removal of pesticide in agricultural run off by granular activated carbon, Bioresource Technology, Vol.102, 5312-5318 pp.

Karimi, L., Salem, A. (2011) The role of bentonite particle size distribution on kinetic of cation exchange capacity. Journal of Industrial and Engineering Chemistry 17, 90–95 pp.

Khan, A.R., Al Waheab, I.R., Al-Haddad, A.A. (1996) Generalized equation for adsorption isotherms for multicomponent organic pollutants in dilute aqueous solution, Environ. Technol. 13–23 pp.

Khan, A.R., Ataullah, R., Al-Haddad, A. (1997) Equilibrium adsorption studies of some aromatic pollutants from dilute aqueous solutions on activated carbon at different temperatures, J. Colloid Interface Sci. 194, 154–165 pp.

Khenifi, A., Bouberka, Z., Sekrane, F., Kameche, M., Derriche, Z. (2007) Adsorption study of an industrial dye by an organic clay. 149-158 pp.

Kilborn (1999). Review of Passive Systems for Treatment of Acid Mine Drainage. Mine Environment Neutral Drainage (MEND) Report 3.14.1.

Kirby, B.J. (2010). Micro- and Nanoscale Fluid Mechanics: Transport in Microfluidic Devices. Cambridge University Press.ISBN 978-0-521-11903-0.

Koble, R.A., Corrigan, T.E. (1952) Adsorption isotherms for pure hydrocarbons, Ind. Eng. Chem. 44, 383–387 pp.

Komadel, P., and Madejova, J. (2006) Handbook of Clay Science, Elsevier.

Koopal, L.K., Van Riemsdijk, W.H., de Wit, J., Benedetti, M.F. (1994) Analytical isotherm equation for multicomponent adsorption to heterogeneous surfaces, J. Colloid Interface Sci. 166, 51–60 pp.

Koumaiti, S., Riahi, K., Ounaies, F. and Thayer, B. (2011) Kinetic Modelling of Liquid-Phase Adsorption of Sulfate onto Raw Date Palm Seeds, Journal of Environmental Science and Engineering, 5, 1570-1580 pp.

Kun, L.E. (1972) A report on the reduction of the sulfate content of acid mine drainage by precipitation with barium carbonate. Anglo American Research Laboratories, D/3/W/1 pp.

Kundu, S. and Gupta, A., (2006) Arsenic adsorption onto iron oxide-coated cement (IOCC): regression analysis equilibrium data with several isotherm models and their optimization, Chemical Engineering Journal, 122, 93-106 pp.

Langmuir, I., (1916) The constitution and fundamental properties of solids and liquids, J. Am. Chem. Soc. 38, 2221–2295 pp.

Laurier, L. (2000) Surfactants: Fundamentals and applications in the petroleum industry, Petroleum recovery institute, Cambridge University Press, 3-22 pp.

Lee, S.H., Song, D.I., Jeon, Y.W. (2001) An investigation of the adsorption of organic dyes onto organo-montmorillonite. 247–254 pp.

Lee, S.M., and Tiwari, D. (2012) Organo and inorgano-organomodified clays in the remediation of aqueous solutions: an overview, Applied Clay Science, 59-60, 84–102 pp.

Lee, S.Y., and Kim, S.J. (2002) Expansion of smectite by hexadecyltrimethylammonium, Clays and Clay Minerals, 50(4) 435–445 pp.

Li, Q., Chai, L., Yang, Z., Wang, Q. (2009) Applied Surface Science 255, 4298 pp.

Li, Z., Willms, C.A., Kniola, K. (2003) Removal of anionic contaminants using surfactantmodified palygorskite and sepiolite. Clays and clay minerals, 51(4) 445–451 pp.

Lopez-Manchado, M.A., Herrero, B., and Biagiotti, J. (2003) Vulcanization kinetics of natural rubber-organoclay nanocomposites. J. Appl. Polym. Sci, 89,1-15 pp.

Madejova, J. (2003) FTIR Techniques in clay mineral studies, Vib. Spectrosc. 31, 1-10 pp.

Madzivire, G. (2009) Removal of sulphates from South African mine water using coal fly ash. BSc (Hons) Chemistry, University of Zimbabwe.

Maree J.P., Hlabela P., Nengovhela R., Geldenhuys A.J., Mbhele N., Nevhulaudzi T., Waanders F.B., (2004) Mine Water Environ. 23 (4) 196–204 pp.

Maree, J.P, Hill, E. (1988) Biological removal of sulphate from industrial effluents and concomitant production of sulphur. Water Pollution Research and Control Brighton, 21, 265-276 pp.

McGinness, S. (1999) Treatment of Acid Mine Drainage, House of Commons Library, Research paper 99/10, 36 pp.

Milavec, P. J. (1999). 1998 Status Report, ARD Set Aside Program. Bureau of Abandoned Mine Reclamation, Pennsylvania, USA.

Mohammed, S. (2009) Removal of Sulfate from Waste Water by Activated Carbon", Al-Khwarizmi Engineering Journal, 5 (3) 72 -76 pp.

Moinuddin, S., Mohammad, M.R., Sadikur, R. (2012) Short and Long Chain Hydrocarbon Transformed from Waste Plastics. International Journal of Chemical Engineering Research,79-90 pp.

Mojovi´c, Z., Milutinovi´c-Nikoli´c, A., Bankovi´c, P., Rabi-Stankovi´c, A., Jovanovi´c, D. (2011) Phenol determination on HDTMA-bentonite-based electrodes. Journal of Hazardous Materials, 178–184 pp.

Motaung S., Maree J., De Beer M., Bologo L., Theron, D. and Baloyi, J., (2008) J. of Water Resources Development, 2 4:3, 433-450 pp.

Mozgawa, W., Król, M., Bajda, T. (2009) Application of IR spectra in the studies of heavy metal cations immobilization on natural sorbents, Journal of Molecular Structure 924-926, 427–433 pp.

Muhammad, N., Amir, W., and Khan, A. (2013) Comparative Study of Laterite and Bentonite Based Organoclays: Implications of Hydrophobic Compounds Remediation from Aqueous Solutions, 78-89 pp.

Muhammad, N., Arita, S., Marsi, and Salni J. (2013) Characterization of Bentonite by XRD and SEM-EDS and Use to Increase pH and Color Removal, Fe and Organic Substances in Peat Water, Journal of Clean Energy Technologies, 1(4) 23-37 pp.

Namasivayam, C., Sangeetha, D. (2008) Application of coconut coir pith for the removal of sulfate and other anions from water. Desalination, 219, 1–13 pp.

Namasivayam, C., Sureshkumar, V. (2007) Removal of sulfate from water and wastewater by surfactant modified coir pith, an agricultural solid ‘waste’ by adsorption methodology. Environmental Engineering Management, 17(2) 129-135 pp.

Nevskaia, D.M., Lopez, E.C., Munoz, V., Ruiz, A.G. (2004) Adsorption of aromatic compounds from water by treated carbon materials. Environmental Science and Technology. 38, 5786–5796 pp.

Ntuli, F., Falayi, T., Moreroa, M. (2014) A kinetic and thermodynamic study of sulphate removal from AMD using fly ash. Biomedical Engineering and Environmental Engineering, Published by WIT Press, 8 pp.

Odom, I.E. (1984) Smectte clay minerals: properties and uses. 391–409 pp.
Özcan, A.S., Erdem, B., Özcan, A. (2004) Adsorption of Acid Blue 193 from aqueous solutions onto Na-bentonite and DTMA-bentonite. Journal of Colloid and Interface Science of The Total Environment, 44-54 pp.

Pálková, H., Hronsky, V., Bizovská, V., Madejová, J. (2015) Spectroscopic study of water adsorption on Li^+, TMA^+ and $HDTMA^+$ exchanged montmorillonite. Molecular and Biomolecular Spectroscopy 149, 751–761 pp.

Pérez-Marín, A.B., Meseguer, V., Ortuno, J., Aguilar, M., Sáez, J., Llorens, M. (2007) Removal of cadmium from aqueous solutions by adsorption onto orange waste, J. Hazard. Mater. B139, 122–131 pp.

Rajkiran R., Kartic, C., Upendra, N. (2008) Synthesis and characterization of novel organo-montmorillonites. Applied Clay Science 38, 204-208 pp.

Ringot, D., Lerzy, B., Chaplain, K., Bonhoure, J., Auclair, E., Larondelle, Y. (2007) Invitro biosorption of ochratoxin A on the yeast industry by-products: comparison of isotherm models, Bioresour. Technol. 98, 1812–1821 pp.

Ríos, C.A., Williams, C.D., and Roberts, C.L. (2008) Removal of heavy metals from acid mine drainage (AMD) using coal fly ash, natural clinker and synthetic zeolites. Journal of Hazardous Materials, 156(1–3) 23-35 pp.

Saljoghi, S., Rafiee, G., Malekpour, A., Safari, A. (2012) Application of Modified Bentonites (SMB and ATB) for Decreasing the Environmental Effects of Phosphate and Sulphate Anions Existing in RAS. Journal of environmental Studies, 38, 10-12 pp.

Sapkota, J. (2011) Influence of clay modification on curing kinetics of natural rubber nanocomposites. 1-57 pp.

Sarkar, B. (2011) Orange II adsorption on palygorskites modified with alkyl trimethylammonium and dialkyl dimethylammonium bromide — An isothermal and kinetic study. Applied Clay Science, 51(3) 370-374 pp.

Sarkar, B., Xi, Y., Megharaj, M. (2012) Bioreactive organoclay: a new technology for environmental remediation, Critical Reviews in Environmental Science and Technology, 42(5) 435–488 pp.

Silva, I., Sousa, F., Menezes, R., Neves, G., Santana, L., Ferreira, H. (2014) Modification of bentonites with nonionic surfactants for use in organic-based drilling fluids, Applied Clay Science 95, 371–377 pp.

Silva, R., Cadorin, L., Rubio, J. (2010) Sulphate ions removal from an aqueous solution: I. Co-precipitation with hydrolysed aluminum-bearing salts. Minerals Engineering, 1220-1226 pp.

Sips, R. (1948) Combined form of Langmuir and Freundlich equations, J. Chem. Phys. 16, 490–495 pp.

Stojiljkovic, S., Stamenkovic, M., Kostic, D., Miljkovic, M., Arsic, B., Savic, Miljkovic, V. (2013) The Influence of Organic Modification on the Structural and Adsorptive Properties of Bentonite Clay and Its Application for the Removal of Lead. Science of Sintering, 45, 363-376 pp.

Su, J., Lin, H.F., Wang, Q.P., Xie, Z.M., Chen, Z.L. (2011) Adsorption of phenol from aqueous solutions by organomontmorillonite, 269, 163–169 pp.

Sven, E. (1979) Industrial waste water management, Studies in environmental science, Published by Elsevier, 2-11 pp.

Thomas, S. (2010) Rubber Nanocomposites: Preparation, properties and application, John Wiley & Sons. 169-171 pp.

Tjong, S.C. (2006) Structural and mechanical properties of polymer nanocomposites. Mater. Sci. Eng, 53, 73-197 pp.

Toth, J. (1971) State equations of the solid gas interface layer, Acta Chem. Acad. Hung. 69, 311–317 pp.

Vega, J.L., Ayala, J., Loredo, J. and García, I. (1995) Bentonites as adsorbents of heavy metals ions from mine waste leachates: Experimental data. 603 pp.

Vijayaraghavan, K., Padmesh, T., Palanivelu, K., Velan, M. (2006) Biosorption of nickel(II) ions onto Sargassum wightii: application of two-parameter and three parameter isotherm models, J. Hazard. Mater. B133, 304–308 pp.

Wang, H., Zhou, A., Peng, F., Yu, H. and Yang, J. (2007) Mechanism study on adsorption of acidified multi-walled carbon nanotubes to Pb(II). J. Colloid Interface Sci. 316, 277–283 pp.

Wanga, H., Jiang, J. (2011) The effect of metal cations on phenol adsorption by hexadecyl-trimethyl-ammonium bromide (hdtma) modified clinoptilolite. Separation and Purification Technology, (80) 658–662 pp.

Waters, J. C., Santomartino, S., Murphy, N., Taylor, J. R. (2003). Acid mine drainage treatment technologies: Identifying sustainable solutions. Paper presented at the 6th ICARD, July 12-18, 2003, Cairns, Australia.

Wright, N. and Hunter, M. J. (1947) Organosilicon polymers. III: Infrared spectra of methylpolysiloxanes: J. Am. Chem. Soc. 69, 803 809 pp.

Xiping, L., Yuhan, L., Zhixing, S. (2008) Synthesis and characterization of Organo-Attapulgite/Polyanaline-Dodecylbenzenesulfonic Acid Based Emulsion Polymerization Method. Institute of Polymer and Engineering. 1-6 pp.

Xu, S., and Boyd, S.A. (1995) Alternative model for cationic surfactant adsorption by layer silicates," Environmental Science and Technology, 29(12) 3022–3028 pp.

Xuea, W., He, H., Zhu, J., Yuan, P. (2007) Spectrochim. Acta A 67, 1030 pp.

Yapar, S., Ozbudak, V., Dias, A., Lopes, A. (2005) Effect of adsorbent concentration to the adsorption of phenol on hexadecyl trimethyl ammonium-bentonite, Journal of Hazardous Materials B121, 135–139 pp.

Zarrouk, A., Hammouti, B., Zarrok, H., Al-Deyab, S., Messali, M. (2011) Temperature Effect, Activation Energies and Thermodynamic Adsorption Studies of L-Cysteine Methyl Ester Hydrochloride As Copper Corrosion Inhibitor In Nitric Acid 2M, Int. J. Electrochem. Sci., 6, 6261 – 6274 pp.

Zhebo C., Huyen N. (2013) Dinh Eric Miller Photoelectrochemical Water Splitting Standards, Experimental Methods, and Protocols, 49-62 pp.

Ziemkiewicz, P. F. and Brant, D. L. (1996) The Casselman River Restoration Project. In: Proceedings Eighteenth West Virginia Surface Mine Drainage Task Force Symposium 1996, Morgantown, West Virginia.

Zvimba, J., Mulopo, J., Motaung, S., Maree, J., de Beer, M. and Bologo, T., (2010) Coal mine acid mine drainage treatment and sludge processing, Natural Resources and the Environment, 1-17 pp.

Appendix 1

Table 1: XRD operating conditions

Parameter	Specification
X-Ray	40 kV , 30 mA
Filter	K-beta filter
Diffracted beam mono.	Fixed Monochro.(U4)
Detector	Scintillation counter
Scan mode	Continuous
Scan speed / Duration time	1.0000 deg./min.
Step width	0.0100 deg.
Scan axis	2theta/theta
Scan range	3.0000 - 90.0000 deg.
Receiving slit #1	1/2deg.

Table 2: SEM operating parameters

Parameter	Specification
HV	20.00 KV
Magnification	1.00 Kx
View field	190.2 µm
Beam intensity	10.00
Size	50 µm

Table 3: FTIR operating parameters

Parameter	Specification
Detector	DTGS KBr
Beam Splitter	KBr
Range	700-4000 cm^{-1}
Optical velocity	0.6329